MONITORING FLUID FRONT MOVEMENT USING PERMANENT RESISTIVITY ARRAYS

BY

MUHAMMAD REAZ UDDIN CHOWDHURY

A Thesis Presented to the

DEANSHIP OF GRADUATE STUDIES

KING FAHD UNIVERSITY OF PETROLEUM & MINERALS

DHAHRAN, SAUDI ARABIA

In Partial Fulfillment of the
Requirements for the Degree of

MASTER OF SCIENCE

In

PETROLEUM ENGINEERING

March 2003

KING FAHD UNIVERSITY OF PETROLEUM & MINERALS

DHAHRAN 31261, SAUDI ARABIA

DEANSHIP OF GRADUATE STUDIES

This thesis, written by, **MUHAMMAD REAZ UDDIN CHOWDHURY** under the supervision of his thesis advisor and approved by his thesis committee, has been presented to and accepted by the Dean of Graduate Studies, in partial fulfillment, of the requirements for the degree of **MASTERS OF SCIENCE IN PETROLEUM ENGINEERING.**

Thesis Committee
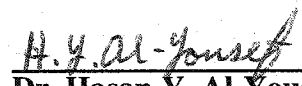
Dr. Abdulaziz U. Al-Kaabi
Thesis Advisor

Dr. Kamal Babour
Member

Dr. Khalid A. Al-Fossail
Member

Dr. Habib Menouar
Member

Dr. Hasan Y. Al-Yousef
Member

Dr. Khalid A. Al-Fossail
Department Chairman

Prof. Osama A. Jannadi
Dean of Graduate Studies

Date: March 22, 2003

ii

DEDICATION

Dedicated to my Parents and my loving Niece "Maisha".

ACKNOWLEDGEMENT

TABLE OF CONTENTS

CHAPTER 4

EXPERIMENTAL APPARATUS AND PROCEDURE.......................... 22

CHAPTER 5

CHAPTER 6

LIST OF FIGURES

Chapter 5

Appendix A

ABSTRACT

FULL NAME: MUHAMMAD REAZ UDDIN CHOWDHURY

TITLE OF STUDY: MONITORING FLUID FRONT MOVEMENT USING

PERMANENT RESISTIVITY ARRAYS

MAJOR FIELD: PETROLEUM ENGINEERING

DATE OF DEGREE: MARCH 2003

Knowledge of fluid movement in the reservoir is a key to reducing production cost and to increasing ultimate recovery. The main objective of reservoir fluid monitoring is to provide a reliable temporal description of the fluid front propagation resulting from fluid injection and production.

This study represents the first experimental work to study the feasibility of fluid front monitoring using Permanent Resistivity Arrays in a well centered in a circular drainage area. A visual sector model that represents $1/16^{th}$ of the circular drainage area was designed and constructed. The production/injection well was equipped with permanent resistivity arrays. Advanced data acquisition system was used to inject current and to measure electric potential.

The experimental data were then simulated numerically using a finite element numerical model developed by Schlumberger. A good match was obtained between laboratory and numerical results. The model was also used to understand the influence of various parameters on the measurements.

The results of this study indicate that resistivity measurements are very sensitive to fluid movement and that Permanent Resistivity Arrays can easily be used to monitor fluid front movement. It was demonstrated through this work that fluid front can be detectable up to a distance equaling twice the length of the resistivity array and the detection level could even be improved several fold if the sensitivity of the measurements are improved. The resistivity measurements were also found to be sensitive to the orientation of the fluid front.

MASTER OF SCIENCE DEGREE

KING FAHD UNIVERSITY OF PETROLEUM & MINERALS

DHAHRAN, SAUDI ARABIA

ملخص

الإســـــــــم : محمد رياض الدين شودري

عنوان الرسالة : مراقبة حركة مقدمة الموائع باستخدام صفوف دائمة للمقاومية .

التــخصص : هندسة البترول

تاريخ التخرج : مارس 2003م.

إن معرفة حركة الموائع في المكمن من أهم العوامل الرئيسة في تخفيض تكلفة الإنتاج, وزيادة الانتاجية الكلية. وإن الهدف الرئيسي لمراقبة حركة الموائع في المكمن هو تقديم وصف مرحلي موثق لانسياب الموائع الناتجة من عمليات الغمر والإنتاج .

وتمثل هذه الدراسة أول عمل تجريبي لدراسة جدوى مراقبة حركة الموائع باستخدام صف دائم للمقاومية في بئر يتوسط حقل دائري. ولقد تم تصميم وانشاء نموذج شفاف لمقطع دائري تمثل جزءاً واحداً من ستة عشرة جزءاً من الحقل الدائري ، مع تزويد بئر الانتاج والغمر بصف دائم من اقطاب كهربائية لقياس المقاومية واستخدام نظام متطور لضخ تيار كهربائي ولقياس الجهد الناتج.

وتم محاكاة البيانات المتحصلة من التجارب حسابياً باستخدام نموذج حسابي مطور من قبل شركة شلمبرجيه . و تم الحصول على نتائج متطابقة مع تلك المتحصلة من التجارب . كما تم استخدام المحاكي في دراسة تأثير العوامل المختلفة على القياسات .

ولقد اظهرت نتائج الدارسة على أن المقاومية حساسة جداً لحركة انسياب الموائع في المكمن وأن نظام الصفوف الدائمة للاقطاب الكهربائية لقياس المقاومية يمكن استخدامها بكل يسر في تحديد حركة مقدمة الموائع على مسافة تعادل ضعف طول صف المقاومية في البئر ، ويمكن زيادة ذلك عدة مرات باستخدام اجهزة قياس اكثر حساسية . وكما أظهرت النتائج أن قياس المقاومية تتأثر بدرجة ميلان المقدمة.

درجة الماجستير في العلوم الهندسية

جامعة الملك فهد للبترول والمعادن

الظهران – المملكة العربية السعودية

Chapter 1

INTRODUCTION

CHAPTER 1

INTRODUCTION

Tracking the movement of reservoir fluids during production has great importance in reservoir management and in improving recovery since it provides advance warning of changes in production behavior. This warning may help to prolong the life of the well. Knowledge of fluid movement in the reservoir is a key to reduce production cost and to increase ultimate recovery.

Currently most of the vital data about the reservoir are obtained under the form of production or pressure behavior. Water breakthrough at a well, however, usually signals a decline in the well's desired production rate. Reliable advance knowledge of the locations of fluid interfaces allows remedial actions to be taken to extend the life of the well.

Geophysical techniques have been used for reservoir delineation and description for several decades. Recently, attempts have been made to adapt geophysical techniques to actively monitor secondary and tertiary recovery processes such as water, and steam flooding. It has been realized that the detection of changes in geophysical response over time can be used to estimate the lateral extent and volume of the reservoir affected by the enhanced recovery processes. The main objective of monitoring is to provide a reliable

temporal description of the fluid front propagation resulting from fluid injection and production. These data are usually supplemented with production data and observation well histories and used to estimate reservoir recovery efficiency and to plan continuation of production cycles. In fact, such data help to optimize the design and to improve control of the well because they provide an independent measurement of the recovery behavior.

The most interesting approach in geophysics for reservoir monitoring is associated with repeating geophysical surveys with great precision at different times during reservoir depletion. This allows the use of time differential data (changes over time) rather than evaluating the reservoir based on a single survey (one time absolute measurement and interpretation). For reservoir monitoring, time-lapse measurements are obviously vital. Besides, time-lapse measurements can be interpreted directly in terms of reservoir parameter changes, rather than by doing absolute interpretations and then comparing them to study the changes in the reservoir parameters.

Electrical methods are more sensitive to fluid content than seismic methods, which are essentially sensitive to the rock matrix properties (except in the case of gas reservoirs). Because of this sensitivity to fluid content, electrical techniques can be used to complement seismic methods in reservoir monitoring. The recent advancements have in borehole electric and electromagnetic transmitters and receivers for cross-hole and subsurface-to-surface electrical surveys opened the possibilities of reservoir monitoring over time for reservoir management.

At present, permanent monitoring systems are increasingly used to measure and record well performance and reservoir behavior from sensors placed downhole during completion. Modern communications provide remote access to measurements of reservoir parameters. Engineers can watch performance continuously, examine responses to changes in production or secondary recovery processes and also have a record of events to help diagnose problems and monitor remedial actions. Most systems in operation record bottom-hole pressure and temperature, but other measurements, such as flow rate, are increasingly becoming common. When pressure and rate are measured within the wellbore, fluid saturation is evaluated around or at some distance away from the wellbore. In the same way that electrical logging resolves the distribution of fluid saturation around the wellbore, permanent-monitoring tools aim at delivering a more complete answer with a greater depth of investigation.

The aim of this research is to study the application of Permanent Arrays of Electrodes as a method for monitoring fluid front movement in a scaled reservoir model. The study will answer the following questions:

- Can we use electrical method to detect fluid front movement?
- If yes,

  - How far can we detect the front?

  - How sensitive is the measurement?

  - What is the effect of controlling factors?

  - Can we numerically simulate the results?

  - What is the effect of front orientation?

Chapter 2

LITERATURE REVIEW

CHAPTER 2

LITERATURE REVIEW

The desire to prevent early water production has created a growing demand for accurate tracking and imaging of fluid front movement in hydrocarbon reservoirs. Various methods were tried to provide an image of fluid movement in the reservoirs. Currently, permanent monitoring methods including permanent electrode arrays are being evaluated in various locations including local Saudi Formations. Following is a summary of work done related to fluid movement monitoring in hydrocarbon reservoirs.

Dunlop, King, and Breltenbach (1991)[1] described a monitoring technique that used repeated seismic surveys to detect saturation changes at locations distant from wells. The monitoring technique integrates the data currently used for prediction of reservoir behavior with measurements made by repeated surface-seismic-reflection surveys. The continuity of seismic information along cross-sections is integrated with the 3-D coverage provided by simulation. This creates a field model in which the fluid location can be verified by direct measurement. Repeated surveys and simulations provide feedback that refines the accuracy of the field model.

Khalaf (1991)[2] used responses from pressure buildup surveys to distinguish between gas and waterfronts and to determine the distance to either of these fronts long before the fronts reach the wellbore in the Umm Sharif field. The gas front behaved as a constant pressure boundary, while water acted as a pressure-support boundary. The field was producing for a long time and the fluid fronts moved significantly from their original locations. The tracking of fluid movement was achieved through TDT logging and monitoring gas and water production.

Mills (1993)[3] used Time-Lapse interpretation effectively in low-salinity formation for quantitative interpretation although formation responses often are masked by larger responses caused by changes in the logging environment. In his work, several techniques, such as using the Gamma ray log to indicate formation water movement, are used to aid interpretation because accurate quantitative interpretation of Pulsed-Neutron-Capture (PNC) logs cannot be achieved in the low salinity formation water environment of the Gippsland basin. This is because formation fluid movement responses are small relative to uncertainties introduced by lithologic variation.

Erga, and Knuston (1991)[4] described the fluid distribution in the Beryl formation, which has a complicated distribution of pressures and fluids. Horizontal permeability restrictions, the result of extensive faulting, subdivided the reservoir into eight inter-related areas as determined by careful analyses of pressure histories, production histories and fluid monitoring. They described the methodology for constructing a conceptual reservoir model for the Beryl reservoir to identify areas of upswept hydrocarbons,

resulting in an aggressive drilling program, and optimize the effort in simulation history matching.

Narayan and Dusseault (1995)[5] showed that three-dimensional electrical resistivity tomography might be used to track propagation of fluid fronts over time. They present general requirements for resistivity tomography in EOR, typical electrode installations to reduce noise and seasonal variations, requirements for a general inversion of a 3-D resistivity problem in EOR, sensitivity analyses for a shallow reservoir case subjected to EOR, and a method of rapid design and evaluation of resistivity monitoring. The analytical tools and technology are now adequate to re-evaluate and develop electrical monitoring for EOR applications.

Brady, Wolcott, and Ferguson (1995)[6] developed and tested a unique method to monitor water movement in a gas cap reservoir in an Arctic environment. The novel surveillance technique for monitoring the water movement had to be developed given the very limited number of wells that penetrate the gas cap, whereas conventional fluid monitoring techniques require drilling numerous observation wells to adequately monitor water movement. Modeling studies indicate that the density changes associated with water replacing gas can be detected using high-resolution surface gravity measurements. Modeling gravity effects of water movement for mass distribution, mass balance and water front detection were also discussed. A test of the gravity meter and essential high-precision station positioning under typical Arctic winter conditions were evaluated using the Global Positioning System (GPS).

Unneland and Haugland (1994)[7] presented experience with and applications of permanent downhole pressure and temperature gauges in the reservoir management of two complex North Sea oil fields, Gullfaks and Veslefrikk. In total, 40 quartz and capacitance gauges had been installed in platform wells for 6 years. The gauges provide invaluable real time data for reservoir management of these two fields and contributed directly to increased daily oil production. The installations proved to be safe and reliable, as well as good investments. The decision to install permanent gauges was based on three primary factors:

1. The need for enhanced reservoir description, especially during the initial production time.

2. Increased production resulting from a combination of less downtime for data acquisition and optimization of reservoir and well management.

3. Safety and operational considerations.

Large investments before production startup are typical for most North Sea developments, requiring a high early production to ensure project profitability. At the same time, reservoir complexity and relatively short field lifetimes necessitate extensive data acquisition during the initial production phase. Permanent gauges supported both requirements by supplying continuous downhole data with a minimum well downtime.

Phillip, Roy, and Walter (1982)[8] used Pulsed Neutron Capture (PNC) Logs to determine residual oil saturation. Previous study showed that, at low values of residual oil saturation (ROS), conventional PNC logging techniques did not have the accuracy necessary for enhanced oil recovery decision-making requirements. So they developed and used special log-inject-log techniques in order to reduce the uncertainty in the values of ROS measured with PNC logs. A study of the uncertainty associated with ROS values determined with PNC logs was made using Monte Carlo simulation techniques. Field data was obtained from tests reported in the literature. Using a more realistic confidence interval of 95%, the expected accuracy of the ROS values was found to decrease by at least a factor of two in tested wells.

Donaldson, Madjidi, and White (1991)[9] presented an experimental work to show that the concept of the focused current logging tool could be extended to cross-well potential measurements to determine the inter-well fluid saturation distribution. A model reservoir, 8 feet in diameter with 20 inches of sand between two layers of shale, was saturated with 80000 ppm of sodium chloride. Eleven wells were located throughout the reservoir and a scaled nine-electrode laterolog was used to provide the focused current. Electrical potentials measured at each well were used to map the isopotential lines. The uniform sodium solution was then changed at one well by injecting fresh water and isopotential maps of the saturation abnormality were made. Dissipation of the saturation abnormality with respect to time, due to counter-current diffusion, was also tracked.

A Finite Element Mathematical Model using Poisson's and Archie's equations was prepared. The exact dimensions of the model reservoir and the experimental input data were used in the computer program. Using these data, the computer program produced maps of isopotential lines. The results indicate that this could be developed into a technique to measure the inter-well saturation distribution in reservoirs. It also could be used for the location of saturation anomalies and discontinuities, caused by geological structure changes, between wells.

Augustin, Kennedy, Morison, and Lee (1988)[10] explained a new logging method, in which the source is a horizontal loop, coaxial with a cased drill hole and the secondary axial fields are measured at depth within the casing. If the casing response cannot be accurately predicted, a separate logging tool employing a higher-frequency transmitter could be used to determine the required casing parameters in the vicinity of the reservoir. The logging technique showed excellent sensitivity to changes in formation conductivity. One of its most promising applications is in monitoring, through repeated measurements, changes in formation conductivity during production or enhanced recovery operations.

Xu and Noel (1993)[11] described how potential data can be obtained for use in electrical resistivity imaging, using a surface linear array of equally spaced electrodes. The aim was to collect a complete data set, which contains all linearly independent measurements of apparent resistivity, with such an array using two-, three- or four-electrode configurations. From this primary data set, it was shown that any other value of apparent resistivity on the array could be synthesized through a process of superposition.

Numerical tests showed that such transformations were exact within the machine error for calculated data but that their use with real field data may lead to noise amplification.

Poirmeur, and Vasseur (1988)[12] showed that hole-to-hole electrical measurements could be used to localize and define the extension of conductive bodies whether or not they were penetrated by the holes. Two promising applications of this electrical method are the optimization of mining boreholes and delineation of fractures. A program was developed to compute the electrical potential caused by direct current injection in an inhomogeneous half-space.

Gorden, Lovell, Miriari and Tezuka (1990)[13] modeled arrays of pole-pole and dipole-dipole electrical logs of ultra long spacing in an environment with a conductive borehole and resistive formation. The forward modeling had been done with 2-D and 3-D finite element codes solving Laplace's equation. Logs of the same electrode configuration had been run in a well drilled in a hot dry rock geothermal reservoir and the same modeling capability had been used to attempt inversion of those logs. The logs showed indications of local mechanical and thermal stress related to micro fractures as well as long but sparse natural fractures intersecting the borehole. The micro fractures were modeled as zones of finite conductivity and the location and conductivity values of those zones were estimated by 2-D iterative modeling.

Imamura (1992)[14] attempted to image the near borehole resistivity structure using the apparent resistivity from normal resistivity logs. An axis metric FEM and 4CST

elements were used to calculate the theoretical apparent resistivity. The apparent resistivity of the FEM result showed good agreement with an analytical solution and a resistor network solution. Using the technique, it is possible to elucidate a variation of resistivity a in radial direction. The technique can potentially be applied to estimate formation permeability, by comparing the image obtained at different times.

Mansure, Meldau, and Weyland (1993)[15] showed how the relationship between the process and formation resistivity, which is an essential part of electrical geo-diagnostic techniques to map thermal recovery processes, is used to interpret electrical well logs and can be used to understand steam flood resistivity changes. Examples are presented of data from steam floods in fields with different reservoir characteristics. Included is a typical heavy-oil steam flood and a steam flood where fresh water is used for the steam generator feed water. Because of differences in reservoir characteristics, changes in resistivity vary from reservoir to reservoir. The information presented includes well logs taken before and after steam flooding and petrophysical measurements sufficient to determine the factors that controlled the resistivity changes in the field.

Kleef and Babour (2001)[16] reported a project launched by Schlumberger and Shell to prove the concept and economic viability of Dynamic Reservoir Drainage Imaging (DRDI). The goal was to provide a time-lapse monitoring of water saturation, allowing evaluation of drainage efficiency in oil and gas reservoirs. To achieve this objective, the resistivity approach was used. In this technique, an array of electrodes is cemented at reservoir level, providing a continuous reading of the formation resistivity. Applications

of this technology include real-time monitoring of water cone development and water table rise, provided there is a sufficiently large resistivity contrast between hydrocarbon and water zones.

In the case of a water flood, as the water front approaches the array the current lines are distorted, resulting in a variation in electrical potentials when compared with the base case with no water. Downhole resistivity was selected for its ability to monitor fluid-front advancement and detect approaching water. Seismic sensors were originally considered as complementary sensors at the beginning of the project. The well completion design was optimized in order to ensure a safe deployment of the electrical array cable and well integrity. On the application side, the data acquired by Dynamic Reservoir Drainage Imaging (DRDI) so far have cast a new light on the dynamic processes taking place in the reservoir. The interpretation of the time lapse DRDI data has shown that the water sweep was vertically uneven and that early water breakthrough was to be expected at the producer wells. Production data and saturation logging confirmed the above interpretation.

Bryant, I.D. et al. (2002)[20] explained the application of electrical measurement technologies to permanent reservoir monitoring. The principle objective of the experiment was to demonstrate the feasibility of monitoring water movement between an injection and an observation well. They were able to generate and present good signal-to-noise ratio and high reciprocity. They demonstrated the viability of using permanently installed resistivity arrays to monitor the movement of oil/water contacts and salinity

fronts that are some tens of feet away from the wellbore. Results demonstrated the feasibility of using such arrays to monitor the movement of oil/water contact from injection, monitoring and production wells.

Charara, M et al. (2002) [21] deployed permanent downhole electrodes successfully in oil wells to track oil fields under secondary recovery such as water flooding, where an even reservoir sweep or zones of bypassed oil could be defined by the proper description of the waterfront advance. They have described the use of pressure buildup from repeated shuts in association with the electrical measurements. They have published a quick look method for interpreting the time-lapse pressure transients with a comparison of the physical and practical advantages of each type of measurement and the domain of application of the two measurements with respect to fluid and reservoir properties.

Chapter 3

STATEMENT OF THE PROBLEM

AND

STUDY OBJECTIVE

CHAPTER 3

STATEMENT OF THE PROBLEM AND

STUDY OBJECTIVE

3.1   STATEMENT OF THE PROBLEM

Reservoir development and management traditionally rely on early data gathered during short periods of logging and testing before wells are placed on production. Additional data are generally required after a long period of production, either as a planned exercise or when unforeseen problems arise. Such data acquisition requires well intervention and always means loss of production, increased risk, inconvenience and logistical problems, and may also involve the additional expense and time of bringing a rig to the location.

Permanent monitoring systems are helpful to avoid the above stated problems. Those systems measure and record well performance and reservoir behavior from sensors placed downhole during completion. Such measurements give engineers information essential to dynamically manage hydrocarbon assets, allowing them to optimize production, diagnose problems, refine field development and adjust reservoir models.

According to the previous literature survey presented in Chapter 2, there has been increasing interest in using permanent downhole arrays to track the movement of the planar front in the reservoir. The following observations were made from the literature survey:

a. There is no previous laboratory work to study permanent downhole arrays of electrodes for tracking of fluid front movement in reservoirs.

b. The idea of using permanent resistivity arrays is relatively new with limited field experience. Further understanding of the factors influencing the measurements is very much needed.

c. There is limited published work on interpreting multiple well data with the use of permanent resistivity arrays.

d. In all the reported studies, the front is assumed as a moving plane. No previous study looked at a front moving toward the well in a radial direction.

e. There is a need to optimize the utilization of wells equipped with permanent resistivity arrays.

Our study was aimed at further advancing knowledge in utilizing permanent resistivity electrodes and the use of electrical methods in tracking fluid movement in reservoirs. A scaled physical model and a numerical simulator were used to study fluid front movement over time in cylindrical coordinate using permanent arrays of electrodes in a single well arrangement with a single source of current.

3.2   OBJECTIVES OF THIS STUDY

The objectives of this study were to:

a. Implement permanent downhole arrays of electrodes in a scaled reservoir model that represents a cylindrical drainage area.

b. Vary the current injection rate, electric potential and spacing of electrodes to get different measurement conditions.

c. Use the setup to measure the change in resistivity due to change in fluid content and distribution.

d. Validate and utilize a numerical model in the analysis of acquired resistance or potential data.

3.3   PROPOSED APPROACH

In order to accomplish the above objectives, the following approach was proposed:

a. Design and construct a scaled reservoir model.

b. Design and implement model wells equipped with permanent arrays of electrodes.

c. Measure the potentials between the array electrodes and a reference electrode located at a distant place.

d. Interpret the experimental data to determine the movement of the fluid front.

e. Validate and utilize a Mathematical Model (developed by Schlumberger) to analyze experimental data.

3.4   STUDY PLAN

The following plan was used to achieve the above objectives:

1. Implement permanent resistivity arrays in an injection / producing well to study the behavior of the resistances with the movement of fluid. From the electrical viewpoint, if there is a large resistivity contrast between the zones mostly saturated with oil and water, the measured resistance should change significantly if the fluid in any zone is changed from oil to water or vice versa. By observing the change in measured resistances, it might be possible to get an indication of the position of the oil water interface.

2. Fabricate a model made of one-inch thick plexiglas sheet to represent a sector in a cylindrical drainage area where a producer well is surrounded by water in all directions.

3. Use a Teflon tube with several electrodes mounted on its surface to represent the well with the permanent resistivity arrays.

4. Eliminate the gravity effect on the orientation of the front by conducting experiments while the model is positioned vertically.

5. Use a state-of-the-art data acquisition system (from Schlumberger) to measure the resistances along the electrodes with respect to the reference electrode.

6. Validate a mathematical model and then use it to analyze the collected data to define the position of the fluid front in the reservoir.

Chapter 4

EXPERIMENTAL APPARATUS

AND

PROCEDURE

CHAPTER 4

EXPERIMENTAL APPARATUS AND

PROCEDURE

4.1 EXPERIMENTAL SETUP

Based on the objectives of this study, there was a need to fabricate two models (one to represent the reservoir and another to determine fluid properties). Their design and implementation were done with the help of the personnel from the Petroleum Engineering Department and the Research Workshop. Below is a description of the two models.

4.1.1 SECTOR MODEL

A transparent 3-dimensional scaled model, made out of plexiglas (one inch thick) was used for the main part of the study. 30-40 mesh glass beads were used to represent the porous media of the reservoir. The model has a wedge shape and represents 1/16th of a polygonal-shaped reservoir. The polygonal shape approximates a cylindrical reservoir with fluid flow in a radial direction (Figure 4.1.1). The length of the two equilateral sides of the sector model is 100 cm each and the base is 40 cm long. The height of the reservoir model is 30 cm when it is in the horizontal position.
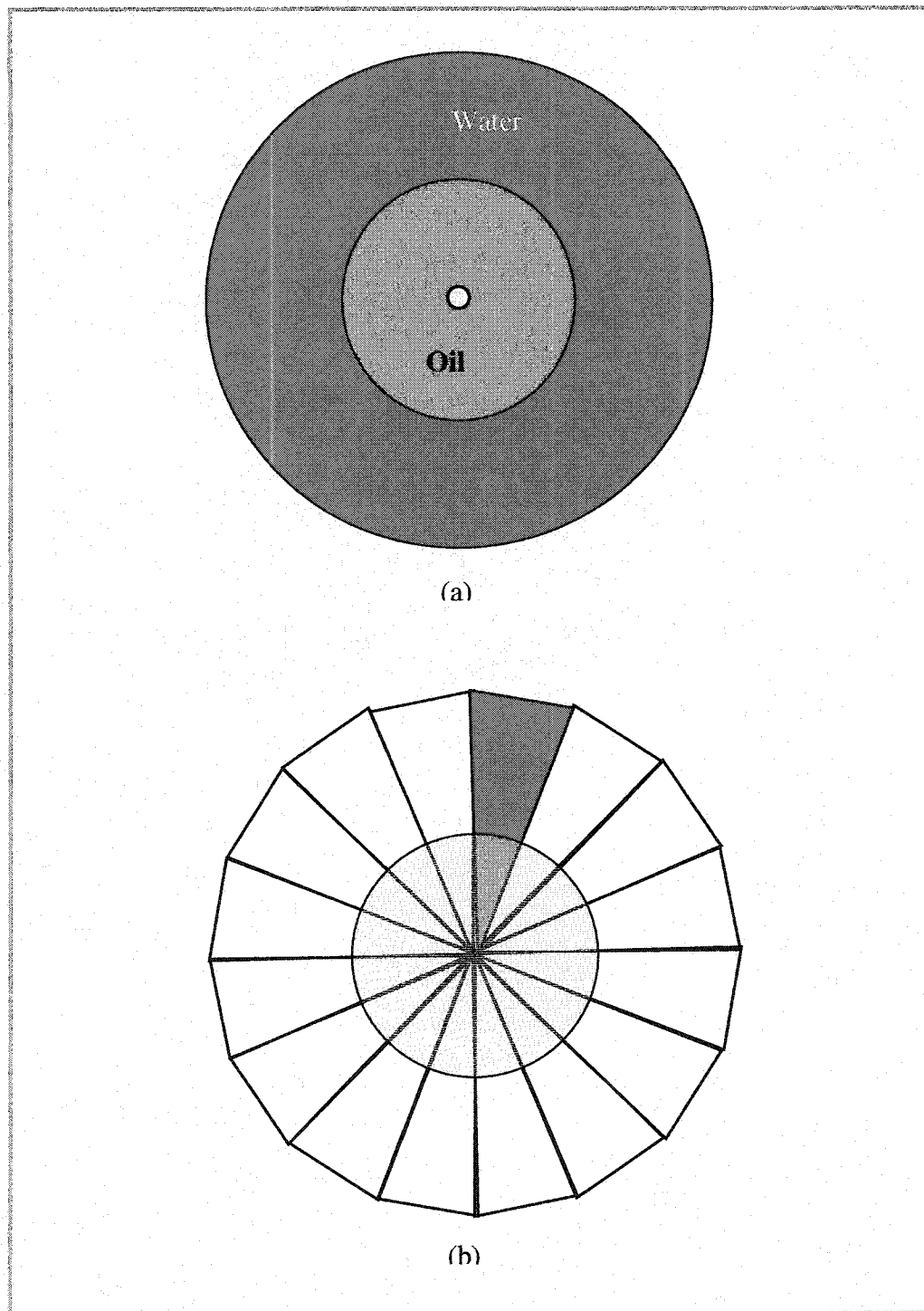
Figure 4.1.1: Top View of (a) Cylindrical Model, (b) Using Sector Model as 1/16th of Polygonal Shape.

All the sides of the plexiglas model were fixed to each other with epoxy glue and long screws to make it completely sealed except for the top cover. The extended portions of the top plate were connected to the extended portions of the bottom plate (shown later in Figure 4.2.3) with screws and nuts keeping the rubber liner in the joint of the top and the side plates only to make it sealed and removable if needed.

Fluids were injected into the sector model using wells. A 30 cm long transparent Teflon tube of 0.6 cm ID was used to simulate the main well (used as production well for most cases) centered in a circular reservoir. The main well was perforated and a filter was mounted in front of the other well. The 30 cm well had 30 perforations per cm. The diameter of the perforations was selected to be 0.4 mm to keep glass beads from getting through during production.

Thirty-one electrodes were mounted on the main well and were connected to the acquisition system to measure electric potential. Two more electrodes were inserted in the base plate of the model; they were used as reference electrodes. Eight electrodes were inserted along the top plate to measure the change of resistivities of the porous media. The top electrode mounted on the well and one of the reference electrodes were used for current injection while the other electrodes on the well and the other reference electrode were used to measure potentials. To improve measurement accuracy and to alleviate difficulties discussed later, extra eighteen electrodes were positioned a few centimeters below the injection well and inserted directly into the porous media from the sides (Figure 4.12 and Figure 4.13).
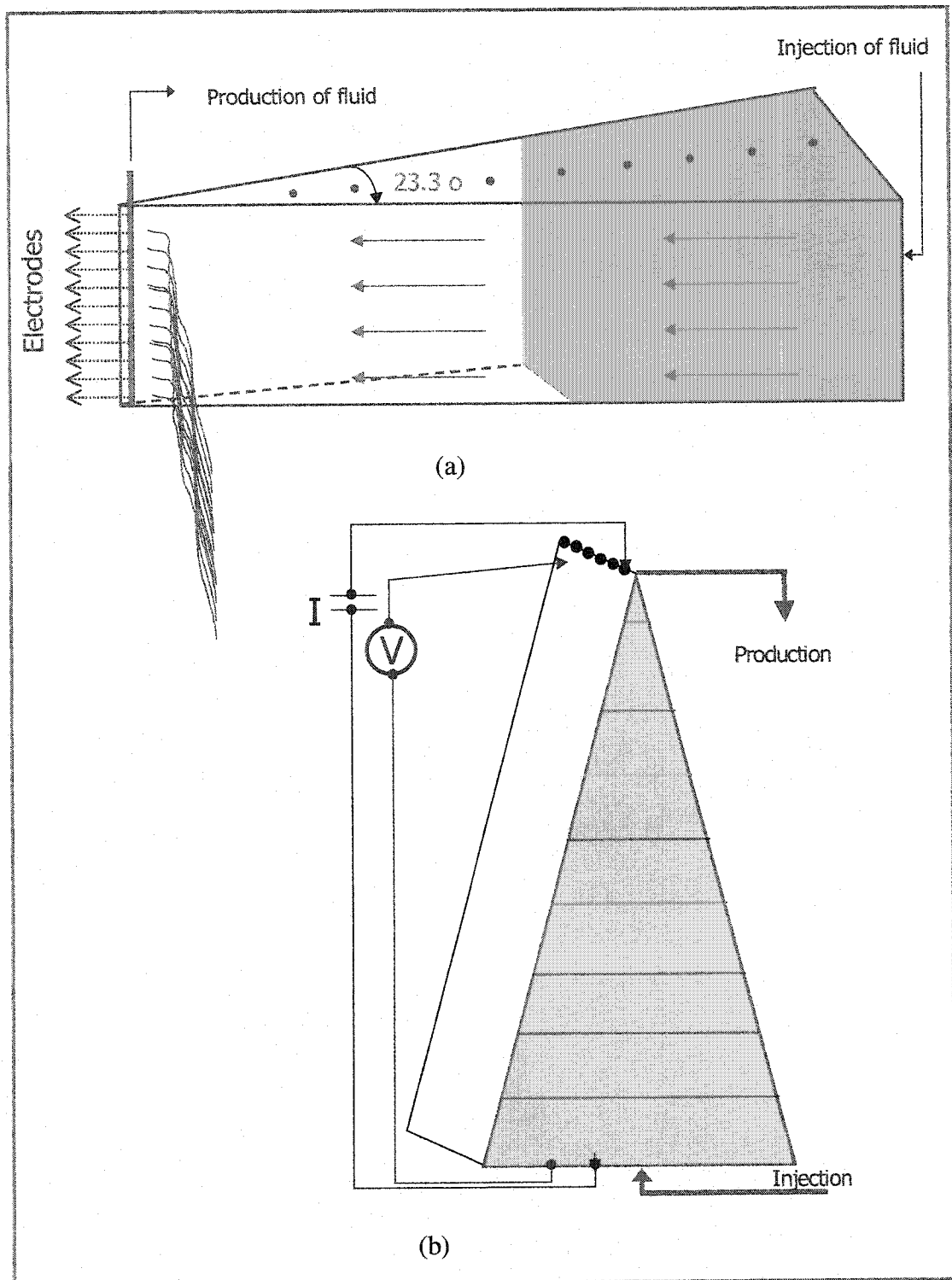
Figure 4.1.2: Schematic of (a) Sector Model, (b) Measurements with the Model Keeping at Vertical Position.
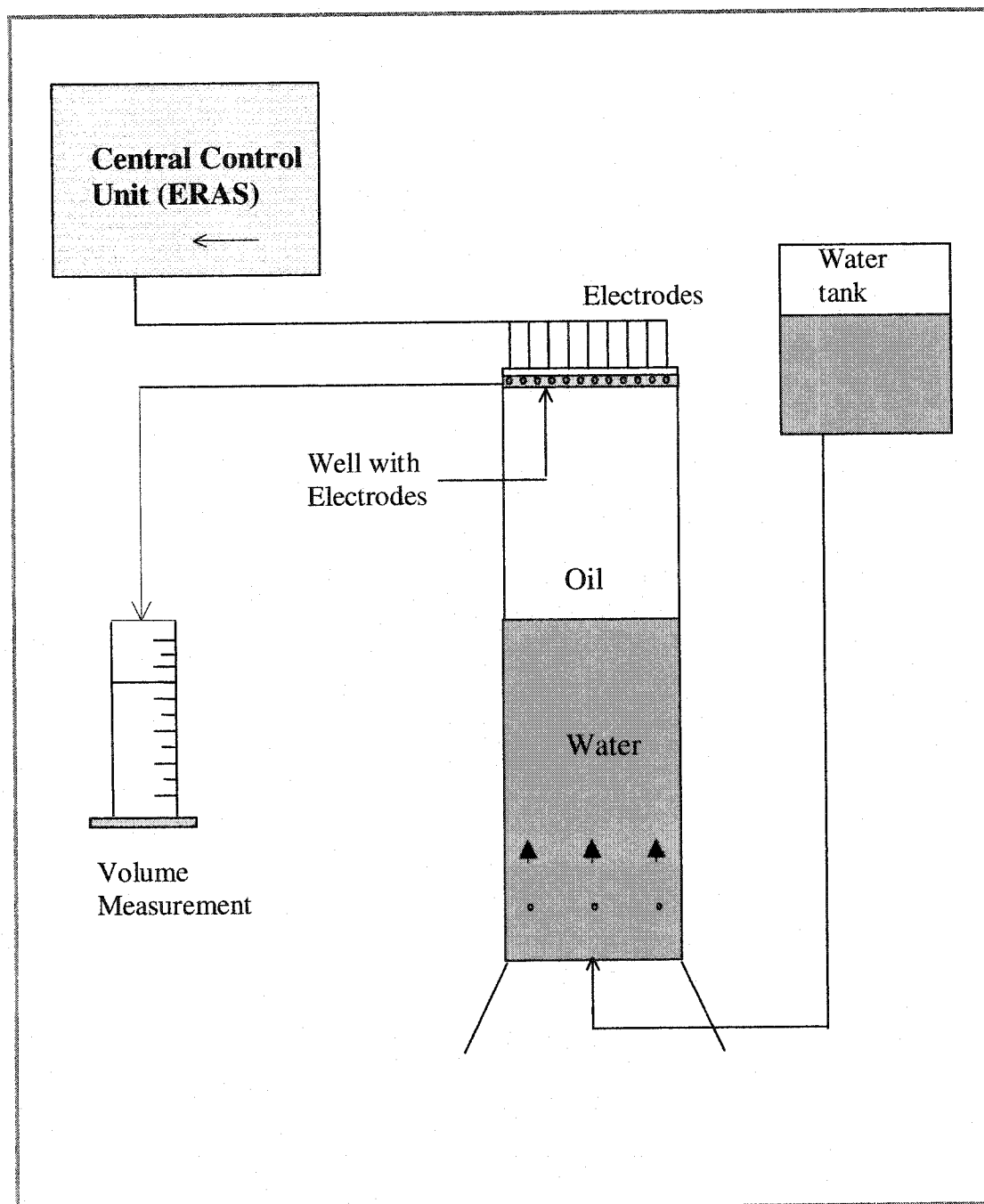
Figure 4.1.3: A Side View of Sector Model.

4.1.2   ONE DIMENSIONAL CYLINDRICAL MODEL

Another physical model, made of Plexiglas, was used for the following reasons:

1.   To establish experimental procedures and measurement conditions before attempting measurements on the sector model,

2.   To become familiar with resistivity behavior under different water salinity and oil combinations, and

3.   To study the maximum allowable resistivity for the fluid pair used to saturate the model with.

This one-D model was cylindrical in shape and fabricated with a plexiglas tube having an inner diameter of 3.98 cm and a length of 37.8 cm. The two ends of the cylinder were closed with Plexiglas plates and two sealed tubes were inserted into those plates with metallic connectors to allow fluid flow through the model. Eleven electrodes were inserted in the cylinder along its length and two others were connected at each end to inject current.   The electrodes were equally spaced (3 cm) along the model and the geometric factor of the cylindrical model is exactly determined. Numerous measurements were conducted using the cylindrical model to understand the change in resistivity and the experimental procedures.

The cylinder was packed in the same way as the sector model. Figure 4.1.4 is a schematic of the cylindrical model and the experimental setup.

(a) Cylindrical Model with ElectrodeS

Tank

Data acquisition system

(b)
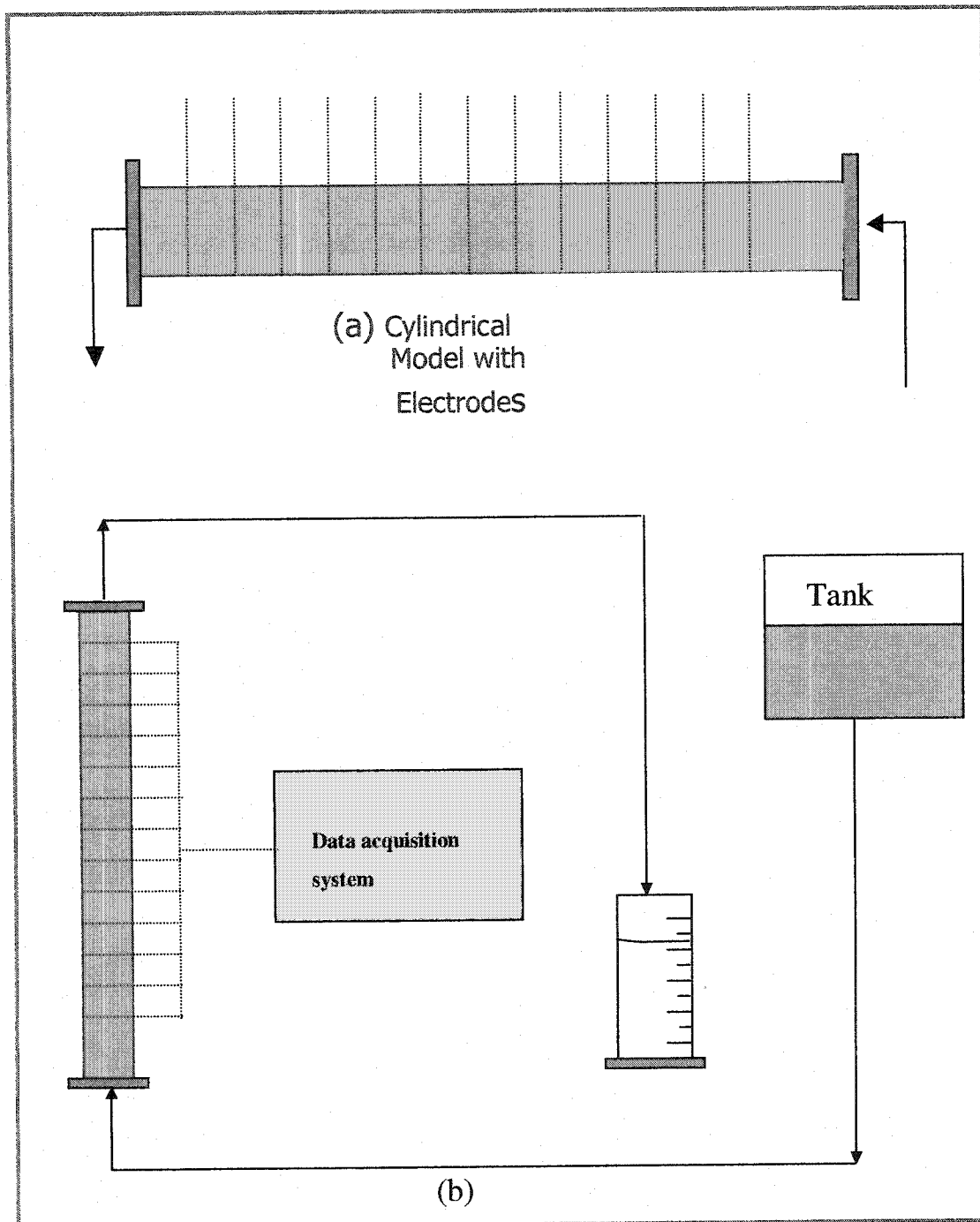
Figure 4.1.4: (a) Cylindrical Model with electrodes (b) Schematic of the

Cylindrical Model with Set-up.

4.1.3   ACQUISITION SYSTEM (ERAS)

The acquisition system is a general-purpose current injection and data acquisition system allowing the following:

- Injection of current between 2 electrodes (Max 2 A, 300V),

- Measurement of potentials, and

- Operation in a frequency band from 0.01 to 500 Hz

The system is controlled by a PC and can perform sequences of current injection and measurement between any combinations of electrodes.

The system was connected to a 110-volt line. Injection of current during the study was limited to 20 mA and the maximum voltage used was 300 V. All measurements were done at 10 Hz. At this frequency, the equation of DC approximation is valid and polarization effects of electrodes are avoided.   The shapes of measured potential and injected current are displayed together with the corresponding values during measurement sequences. This feature allows the detection of any error during measurement. The system was originally designed for actual field measurements. Acquisition sequences (defined as scenario) can contain infinite loops allowing continuous measurements. All the measurements can be stored in the database and can be monitored from anywhere at any time by remote access. The acquisition software is based on Labwindows/CVI. The Following components were required for the software configuration of the ERAS setup: Labwindows/CVI 5.5.1, NiVisa 2.01, Niswitch 1.5, IVI Engine 1.6 and NI-DAQ 6.9.

4.1.4 VACUUM PUMP

A Vacuum pump was used to evacuate the model. The pump has a vacuum pressure gauge ranging from a maximum pressure of 1200 mbar to a minimum of 0-mbar. The vacuum pump along with a fluid displacement pump was also used to saturate the model with fluids.

4.1.5 VOLUME MEASURING DEVICES

Graduated cylinders of various volumes were used to collect and determine the volumes of injected and produced fluids.

4.1.6 AUXILIARY EQUIPMENTS

The Fann Resistivity Meter (model 88c) was used to measure brine resistivity. The Terratek Resistivity Meter was also used for the resistivity measurement of the saturated porous media.

An MPH I-220 Helium Porosimeter was used to measure the porosity of the porous medium.

The Viscosities and densities of kerosene and brine were measured using a viscometer and a hydrometer, respectively.

A manual polyethylene sprayer pump was used to inject brine in the model when the flow rate achieved by gravity was very low. The sprayer pump was pressurized to 1 bar.

Fittings and valves, weighing balances, pressure gauges, a potentiometer, an ammeter, resistivity arrays, and a manometer were also used at different stages of the experiments.

4.1.7 NUMERICAL MODEL

A mathematical model developed by Schlumberger was validated and then used to analyze experimental data. The model can be used to simulate a reservoir with water movement in any direction after a little modification of the input file used to provide the required inputs for the model. The geometrical description of the reservoir is entered in cylindrical coordinates. Electrodes are located at the nodes of the grids. To get the potential distribution using the numerical model, it is necessary to define the position of the fluid front and also the resistivities of different fluid zones.

4.2   FLUIDS AND POROUS MEDIA USED

4.2.1   FLUIDS

Oil and brine were used to simulate zones of high and low resistivity. Due to a limitation of the acquisition system towards the high values of impedance, it was necessary to choose the water salinity and oil viscosity so that when brine was displaced with oil, residual brine saturation was high enough to generate conductivity that was within the limits of the acquisition system. At the beginning of this study, mineral oil with high viscosity represented the oil phase. When it was injected in the model, it displaced almost all the water from the porous media leaving a highly resistive zone behind, which exceeded the limits set for the acquisition system. Several combinations of oils were tested before selecting pure kerosene to represent the oil phase. Brine with a concentration of 200,000 ppm was used to represent the conductive medium. Green coloring was added to the brine to show the movement of the water phase in the model (Figure 4.2.1). The color was insoluble in kerosene and did not stain the porous media, which helped to distinguish the water phase from the oil phase (Figure 4.2.2). The specific gravity of kerosene used was 0.78 and viscosity was 1.27 cp, and the specific gravity of the brine was 1.154 (after the addition of color) and its viscosity was 1.67 cp. All the measurements were conducted at room temperature (about 24 degrees Celsius).

Figure 4.2.1: Photograph of Fluid Front as Seen From the Side of Sector Model (front view).
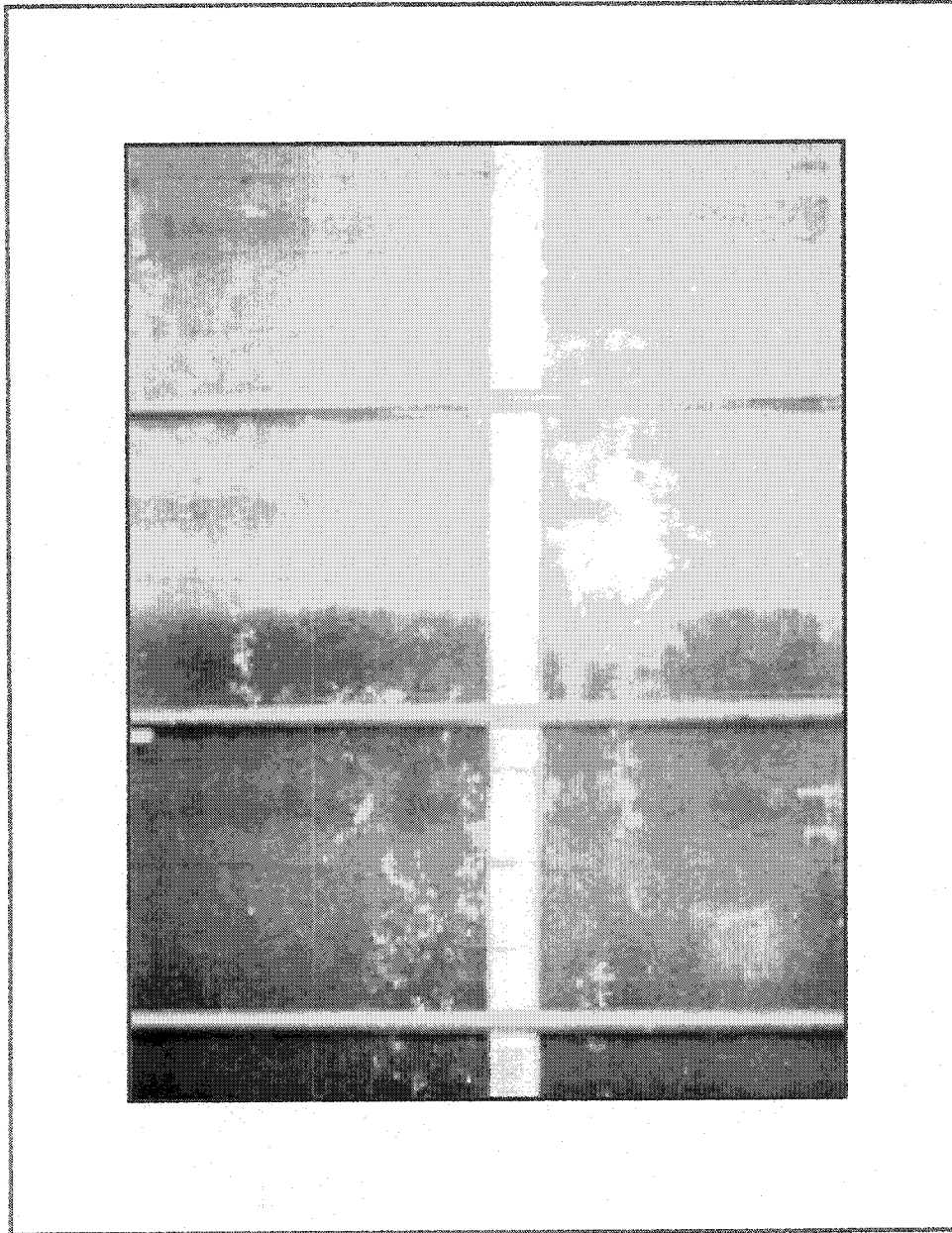
Figure 4.2.2: Photograph of Fluid Front as Seen From the Side of Sector Model (side view).

4.2.2 POROUS MEDIA

Glass beads were used to represent the porous media in the physical models. Only spherical beads that passed a 30-mesh screen and retained by a 40-mesh screen were used for this experiment. Good packing of the porous media was assured through the use of a large electric vibrator. After a few hours of continuous vibration, the level of the glass beads went down indicating compaction, after which more glass beads were added and vibration was continued. The total requirement of glass beads to fill the model was about ninety kg. After filling the model, the top cover was attached carefully to the bottom plate using nuts and bolts with screws to avoid any leaks (Figure 4.2.3).

Porosity and permeability were selected to cover the practical scaling criterion. The porosity measurement of the pack was based on the volumetric method, which involves the measurements of both bulk, and pore volume.

To measure the porosity of the glass beads pack, the measurement cup of the Helium Porosimeter was filled with the metal disks (the billets) and also with the glass beads and vibrated to compact the beads. The average porosity obtained from the Helium Porosimeter was 37.5%.

A tube packed with the same glass beads was used to measure permeability based on Darcy's law. The absolute permeability at 100% water saturation was 128 Darcys keeping the tube at horizontal position. A water manometer was used to achieve good accuracy in measuring the differential pressure for this high permeability.
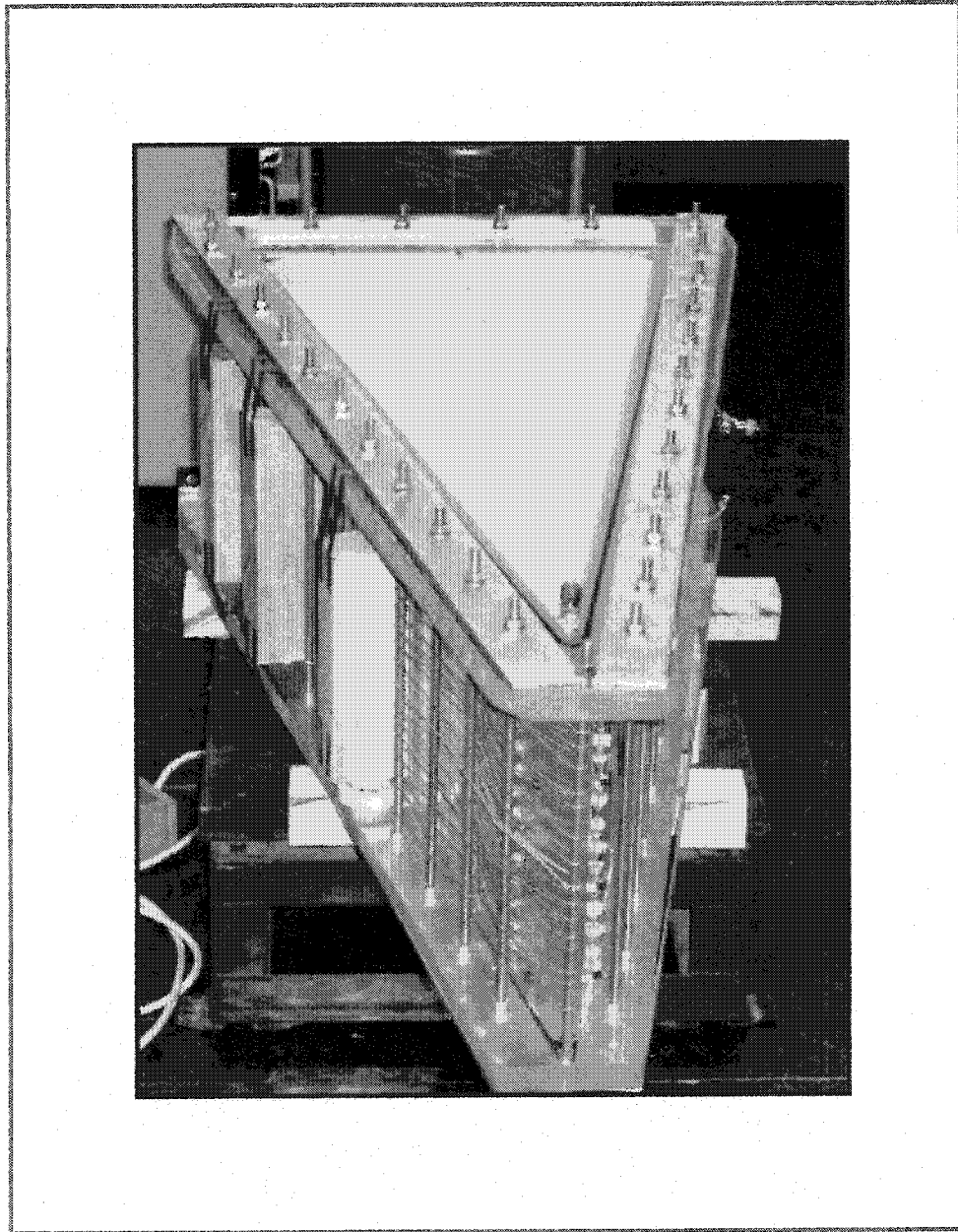
Figure 4.2.3: Photograph of Sector Model on the Vibrator.

4.3   EXPERIMENTAL PROCEDURES

4.3.1   PROCEDURES FOR THE CYLINDRICAL MODEL

The cylindrical model was used to select the best combination of oil-water to be used in the sector model to conduct the experiment. It was also used to measure the resistivity of the different fluid zones to use as an initial input for the numerical model.

In the cylindrical model, the two metallic connectors at each end were used as the current electrodes for measurements of resistance. Eleven electrodes, 3 cm apart were used for the measurement of potential drop, which is defined as a 4-point measurement (Figure 4.1.4).

The model was first filled with brine, which was replaced with kerosene to get the connate water saturation and again brine was injected from the bottom to get the residual oil saturation. The electrodes of the both arrays were connected to the central control unit with copper wires and used for measurements of potential drops for all the displacements. Resistances were measured to observe the movement of water in the model. Measured Resistances varied significantly with change in resistivity of oil saturated and brine saturated zones.
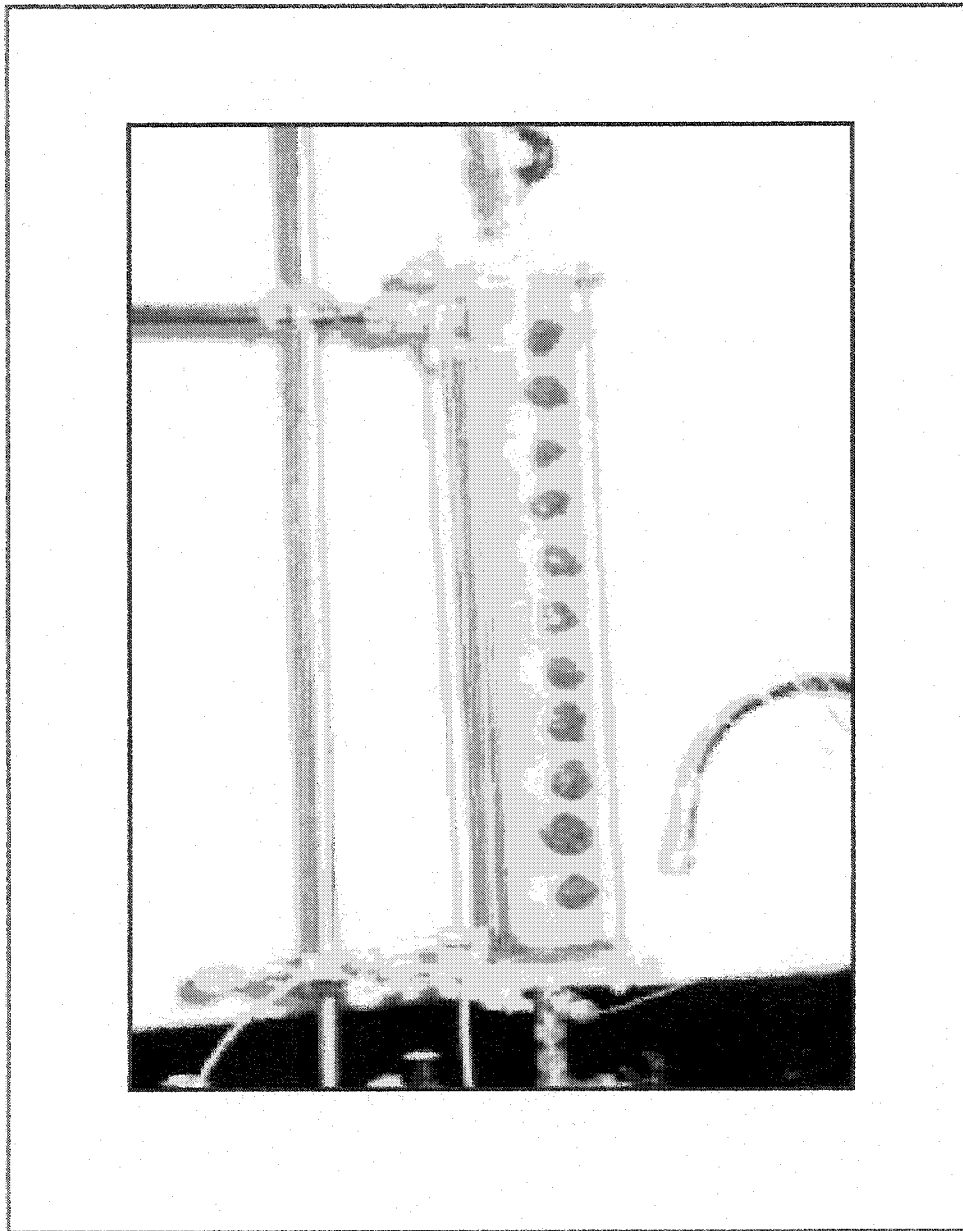
Figure 4.3.1: Photograph of Cylindrical Model With the Accessories.

4.3.2 PROCEDURES FOR THE SECTOR MODEL

The experimental procedures for the sector model were divided into two parts. Firstly, the experiment was conducted keeping the model in an upward position (the well and its electrodes remained at the top) as it is shown in Figure 4.3.2 and secondly, to simulate an injection well, keeping the model in an inverted position (the well and the electrodes remained at the bottom) as it is shown in Figure 4.3.3. The sharp end of the sector model did not allow appropriate compaction when the model was in the upright position. Due to low compaction, water saturation was locally very low, which increased the local resistivity and limited the injection of electric current when the model was saturated with oil at connate water saturation. So, the model was inverted to have a better contact of the electrodes with the porous media to improve the quality of the measurements. The experiment was divided into seven parts referred to as seven cases. The first two cases were conducted keeping the reservoir model in an upward position and the next three cases were conducted keeping it in an inverted position. The last two cases were conducted by tilting the radial model to an angle of 25 degrees from the vertical axis. Before starting the actual experiment, the physical properties of the model were measured to determine different parameters associated with the experiment and the resistivity measurement.
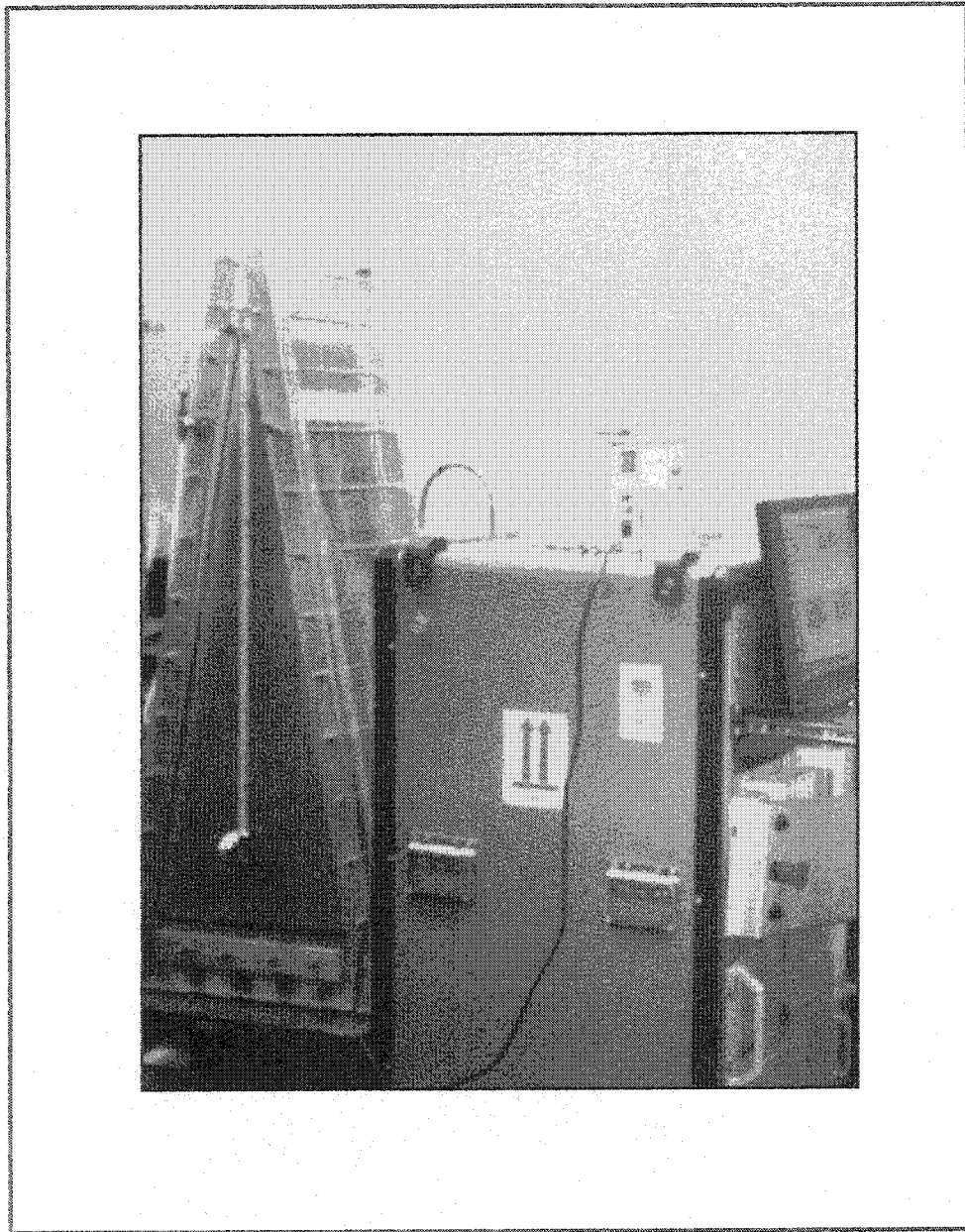
Figure 4.3.2: Photograph of the Sector Model With ERAS.

Figure 4.3.3: Photograph of Sector Model While Inverted.

For the first part of the experiment, the following procedures are applied:

4.3.2.1 MEASUREMENTS OF PHYSICAL PROPERTIES:

1. The sector model was cleaned properly and vibrated after filling to get a packing similar to a compact reservoir. Then, air was evacuated from the model for several hours until the vacuum pump read close to absolute zero pressure.

2. Brine with a concentration of 200 kppm was injected to saturate the pack until a steady state condition was reached. The total volume of brine required to fill the model was 22.3 liters.

3. The bulk volume of the sector model was calculated using the dimensions of the model before filling it with glass beads. The bulk volume of the model was 59.2 liters. Brine required to fill the pores of the triangular model was 22.3 liters from which the calculated porosity was 37.67%, which is close to the one obtained using the Helium Porosimeter (37.5%).

4. Kerosene was then injected into the water-saturated model until no more water production was observed. At this stage the connate water saturation was calculated. 20.6 liters of water were recovered at the end of injection in the model and the calculated connate water saturation was 8.04 percent.

5. Brine was again used to displace the kerosene from the model to calculate the residual oil saturation in the model. The amount of injected kerosene was 20.6

liters and recovered kerosene during displacement was 17.9 liters. So, the calculated residual oil saturation was 13.1 percent.

4.3.2.2 RESISTIVITY MEASUREMENTS

An array of electrodes was inserted in the main well and another set of electrodes was inserted later with two reference electrodes located on the surface to inject current and to measure the potential drops with respect to each of the array electrodes. Measurements were conducted using both sets of electrodes at different stages of kerosene injection in the model and also at different stages of kerosene displacement with water to facilitate the comparison of resistances obtained in the two situations, which helped to check the accuracy of resistance measurement. Two reference electrodes were placed at the other end of the sector model. Current was injected through the first electrode of each array (source electrode) with respect to one of the reference electrodes and the potential drop was measured using the other electrodes of the array with respect to the other reference electrode. Potential was measured between the reference electrode and only one electrode located in the array each time (Figure 4.3.4). The same resistance measurement procedure was repeated for the rest of electrodes.

A central control and acquisition unit, defined as Electrical Resistivity Array Software (ERAS), was used to facilitate the operation and control of the associated electrical equipment. The electrical current to the source electrode, return current potentials from the monitoring electrodes, and tuning of the signal generator, were all provided through

the control unit. ERAS consists: a signal generator module capable of providing a wide variety of frequencies and wave-forms, a digital multi-meter module, and an oscilloscope unit capable of monitoring two signals simultaneously--current signal and potential signal.

Another type of measurement was tried to detect the water front movement in the reservoir, defined as a 4-point measurement. For this case, the potential drop was measured between the last electrode and any other electrode of the same electrode array. The potential drops were then connected by isopotential lines on a map of the model reservoir to yield maps of the potential distributions within the reservoir. As there was a sufficiently large resistivity contrast between the hydrocarbons and water zones, the water front movement or water table rise caused a significant deflection in the isopotential lines indicating the advancement of the water front (Figure 4.3.5).
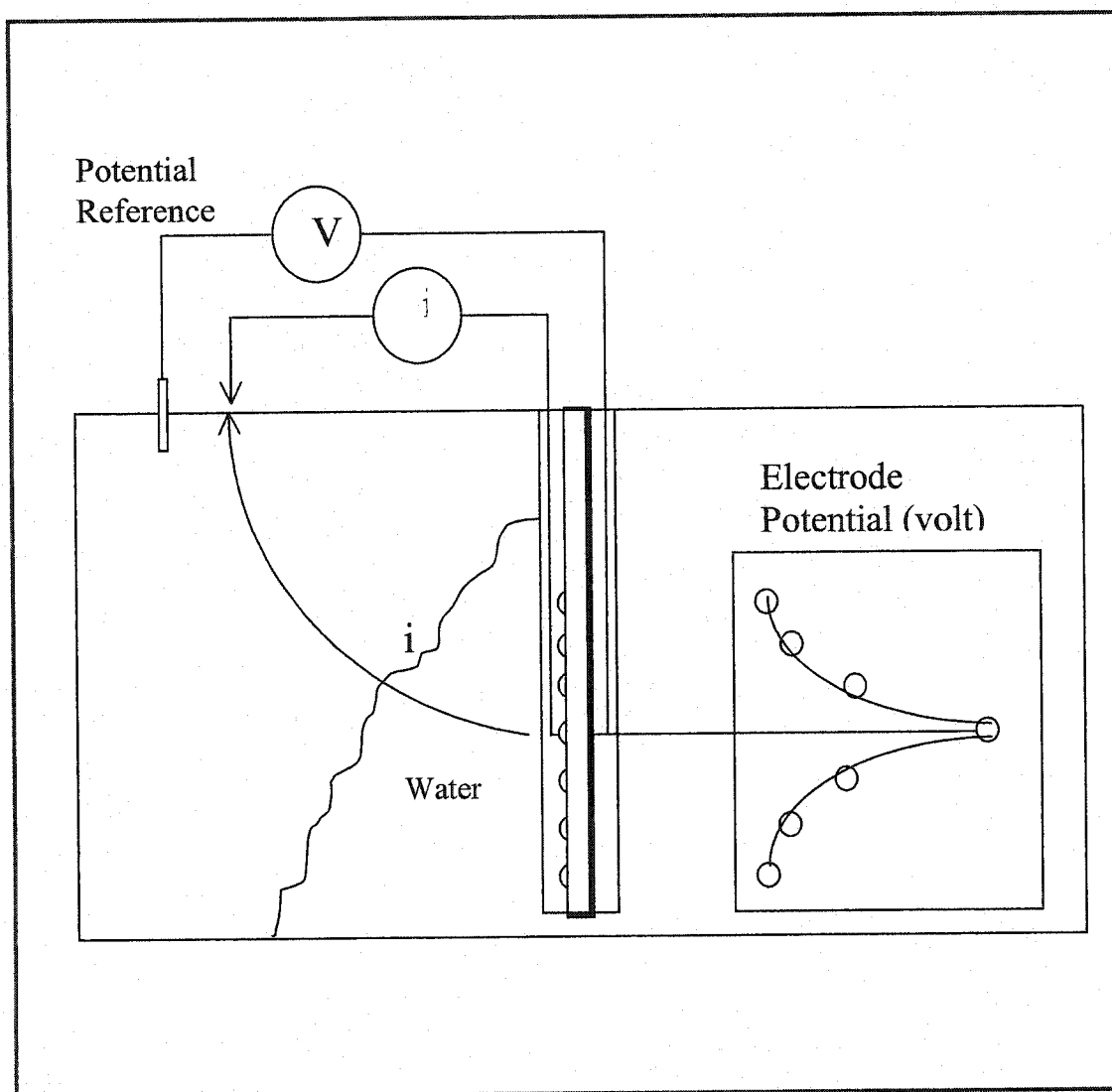
Figure 4.3.4: Measurements Using Array of Electrodes and Reference Electrode.
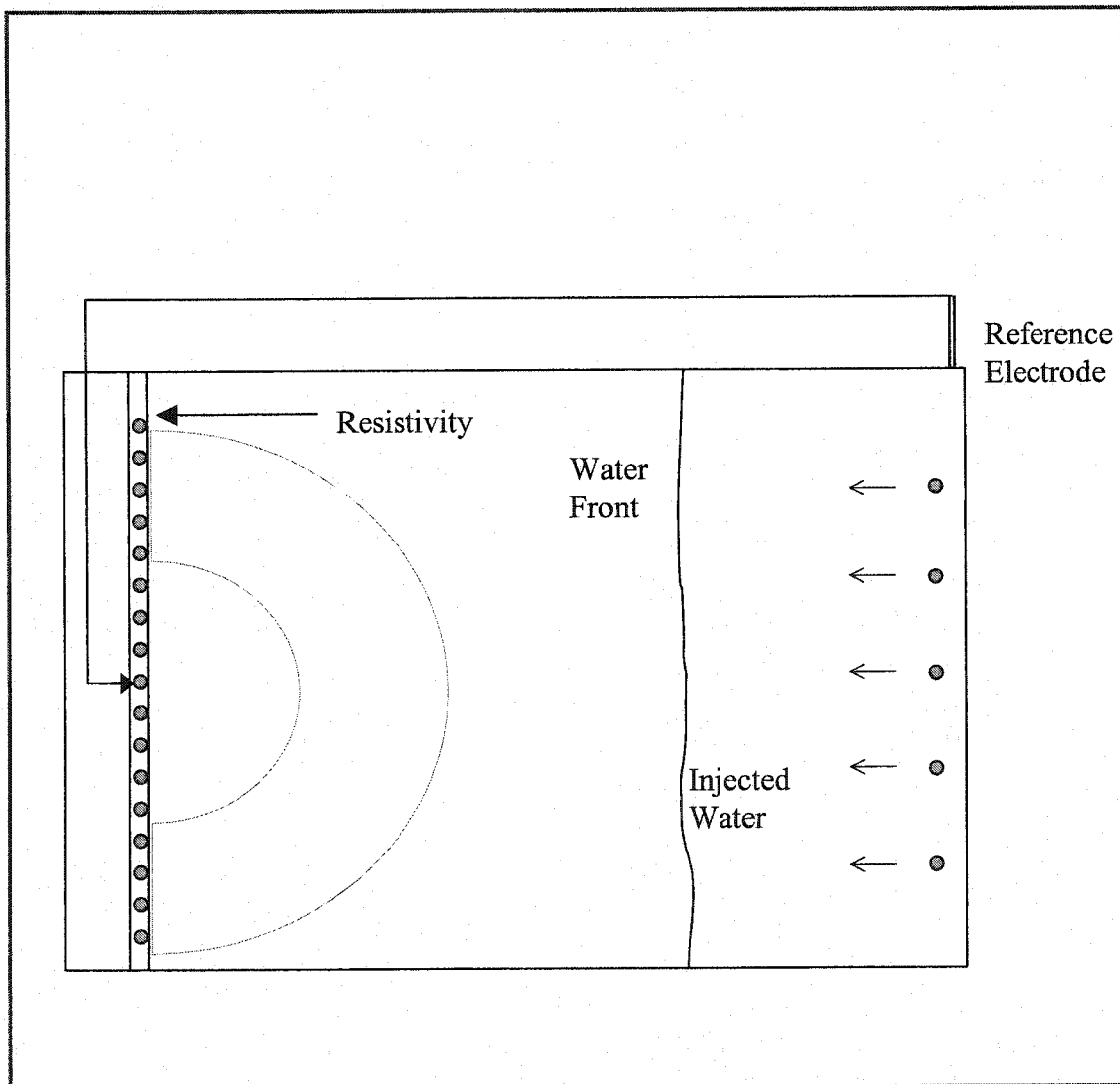
Figure 4.3.5: 4-point Measurement Without Reference Electrode.

4.4   ANALYSIS OF RESISTIVITY MEASUREMENTS

In the experiment, we obtained the potential drop knowing the position of the front. In practice, we are interested in the inverse problem: Can we deduce the position of the interface (resistivity distribution) from the potential distribution.

The classical procedure to solve the inverse problem can be described as follows:

Let F be the direct model allowing one to compute the distribution of potential in the reservoir for a given set of model parameters P (resistivity, position of electrodes).

Let F (P) = V (z), be the potential distribution and P_0 be an initial Potential distribution.

Neglecting second order terms we can write,

$$\left(\frac{dF}{dP}\right)_{p=p_o} = \frac{F(P)-F(P_o)}{P-P_o}$$ ....Equation 4.1

This can be re-written as:

$$\left(\frac{dF}{dP}\right)_{p=po} \times (P-P_o) = F(P) - F(P_o)$$ ....Equation 4.2

Where:

- P is the set of unknown parameters (resistivity distribution),

- P_0 is the initial guess of parameters, (known)

- F(P) are the measured potential, (known)

- F(P_0) are the calculated potentials for the initial set of parameters P_0 (known).

The term dF/dP, called the sensitivity matrix or Jacobien matrix expresses the sensitivity of the measurements to each parameter. Each term of this matrix can be computed using 2 runs of the direct model.

The equation has the form of $\underline{A}*\underline{X} = \underline{B}$. Where, $\underline{A}$ is the sensitivity matrix, $\underline{X}$ is the unknown vector of parameters and $\underline{B}$ is the vector expressing the difference between the measured and computed potentials. This matrix equation can be solved using classical techniques available in the literature (references 23 and 24). Detailed description of the solution is out of scope of this study.

Fortunately, in our simple case, the number of unknown parameters is only 1, and a trial and error procedure was sufficient to invert the problem.

The following procedure was used to determine the position of the fluid front from the potential measurements:

1. Run the simulation software with an approximate value of the front position.

2. Visualize the difference between the measured potentials and the computed ones.

3. Guess from the sign of the difference in which direction the front must be moved.

4. Run the simulation software with this new value.

5. Iterate the process (2) until the difference is below the measurement noise.

The resistivities of the fluid zones in the model were inserted as the inputs to the numerical model to obtain the apparent resistances for different front distances. To

calculate the resistivity of different fluid zones, the cylindrical model was used, and was packed using the same procedure to obtain the same reservoir characteristics.

For the second part of experiment with the sector model only, the displacement procedure was followed inverting the model in the opposite direction, as the physical properties were known earlier. The model was again flushed with brine (12 pore volumes of brine were circulated) to remove all the residual oil obtained from the previous oil injection and to get almost 100% brine saturation before inverting it for measurement of resistances from an injection well. The model was physically put upside down and the well was located in this case at the bottom along with the electrodes. The brine was displaced with kerosene to get the connate water saturation and, subsequently, brine was re-injected to displace the kerosene similar to the case of a water injection well. Again, (for only one case) the brine was displaced with kerosene similar to the case when water is produced from injection well to measure the relative permeabilities. Three sets of measurements (three cases) were conducted using the two sets of electrodes while displacing brine, oil and again brine.

Sensitivity of the numerical model to the movement of fluid and also to the change of resistivity of the fluid was calculated using different resistivity values for different fluid phases and also using different fluid front positions as the input for the numerical model.

Chapter 5

INTERPRETATION OF RESULTS

AND DISCUSSION

CHAPTER 5

INTERPRETATION OF RESULTS

AND DISCUSSION

5.1   EXPERIMENTAL RESULTS AND DISCUSSION

Experiments were conducted in the sector model and also in the 1D cylindrical model. The main experimental results were obtained using the sector model. The results obtained were used to validate the mathematical model.

5.1.1   CYLINDRICAL MODEL

Before starting experiments with the large sector model, it was necessary to observe the change in resistances due to changes in fluid content and to understand the measurements in a small model. The small cylindrical model was used to select the best combination of oil-water to be used in the sector model. The acquisition system used for this experiment had a limitation in measuring infinite resistance. So, there was a need to optimize the combination of fluids used in order to get the maximum resistivity contrast between the oil and water phase within the limit of the acquisition system. The cylindrical model was also used to get the resistances implied by different fluid phases.

Knowing the geometric factor for the cylinder, resistivities for different fluid phases were calculated from those resistance data and the resistivities were used in the numerical model as an input for the initial resistivities of different fluid phases in sector model.

Current was injected using the electrodes at each end of the cylinder and the electrodes mounted along the model were used to measure the resistance with respect to a reference electrode placed at the bottom of the model. The electrodes in the array were placed three centimeters apart and completely penetrated across the diameter of the media from one end to the other. Measurements were also conducted using pairs of electrodes while one fluid was injected in the model from one end and another fluid was produced from the end. As the geometric factor for the cylinder was known, resistivities for different fluid zones were calculated from the measurements. Several combinations of oil and water were used in the model before going for the selection of kerosene and 200,000 ppm brine for the experiment.

Measurements made with the cylindrical model greatly helped to understand the different factors controlling of the measurements and it was possible to correlate the position of the fluid front in the cylinder directly with the measurements. Those measurements were divided into two cases (Figure 5.1). At first (Case A), the cylinder was 100% saturated with brine and then oil was injected from the top to reach connate water saturation. In Case B, brine was injected from the bottom to simulate upward water-oil contact movement. In both cases, resistances were measured at different front positions and were shown in Figure 5.2 and 5.3, respectively.
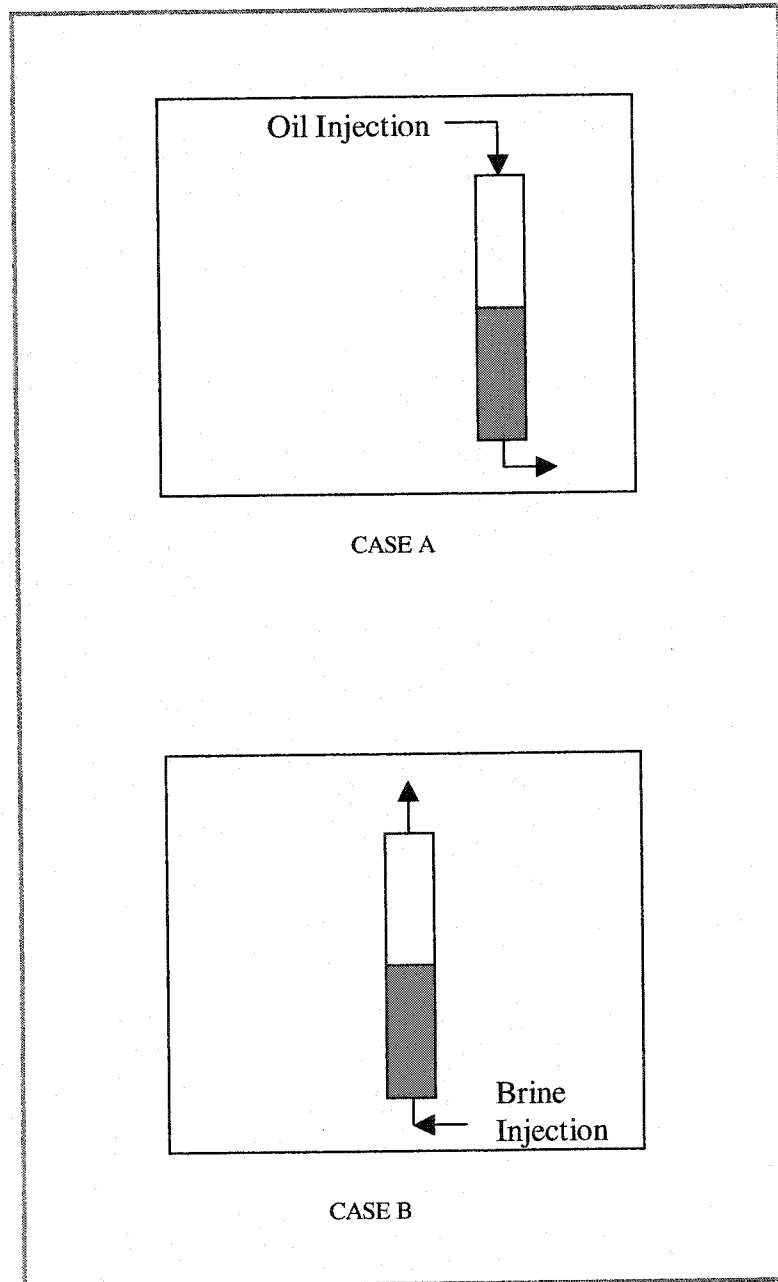
Figure 5.1: Block Diagram of Different Cases for the Cylindrical Model.

5.1.1.1 CASE A

Injection of Oil in the 100% Water-Saturated Cylindrical Model:

The objective of this run was to make a series of injections into the top of the brine saturated cylindrical model to reach connate water saturation. After each injection, time was allowed for the fluids to reach equilibrium and to clearly visualize the front. At each equilibrium stage, the resistances were measured.

Results obtained from this run are presented in figure 5.2. The inset at the top shows the oil-water interface at different positions relative to the potential electrodes in the cylinder. From the results obtained from this experiment, it was possible to correlate the behavior of resistance directly to the position of the front.

5.1.1.2 CASE B

Injection of Brine in the Cylindrical Model at Connate Water Saturation:

The objective of this run was to simulate water displacing the oil from the bottom of the cylinder to get the residual oil saturation. This kind of phenomenon is often observed in producing wells. The measurements gave an idea about the change in resistance due to water encroachment and also described the resistivity of the different fluid phases. Results are presented in figure 5.3. The inset shows different front positions in the cylinder for the measured data with the same color.
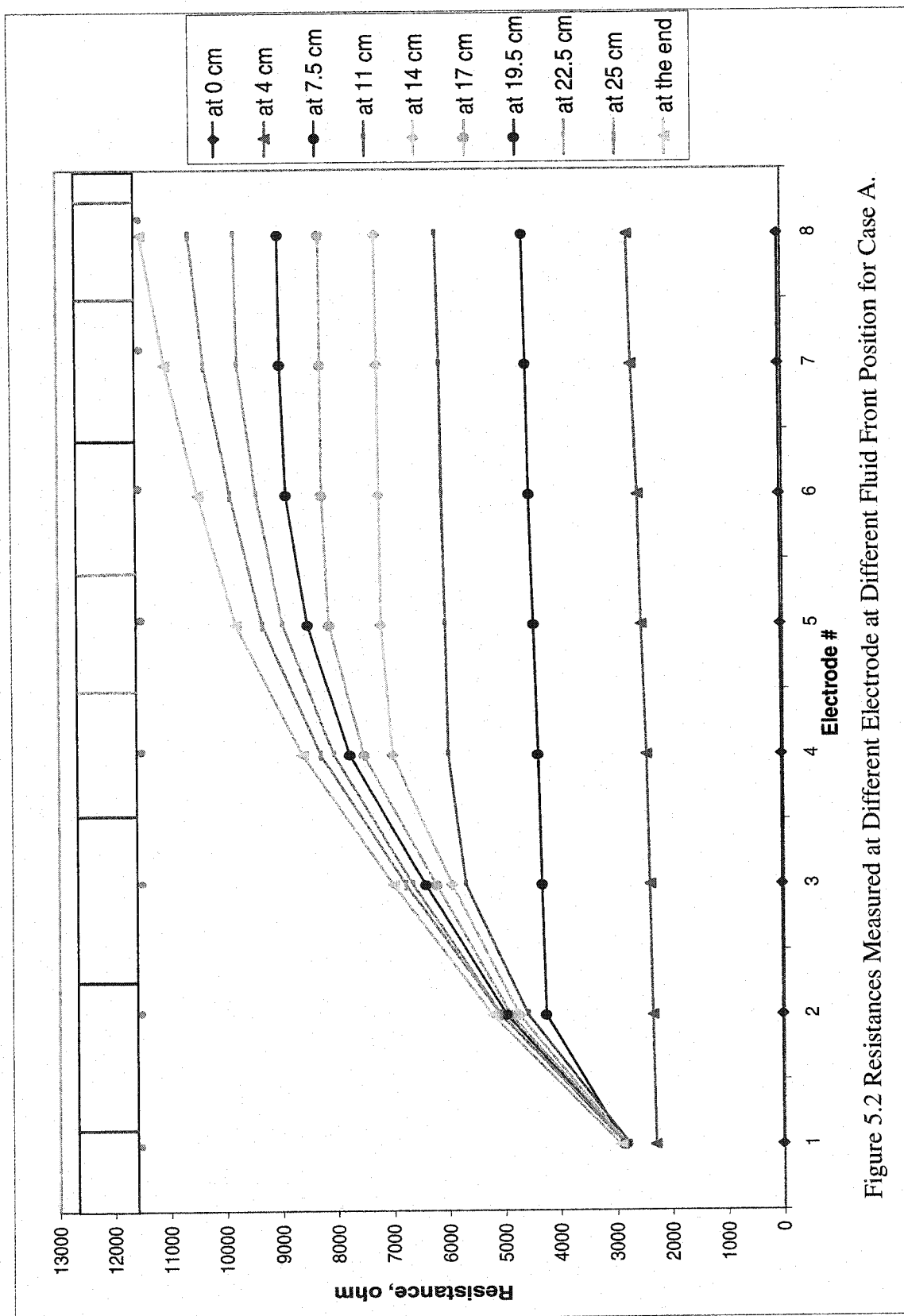
Figure 5.2 Resistances Measured at Different Electrode at Different Fluid Front Position for Case A.

Figure 5.3: Resistances Measured at Different Electrode at Different Fluid Front Position for Case B.
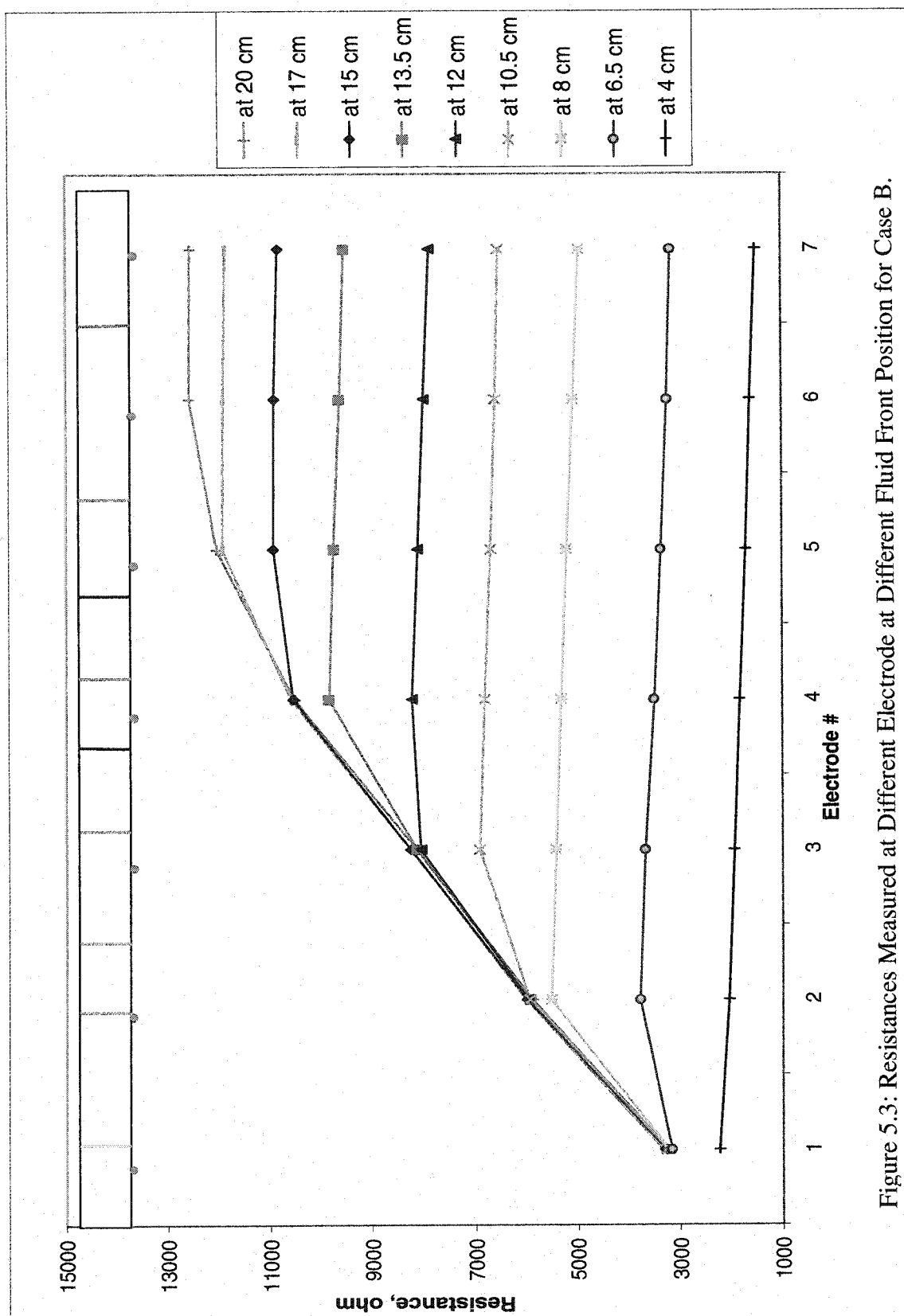
5.1.2 SECTOR MODEL

In the sector model, one set of electrodes was mounted on the main well to simulate the actual permanent downhole electrodes arrangement. That set contained 31 electrodes (1 cm apart from each other) and was defined as the first set of electrodes. However, to have a better control on the position of electrodes and due to contact problems with the porous medium, a new set of electrodes was inserted in the porous medium in a line parallel to the well and at a distance of 1.5 cm from the well. This set was defined as the second set of electrodes and it contained 18 electrodes (1.5 cm apart from each other). Experiments were conducted in the model using both sets of electrodes. In each set, the first electrode was used as the current injection electrode and the others were used for resistance / potential drop measurement. Initially, the model was kept in a vertical position (sharp end with the well and the electrodes are at the top) and the injection of fluids and measurements of resistance were conducted in the model as it is done for an oil producing well in a reservoir. Later, the model was kept in an inverted vertical position (sharp end with the well and electrodes at the bottom) to have a more compacted porous media in the vicinity of the electrode arrays. Measurements made in this condition represented the measurements from an injection well in the reservoir. Also, experiments were conducted keeping the model in an inclined position (25 degree-angle from the vertical axis) to observe the effect of front orientation on the measurements. For an easy understanding of all the measurements made in different measurement conditions, the

experiments were divided into seven cases. Those seven different cases are shown in figure 5.4 and 5.5. The cases are summarized below:

1. **Case 1**: Injection of oil in the brine-saturated model from the top keeping the sharp end at the top to obtain connate water saturation for a producing well.

2. **Case 2**: Injection of brine in the oil-saturated model from the bottom keeping the sharp end at the top to obtain residual oil saturation, which will represent water encroachment to an oil producer.

3. **Case 3**: Injection of oil from the top in the brine-saturated model keeping the sharp end at the bottom to obtain connate water saturation for an injection well.

4. **Case 4**: Injection of brine in the oil-saturated model from the bottom keeping the sharp end with the electrodes at the bottom to obtain residual oil saturation, which represents a brine injection well.

5. **Case 5**: Re-injection of oil from the top in the brine injected model with residual oil keeping the electrodes at the bottom. This represents the injection well used to calculate the relative or end point effective permeability of both the brine and oil bearing media in the vicinity of the injection well.

6. **Case 6**: Injection of oil from the top in the brine-saturated model keeping the sharp end at the bottom when the model was tilted at an angle of 25 degrees to the vertical axis to obtain connate water saturation.

7. **Case 7**: Injection of brine from the bottom in the oil-saturated (at connate water saturation) model to obtain residual oil saturation when the model was in the tilted position as in case 6.

While conducting the experiments, there were some errors introduced due to the displacement of electrodes in the first set of electrodes. From the Theory of Electricity Flow, it is known that the potential drop is inversely proportional to the distance from the current injection source and the same proportion was found for error calculation. Calculated error was found to be maximum for the closest electrode to the current injection electrode and decreased with distance. It was the minimum for the furthest electrode from the current injection electrode. For a 2 mm displacement of the electrode in the sector model, the error in measurement was more that 40 percent for the first electrode and it decreased to 1.2 percent for the farthest electrode.

Accordingly, it was decided to exclude all the results from the analysis with an error of more than two percent. So, measurements made with the first 13 electrodes of the first set were excluded from the analysis and the other 18 electrodes were used to compare with the numerical ones. The behavior of error introduced for a displacement of 2 mm is shown in figure 5.6.
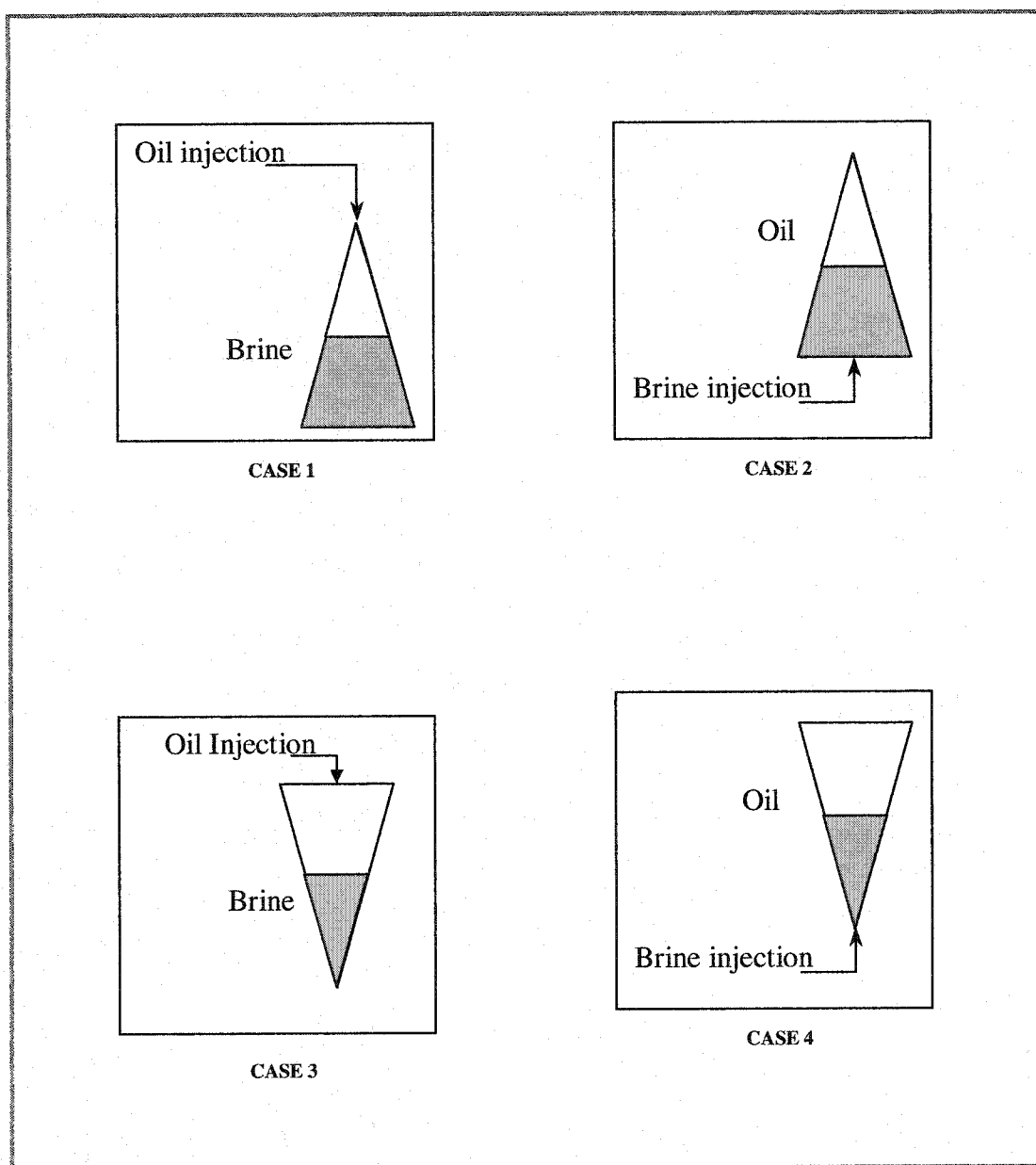
Figure 5.4: Cross-sectional Schematic for Cases 1 to 4.
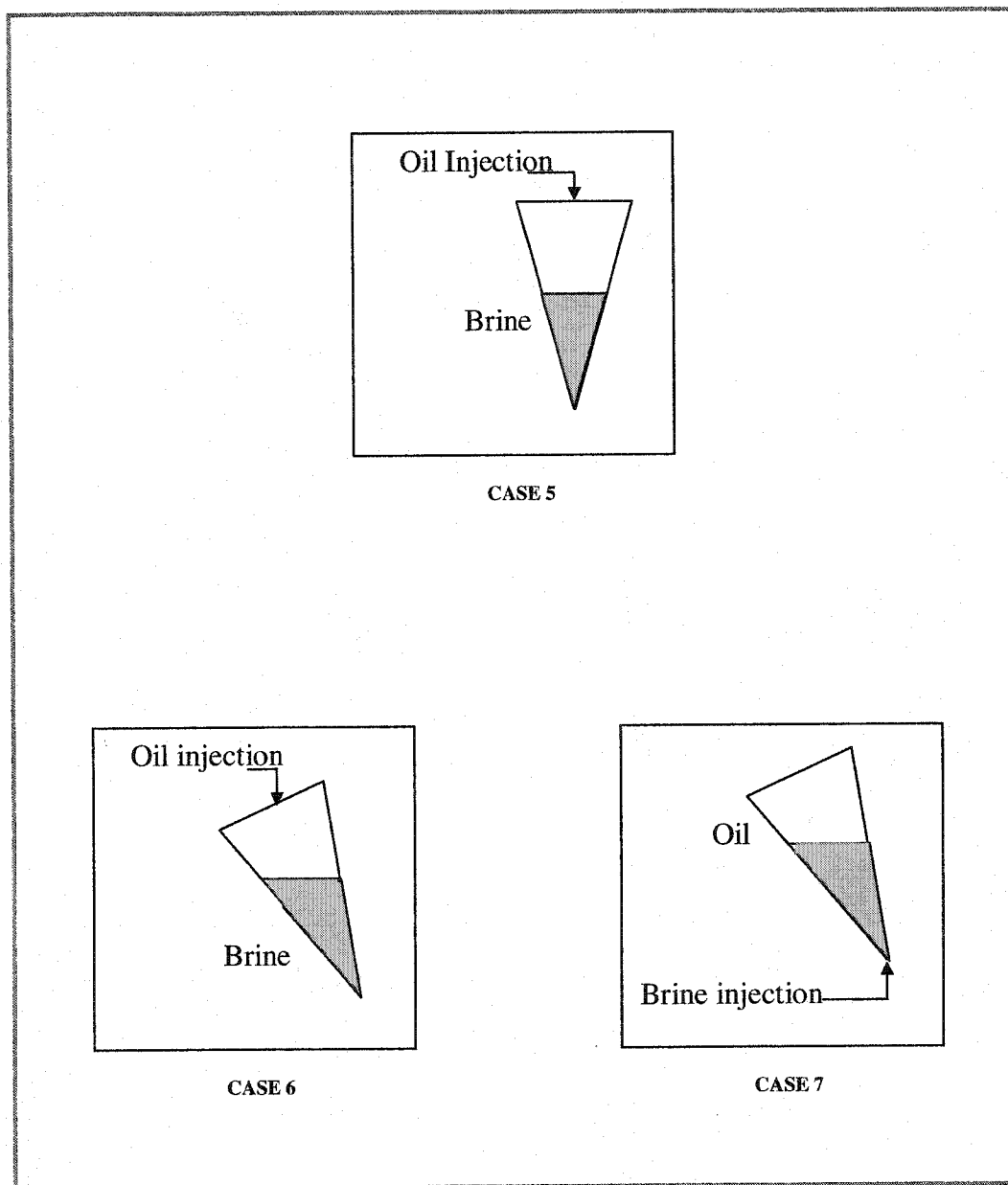
Figure 5.5: Cross-sectional Schematic for Cases 5 to 7.
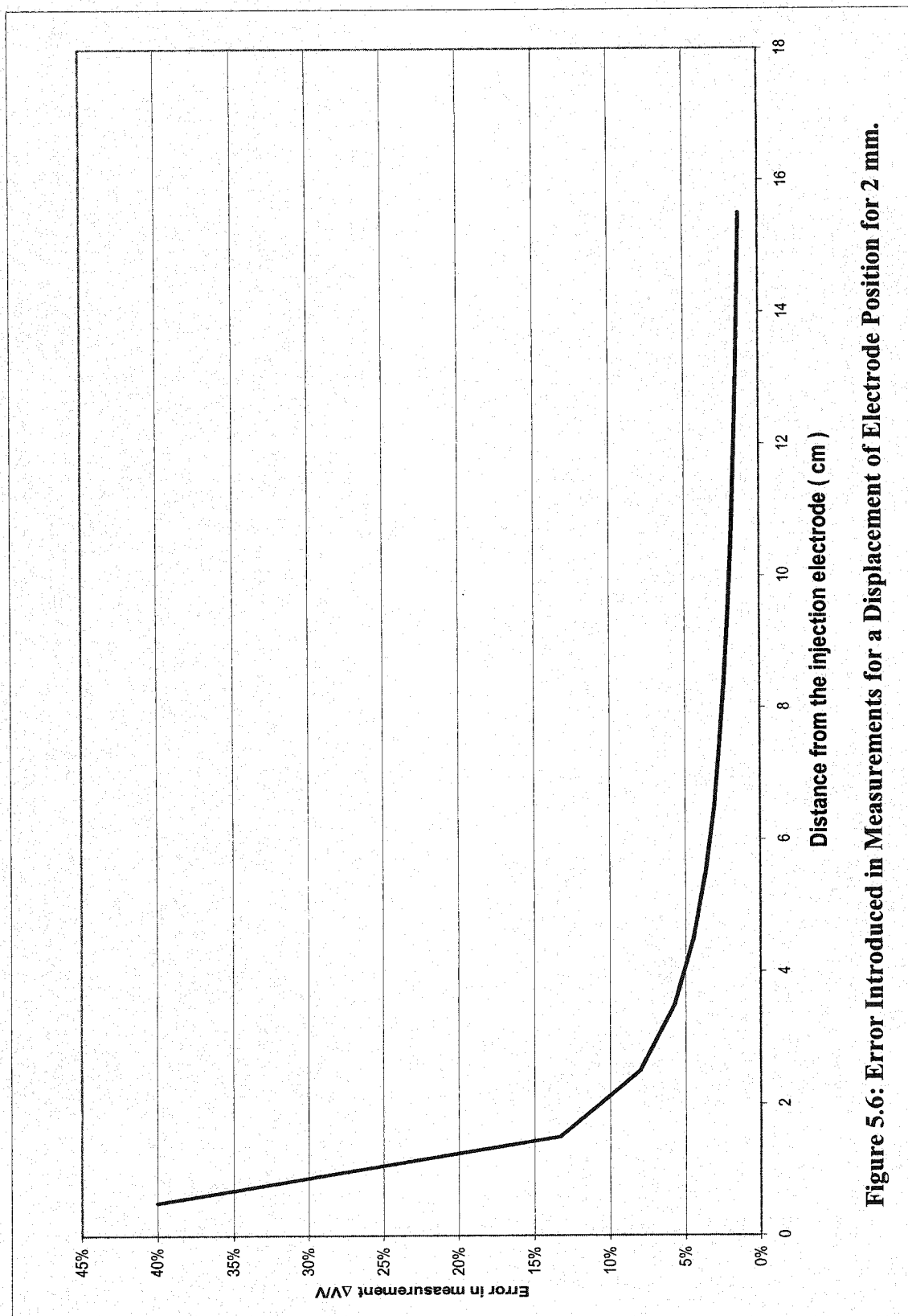
Figure 5.6: Error Introduced in Measurements for a Displacement of Electrode Position for 2 mm.

5.1.2.1 CASE 1

Injection of Oil in the

Brine-Saturated Model:

Oil injection
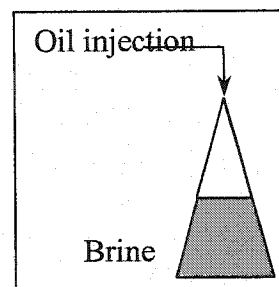
Brine

CASE 1

At the beginning, the model was 100% saturated with brine with a concentration of 200,000 ppm. Oil was injected to displace the brine and to obtain connate water saturation. Oil was injected in the model in stages with an equilibrium time of about 30 minutes between each injection stage. After visual detection of the oil-water interface at the end of each equilibrium stage, resistances were measured using the ERAS system. A 0.02-ampere current was supplied between the first electrode of the array in the well and the reference electrode at the other end (surface) of the model. Resistances were measured at each of the potential electrodes of both of the arrays with respect to the other reference electrode.

To complete each set of measurements, almost 7 minutes were required. As indicated earlier and due to contact problems, the electrodes of the first set were not in good contact with the porous media. Accordingly, there were some errors introduced in the measurements of the first electrode, especially with those electrodes that were very close to the injection electrode. The measurements of such electrodes were excluded from the analysis.

After displacing water with oil, connate water saturation was calculated to be 8.04 percent. The water, which was produced, was collected to calculate the connate water saturation. The measurements at different front positions are plotted and presented in Figure 5.1.1 for the first set of electrodes (Case 1-a) and in Figure 5.1.2 for the second set of electrodes (Case 1-b). The first set of electrodes was not able to measure properly the change in resistance due to change in fluid content as the front approached a distance of 70 cm from the current injection electrode. The fluid front was not clearly detectable further than that distance using the first set of electrode. This might be due to the improper contact between the porous media and the first set of electrodes.

66
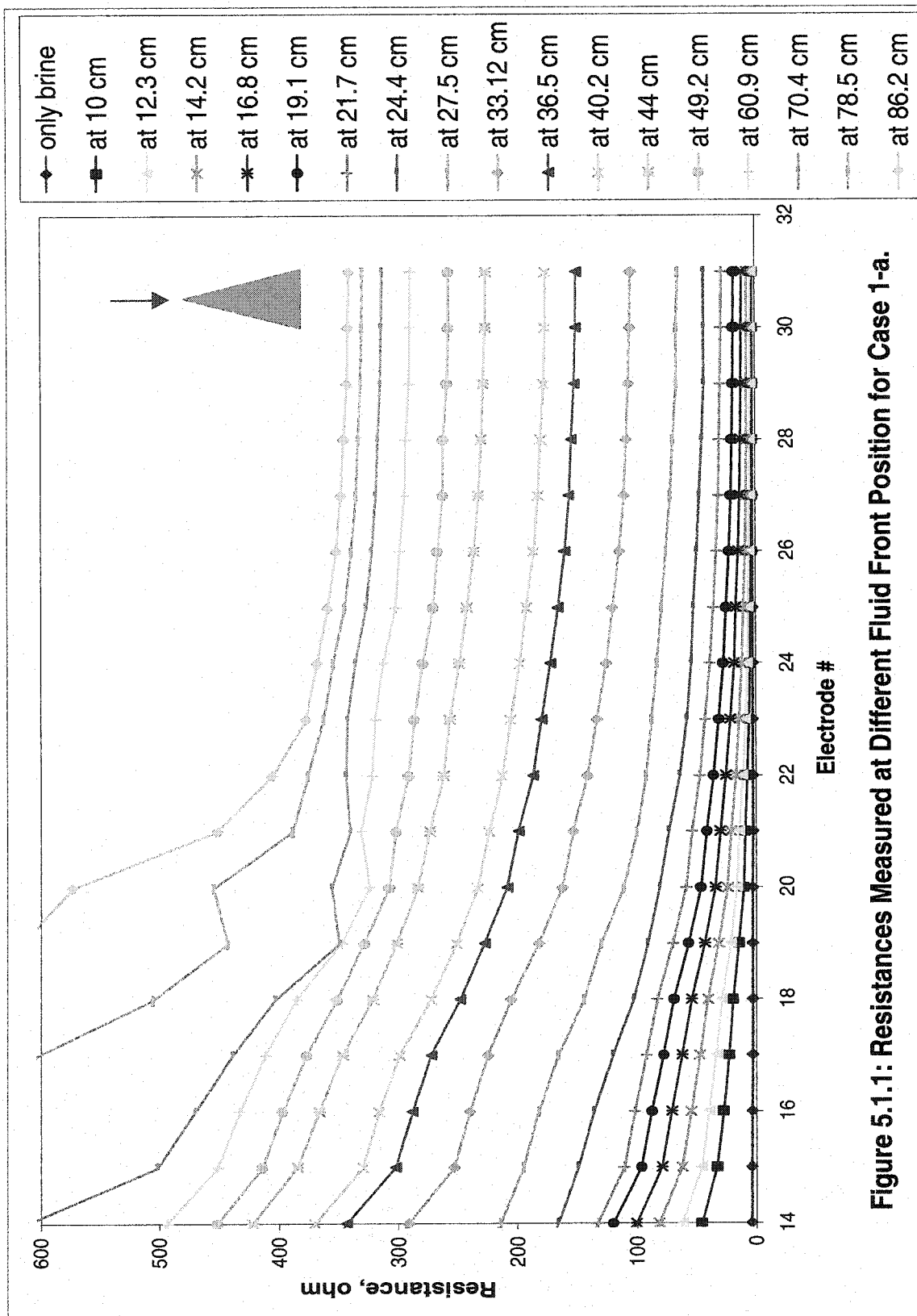
Figure 5.1.1: Resistances Measured at Different Fluid Front Position for Case 1-a.
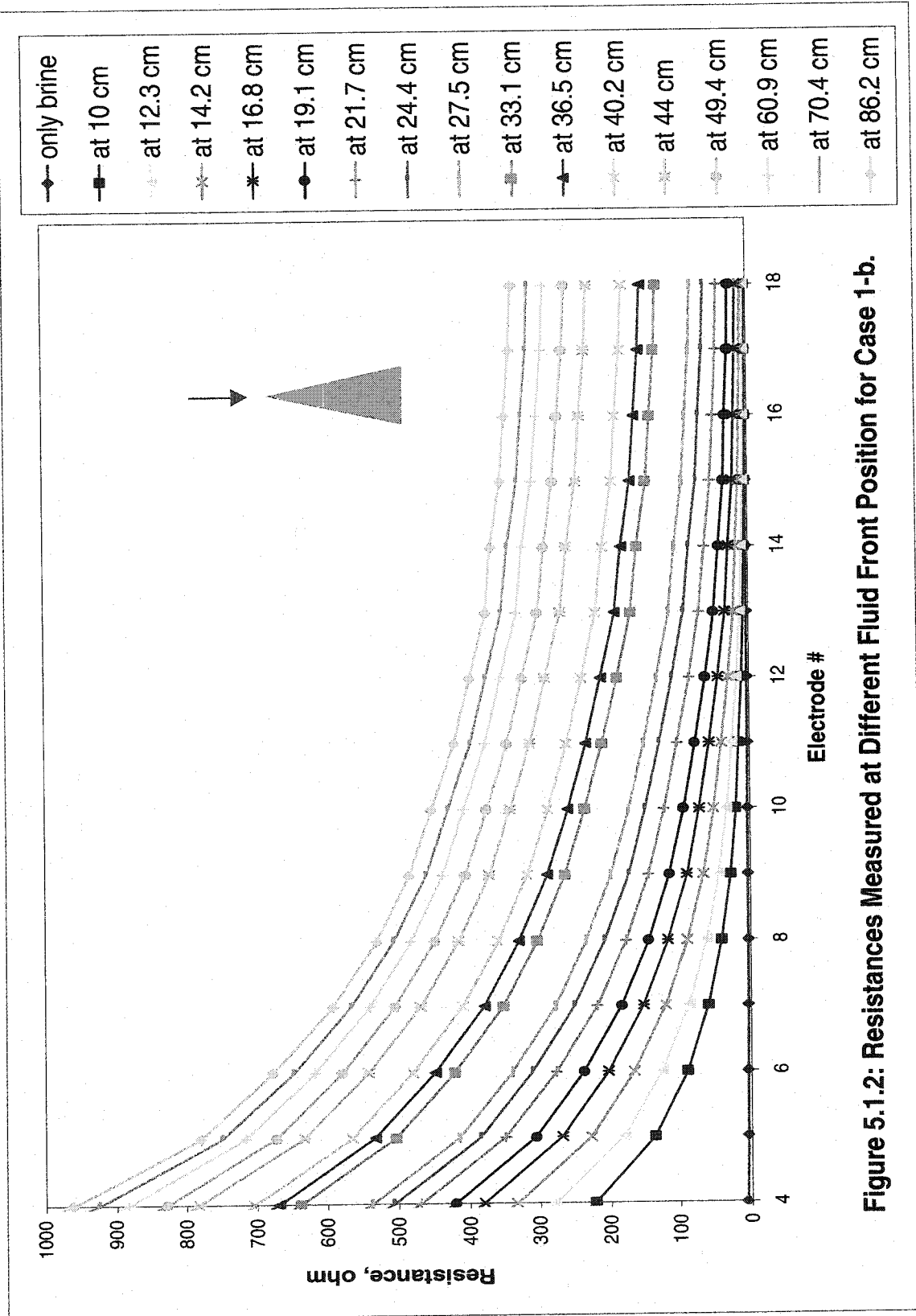
Figure 5.1.2: Resistances Measured at Different Fluid Front Position for Case 1-b.

5.1.2.2 CASE 2

Injection of Brine in the

Oil-Saturated Model:
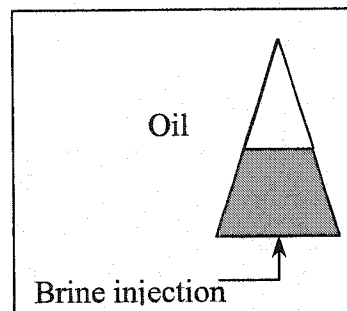
CASE 2

The model at this stage simulates a radial reservoir with a uniform porosity and permeability surrounded with an aquifer, which is producing oil using the producer at the center. In this case, brine was injected from the bottom of the reservoir model. Produced oil was measured to calculate residual oil saturation in the reservoir model at the end of the displacement.

As the waterfront approached the well, resistances were measured at different oil-water interfaces (water front) using both sets of electrodes. The potential drop was the maximum at the closest distances, and measurements were always erratic in the vicinity of the injection electrode (specially with the first set of electrodes). Measurements made with the electrodes too close to the injection electrode were excluded from the presentation.

Measurements were plotted and presented in Figure 5.1.3 for the first set of electrodes (Case 2-a) and in Figure 5.1.4 for the second set of electrodes (case 2-b). In both cases, erroneous measurements of the closer electrodes were excluded.

At the end of the run (Case 2) the calculated residual oil saturation was about 13.1 percent. Although the residual oil saturation was not constant all over the model due to the significant gravity force acting on the fluid, it was assumed to be uniform throughout the model.

Figure 5.1.3: Resistances Measured at Different Fluid Front Position for Case 2-a
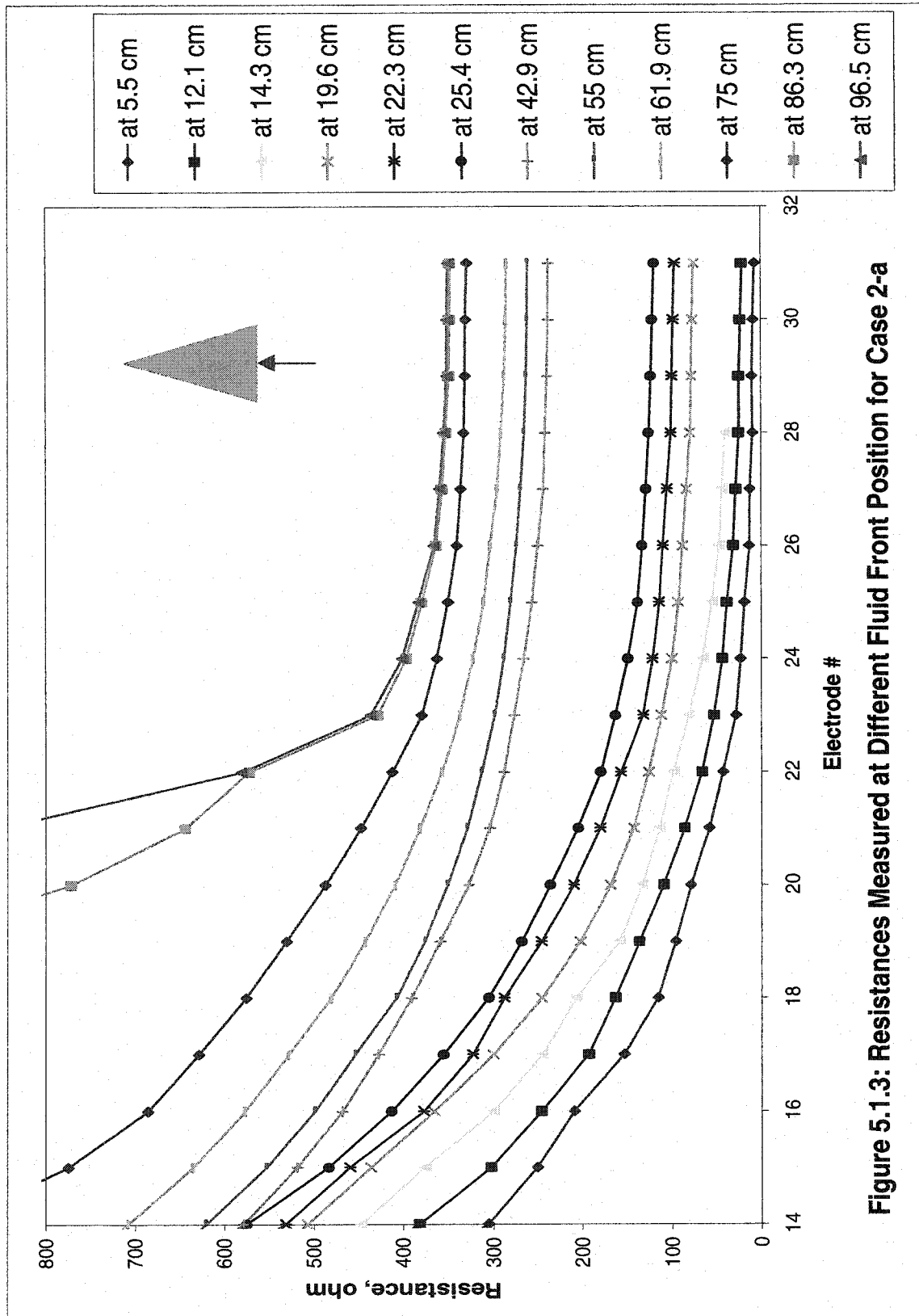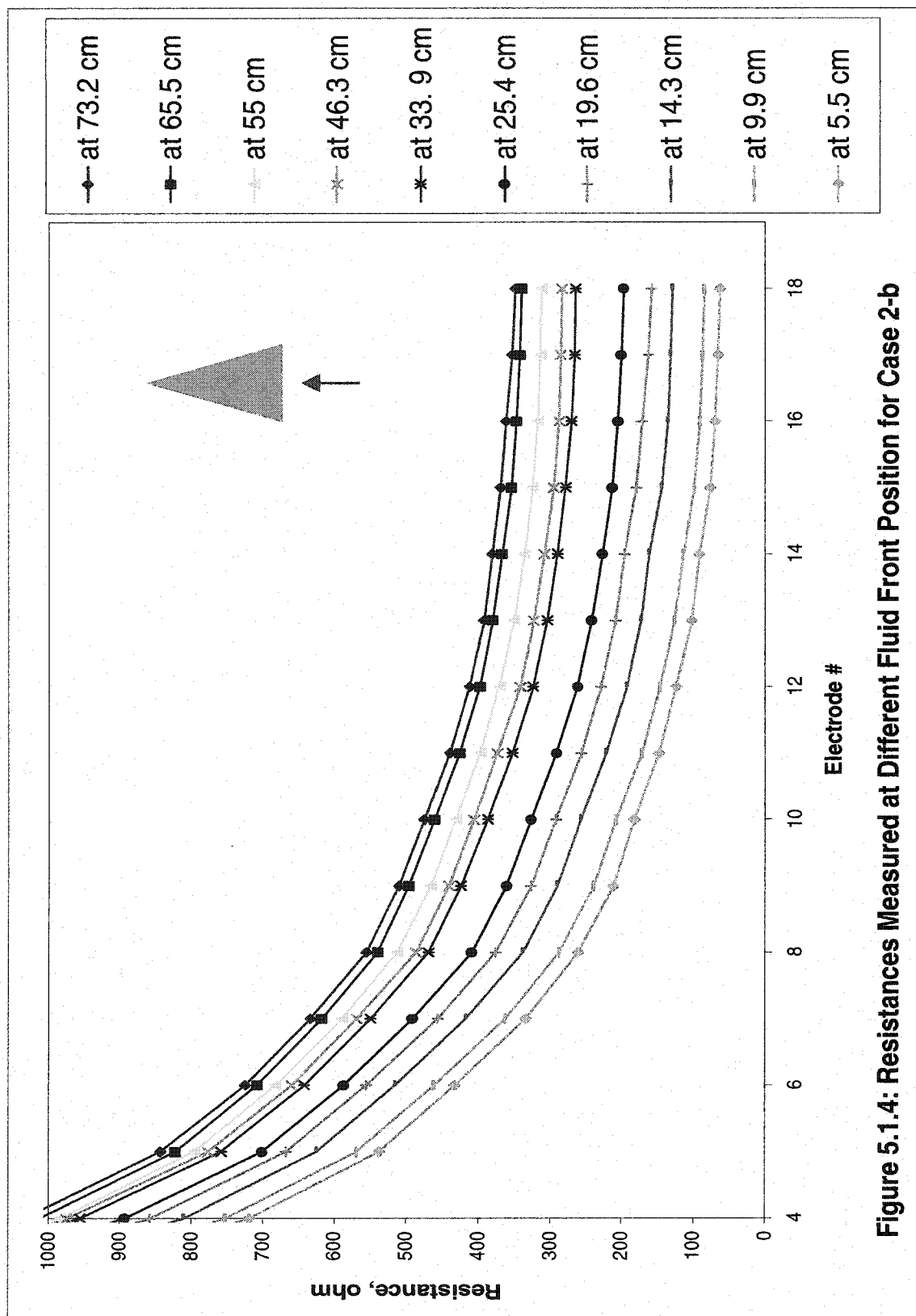
Figure 5.1.4: Resistances Measured at Different Fluid Front Position for Case 2-b

Legend:
- at 73.2 cm
- at 65.5 cm
- at 55 cm
- at 46.3 cm
- at 33. 9 cm
- at 25.4 cm
- at 19.6 cm
- at 14.3 cm
- at 9.9 cm
- at 5.5 cm

X-axis: Electrode #
Y-axis: Resistance, ohm

5.1.2.3 CASE 3

Injection of Oil in the

Brine-Saturated Model:

Oil Injection

Brine
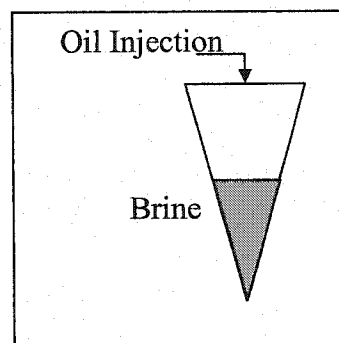
CASE 3

In this case, the reservoir model was vertically inverted with the well and electrodes at the bottom to get a more compacted porous media in the vicinity of the electrode arrays and to improve the measurements. Measurements conducted in this condition are completely different than those conducted in the previous cases as the environment of measurement is completely different.

Before starting the experiment, the model was flushed several times with brine at a high circulation rate to reduce residual oil saturation to the minimum. The circulation of brine was continued until no oil droplets were observed in the effluent. Almost 12 pore volumes of brine were needed to make the model almost fully water-saturated. The circulation rate was about 2-liters/ minute.

To obtain connate-water saturation, oil was injected in the model and resistances were measured using both sets of electrodes at different oil-water interfaces as it was done in Case 1. But here the electrodes were immersed in the water phase, which is just opposite

to the situation in Case 1. Therefore, resistances measured in case 3 were very low compared to that of Case 1.

These measurements were far better than the measurements in Cases 1 and 2 as the main well was at the bottom and the electrodes mounted on the well were in good contact with the porous media. It was also easier to simulate the results obtained by all the electrodes, including the ones closer to the injection electrode as the injected current was very low in the brine media compared to when the electrodes were immersed mostly in the oil zone.

The results obtained are plotted in Figure 5.1.5 for the first set of electrodes (Case 3-a) and in Figure 5.1.6 for second set of electrodes (Case 3-b). It should be noticed here that the measurement condition for case 3 was completely different than that of Case 1 or Case 2. In Case 1 and Case 2, both of the sets of electrodes were immersed in the oil phase for most of the time and the change of potential was very high for each cm of fluid movement due to the high resistance of the oil zone. But for Case 3 and for the later cases the electrodes were immersed in conductive media and the change in potential due to fluid movement was completely different. So, for Case 1 and Case 3, there was a big difference in measurement conditions and measurements for one case are not comparable with the other. For the same reason, measurements made by ERAS in this case were faster than before.

Figure 5.1.5: Resistances Measured at Different Fluid Front Positions for Case 3-a.
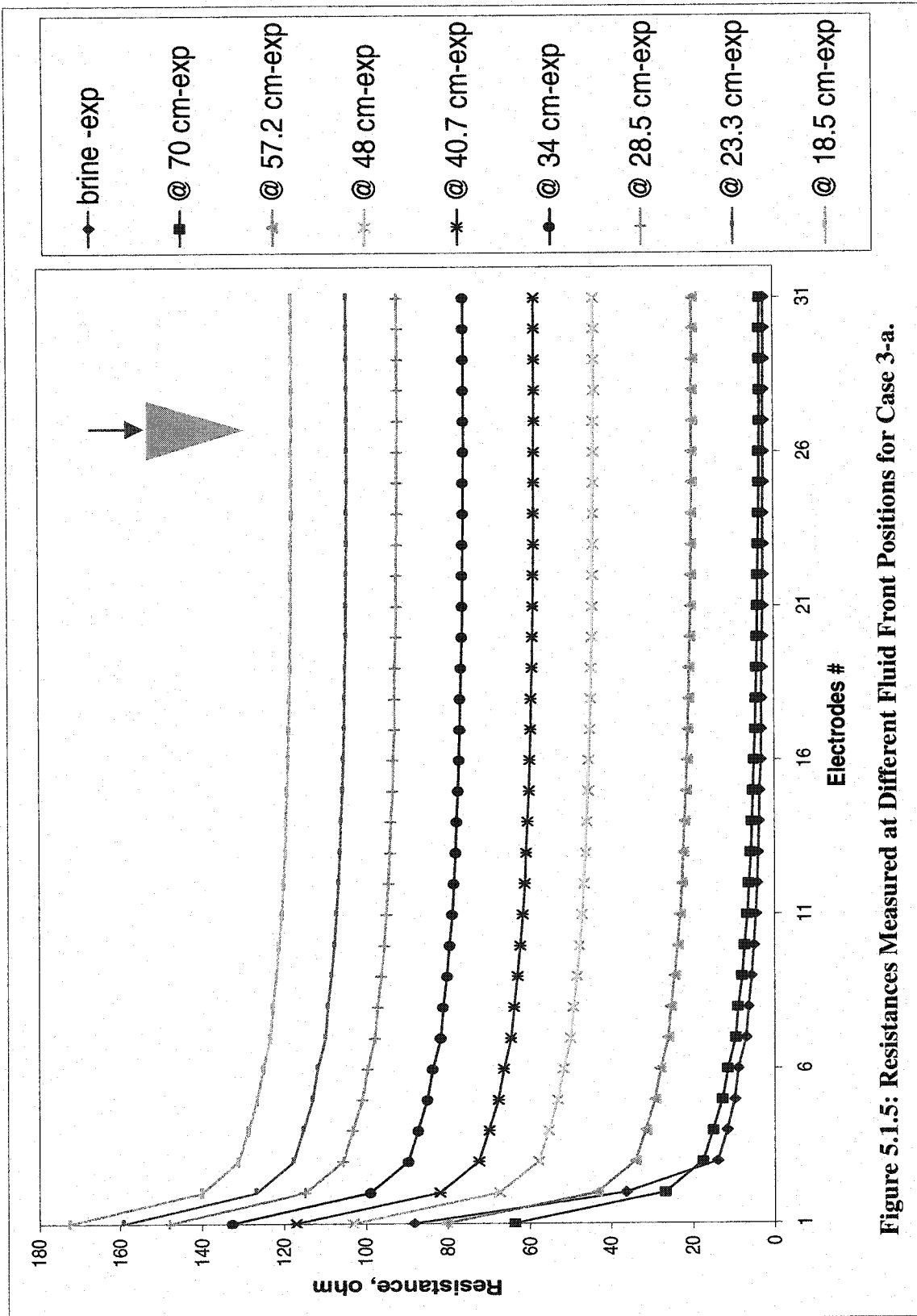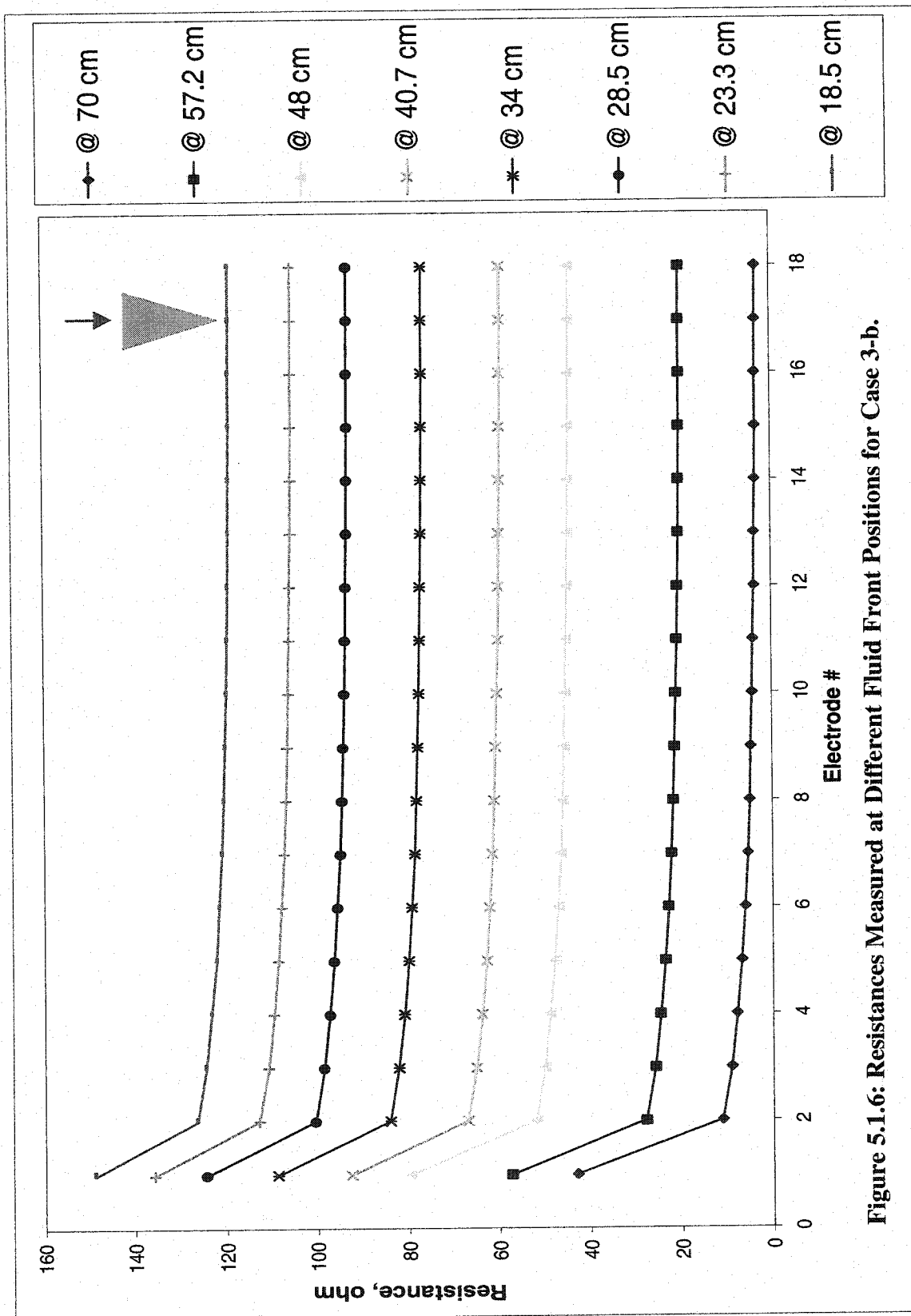
Figure 5.1.6: Resistances Measured at Different Fluid Front Positions for Case 3-b.

75

5.1.2.4 CASE 4

Injection of Brine in the

Oil-Saturated Model
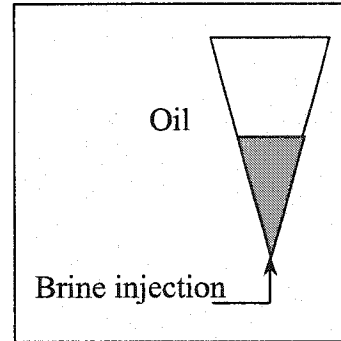
CASE 4

This case started with the model at connate-water saturation. Brine was injected from the bottom to displace oil as it is done in an injection well. This run was conducted to monitor the change in resistances due to the advancement of the injection fluid. Obviously, mention that the measurement condition for this case is also completely different from that of Case 1 or Case 2.

The experiment was continued until residual oil saturation was obtained. Measurements conducted during this run were also faster using the ERAS system, as it was in Case 3.

The resistivity data were plotted in Figure 5.1.7 for the first set of electrodes in the well (Case 4-a) and in Figure 5.1.8 for the second set of electrodes (Case 4-b). If the measurements are compared with those obtained from case 2, it is found that the slope of the lines connecting each measurement point by each electrode are different for the two cases. This difference is also related to the measurement environment, as in case 4 the measurement environment is facing very low impedance compared to case 2.
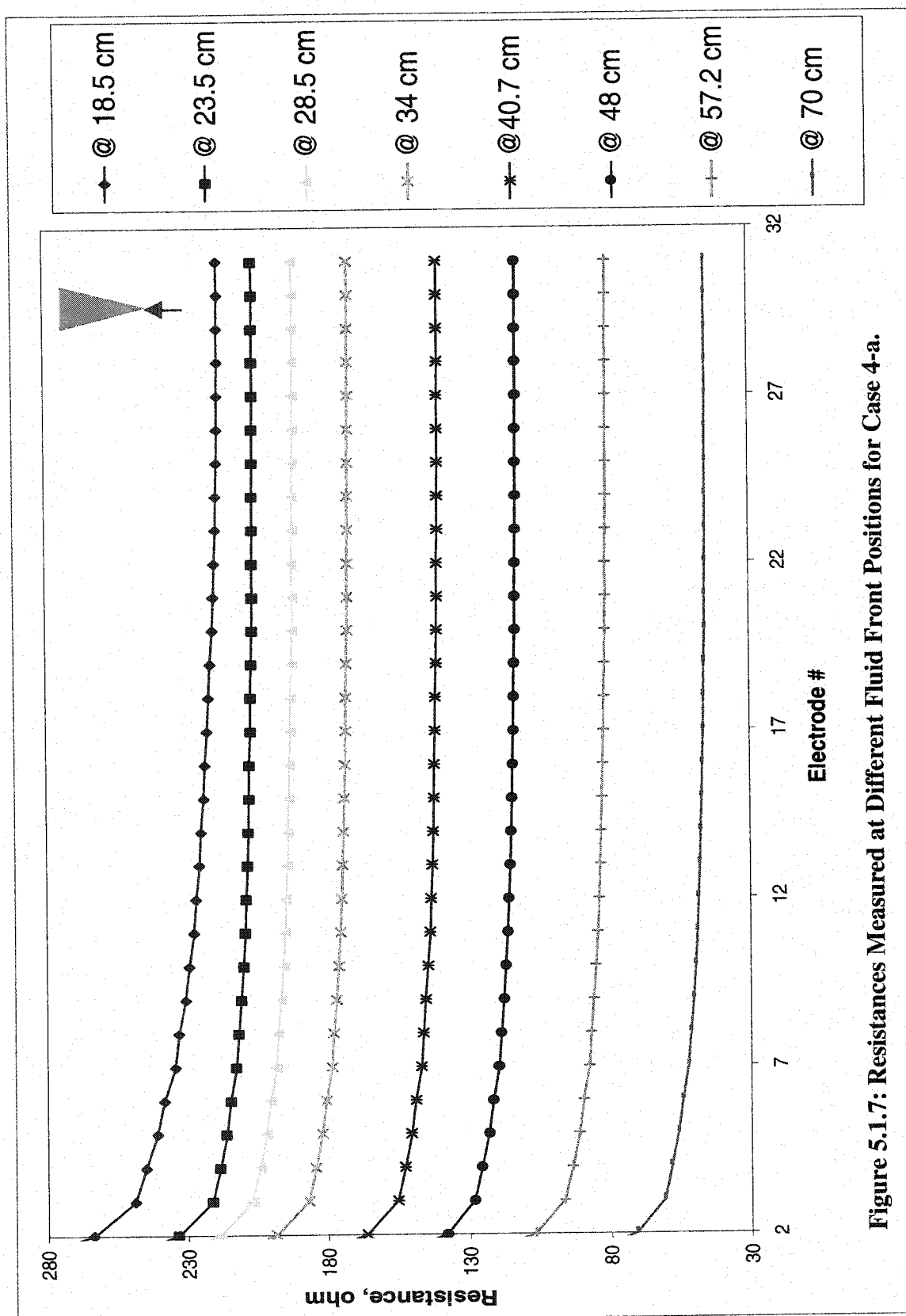
Figure 5.1.7: Resistances Measured at Different Fluid Front Positions for Case 4-a.

Figure 5.1.8: Resistances Measured at Different Fluid Front Positions for Case 4-b.
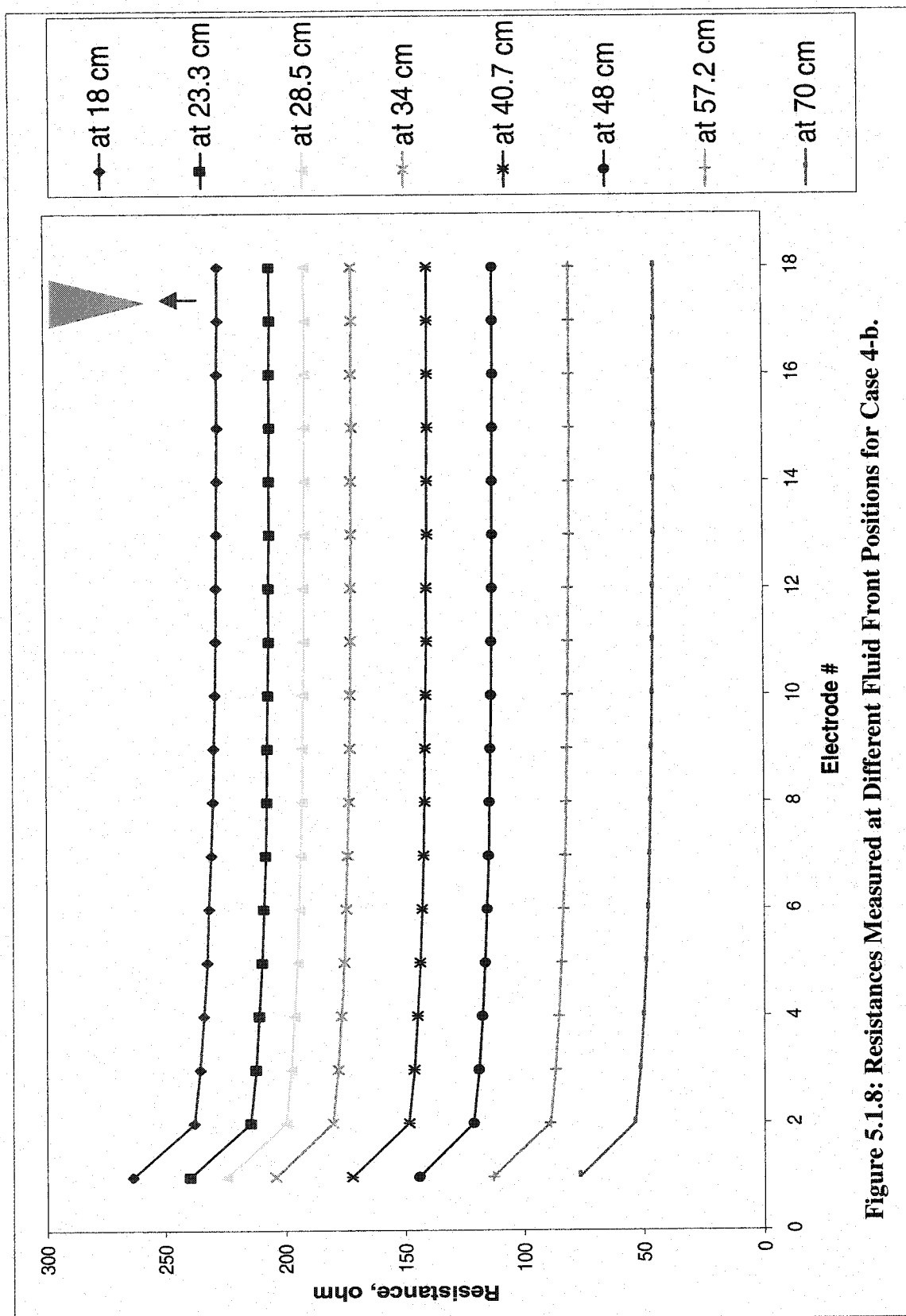
5.1.2.5 CASE 5

Re-Injection of Oil when

Model at Residual Oil Saturation:

Oil Injection

Brine
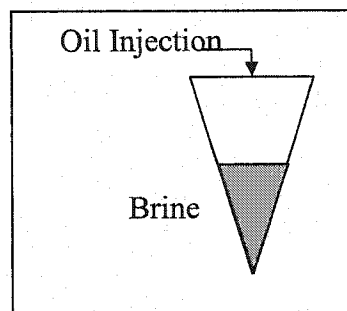
CASE 5

Although this case does not have any direct practical application in the field, this kind of experimental run could help in the determination of relative permeabilities in the vicinity of the injection wells in the field. To simulate those situations, oil was re-injected into the model when it was at residual oil saturation. The measurement condition was the same as it was for Case 3.

Resistances were plotted in Figure 5.1.9 for the first set of electrodes (Case 5-a) and in Figure 5.1.10 for the second set of electrodes (Case 5-b) as it is done in other cases. The results are almost similar to case 3, but the resistances are higher than those obtained in that case.

The quality of the measurements indicated that the electrodes were in good contact with the porous media and the smoothness of the data set indicates an easy injection of current in the conductive media.

Figure 5.1.9: Resistances Measured at Different Fluid Front Positions for Case 5-a.
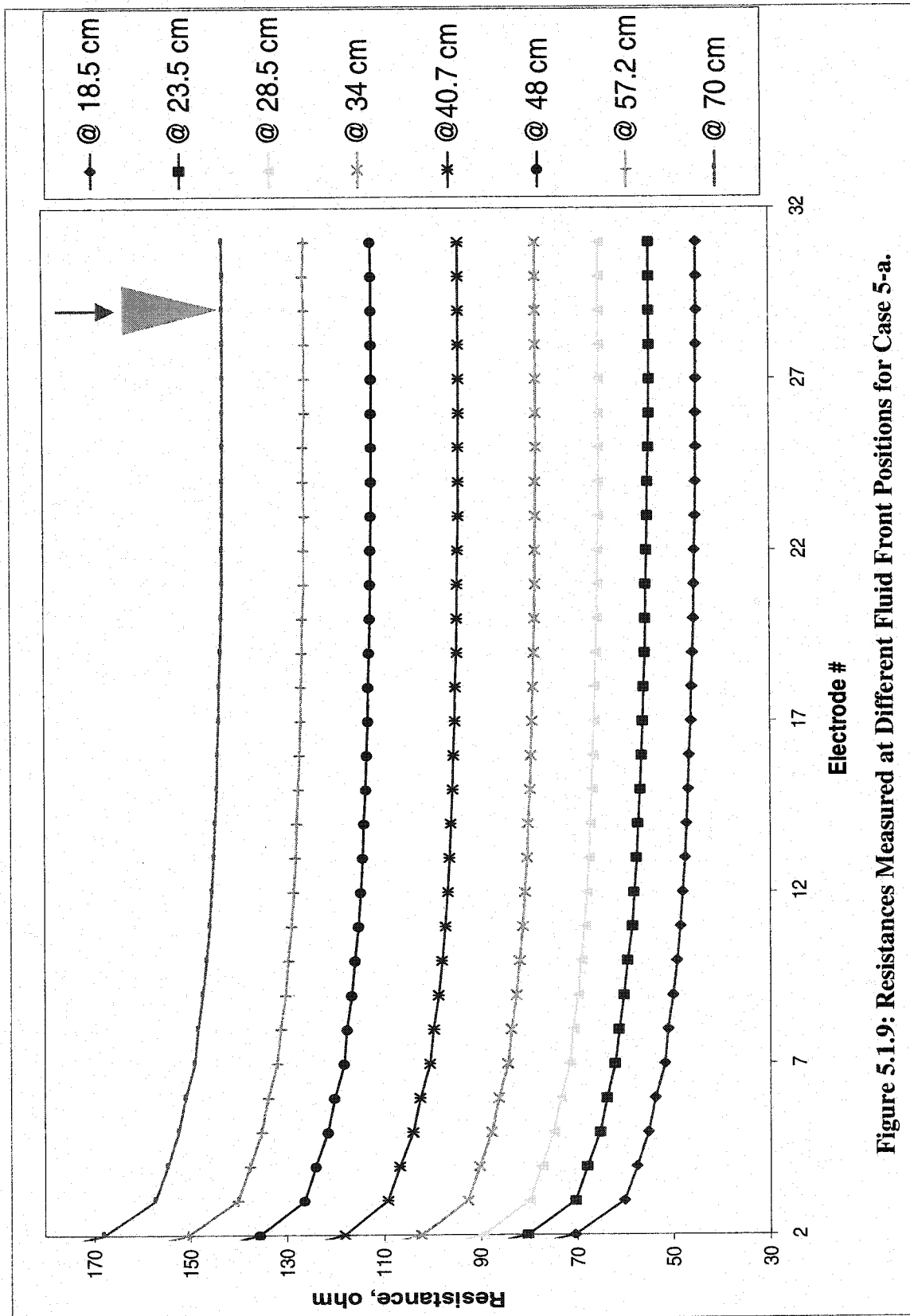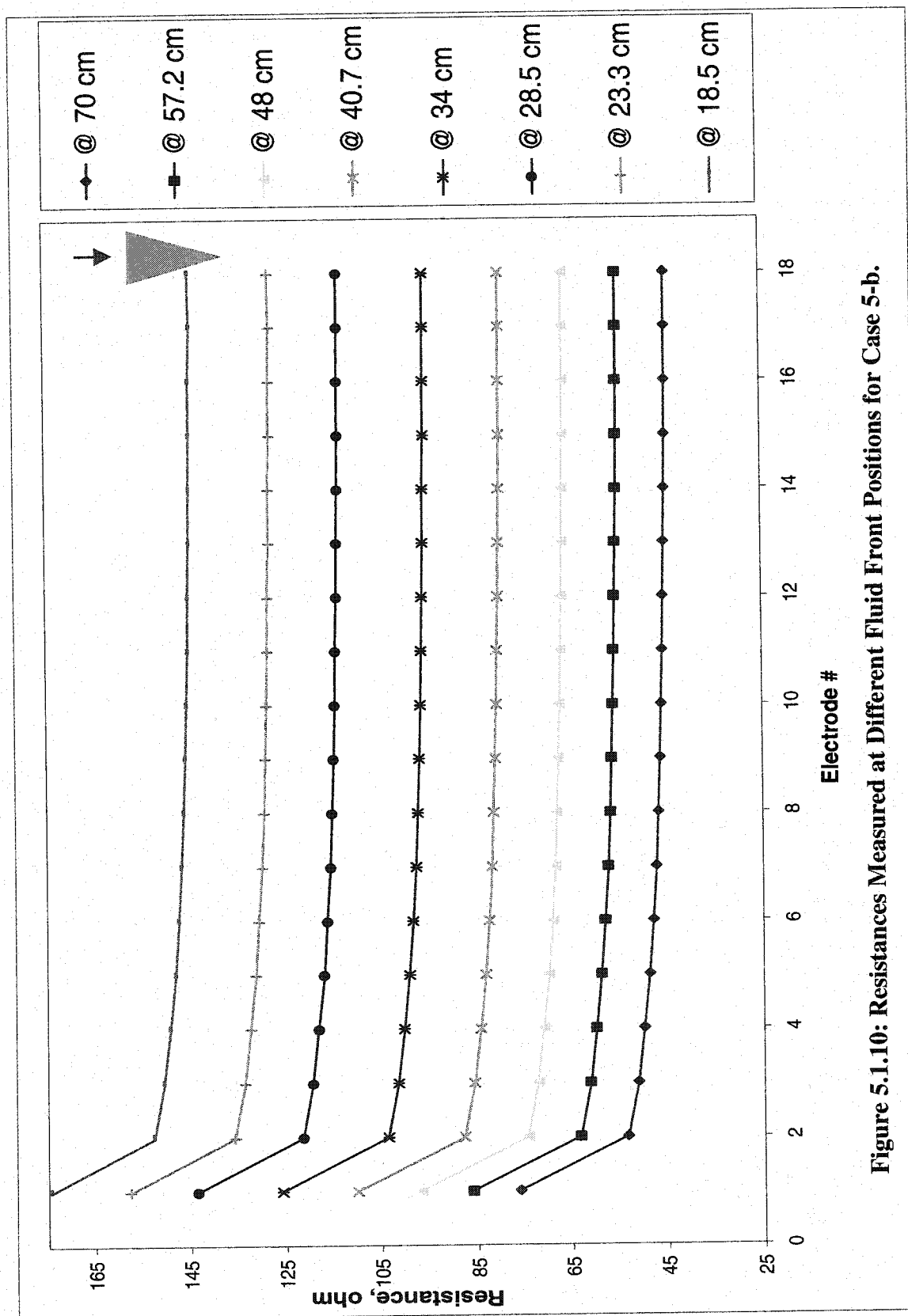
Figure 5.1.10: Resistances Measured at Different Fluid Front Positions for Case 5-b.

5.1.2.6 CASE 6

Injection of Oil in a 25-Degree

Tilted Model:
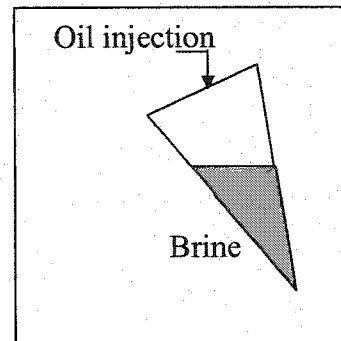
CASE 6

The objective of this experiment was to observe the sensitivity of measurements to the change in front orientation. In this case, the model was tilted to an angle of 25 degrees from the vertical axis. Initially, the model saturation was restored to nearly water saturated, and then oil was injected in stages to simulate the advancement of the front.

After each injection cycle, the model was allowed to reach equilibrium and resistances were measured using the ERAS system. To allow comparison and to evaluate the effect of tilting on measurements, the same front positions were used as in Case 3.

The measurements are plotted in Figure 5.1.11 using the first set of electrodes only. Also the measurements of Case 3 are plotted to have a clear comparison with the measurements made by keeping the model at vertical position. From the measurements for each position it is clear that of fluid front orientation.
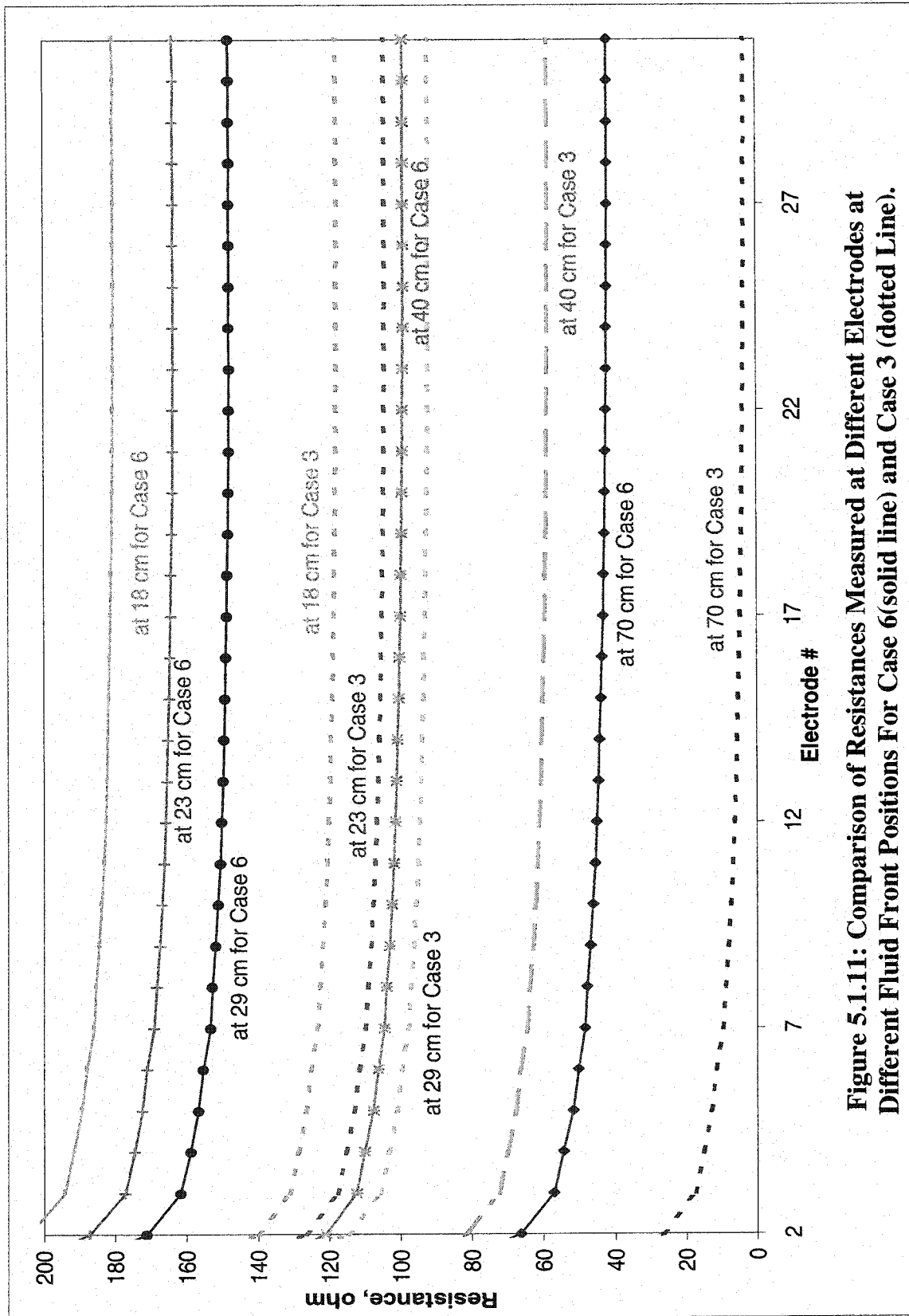
Figure 5.1.11: Comparison of Resistances Measured at Different Electrodes at Different Fluid Front Positions For Case 6(solid line) and Case 3 (dotted Line).

5.1.2.7 CASE 7

Injection of Brine in the

Model Keeping the Model

At an Angle of 25 Degrees

To the Vertical Axis:
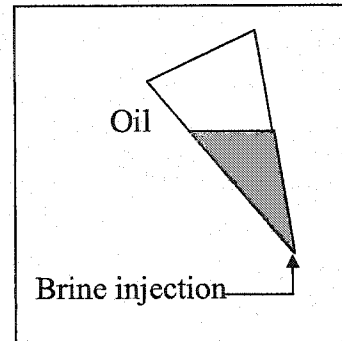
CASE 7

The objective of this run was the same as it was for Case 6. Measurements made in this Case (Case 7-a: For injection of water and Case 7-b: For re-injection of oil) were compared to those results obtained in Cases 4 and 5.

The procedure was the same as it was in Cases 4 and 5, except the model was tilted at 25-degrees. The measurements at different front positions were plotted in Figure 5.1.12 for the injection of brine (Case 7-a) and in Figure 5.1.13 for the re-injection of oil (Case 7-b). In this case, the second set of electrodes was not used for measurements, as the results obtained from the first set were sufficient to observe the difference in measurement and also to compare with the measurements made in the vertical position. In all the cases, the difference in measurements was significant enough to signal the effect of the fluid front orientation on the measurements.

Figure 5.1.12: Comparison of Resistances Measured at Different Electrodes at Different Fluid Front Positions For Case 7(a)(solid line) and Case 4 (dotted Line).
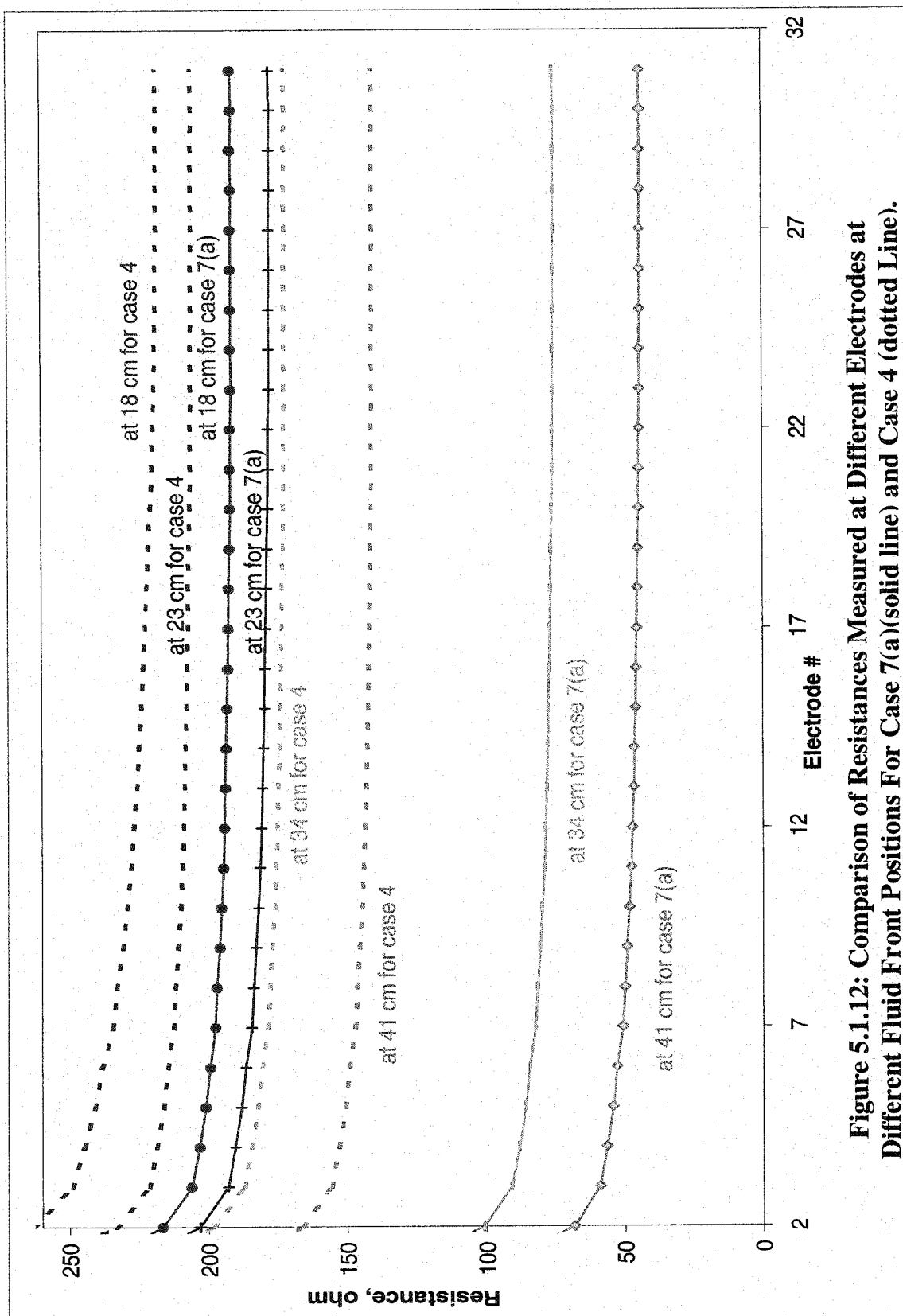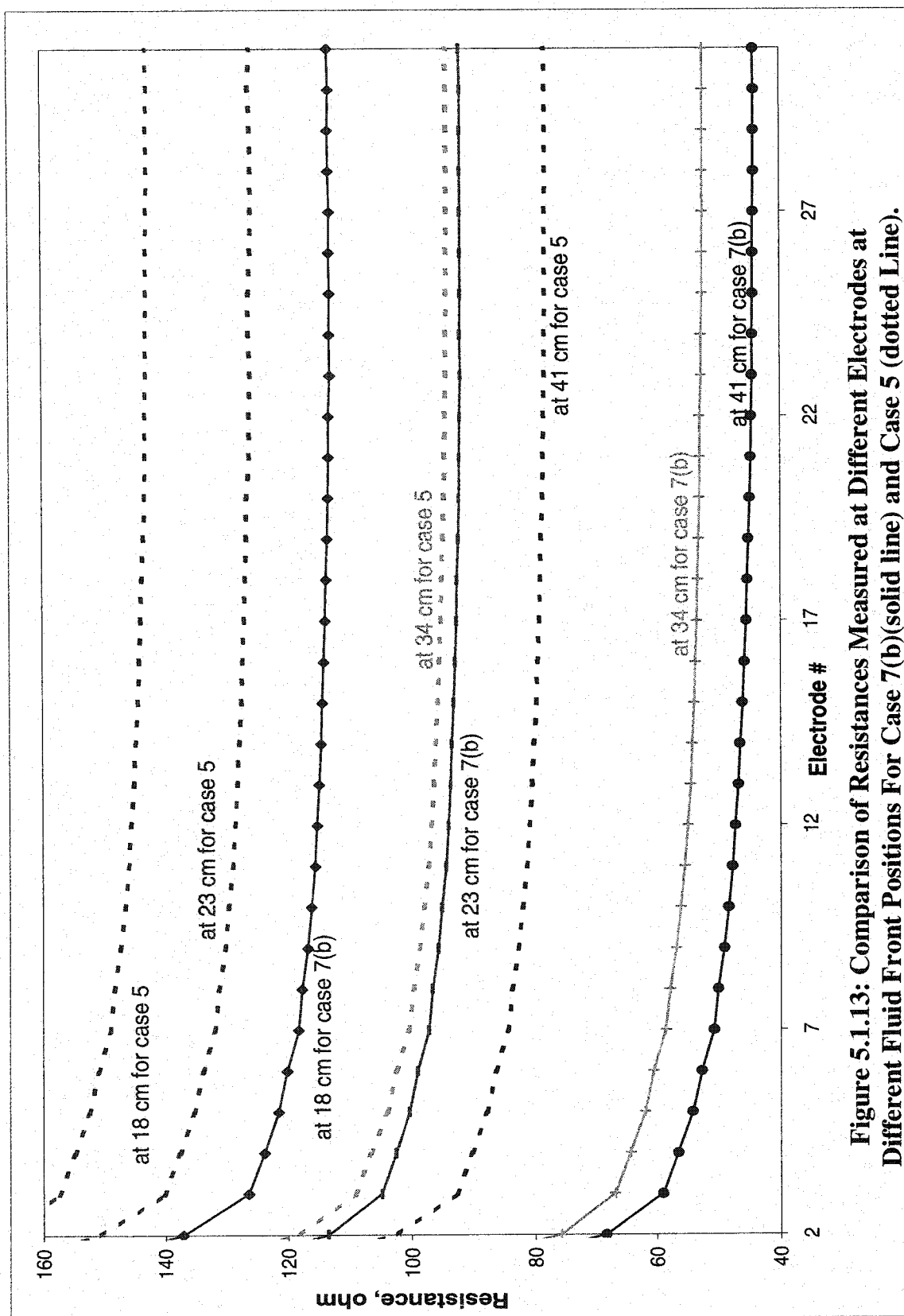
Figure 5.1.13: Comparison of Resistances Measured at Different Electrodes at Different Fluid Front Positions For Case 7(b)(solid line) and Case 5 (dotted Line).

5.2 NUMERICAL RESULTS AND DISCUSSION

The experiments conducted on the sector model were simulated using a numerical model developed by Schlumberger. Simulated results were compared to the experimental results. The model was approximated by a cylindrical grid system in three-dimensional coordinates. In order to generate resistances for each front position, the numerical model required the resistivities of different zones across the fluid front, the position of the fluid front, and the definition of the position of the electrodes as inputs.

The model is based on the Finite Element Scheme and is written in FORTRAN. The model is used to simulate water front movement in a radial direction in a cylindrical reservoir surrounded by an aquifer. This model can be easily used to simulate a reservoir with planar front movement after some modifications to the input files. It can also be used to simulate a waterfront approaching the well at an angle. The geometrical description of the reservoir is entered through the definition of a grid in cylindrical coordinates. The grid size is variable. Fine cell sizes are used in the vicinity of the borehole and much larger cells are defined near the border of the model. Electrodes are located at the nodes of the grids.

The program computes the potential distribution resulting from an injection of current between an electrode located on the axis of symmetry (the well) and a return electrode

located at infinity. From this potential distribution, apparent resistivities between any set of electrodes are computed further on. The program solves the DC current laws (can be used for AC current also at very low frequencies) as described by the equations below:

$$\vec{J} = \sigma \cdot \vec{E} \quad \text{(Ohm's law)} \qquad \dots\dots\dots\dots\dots\dots\dots\dots\dots\dots\text{Equation 5.1}$$

$$\vec{E} = -\vec{\nabla}.V \quad \text{(Potential definition)} \qquad \dots\dots\dots\dots\dots\dots\dots\dots\dots\text{Equation 5.2}$$

$$\vec{div}(\vec{J}) = \delta_{i,j} \quad \text{(Current preservation)} \qquad \dots\dots\dots\dots\dots\dots\dots\dots\dots\text{Equation 5.3}$$

Where $\delta_{i,j} = 0$ everywhere except at the source location where it is equal to J, the current injected.

Combining the above three equations yields:

$$div(-\sigma.\nabla.V) = \delta_{i,j} \quad \text{this is solved under the equivalent form:}$$

$$\nabla^{2}(-\sigma.V) = \delta_{i,j} \quad \text{(Lap lace equation)} \qquad \dots\dots\dots\dots\dots\dots\dots\dots\dots\text{Equation 5.4}$$

Equation 5.4 is discretized at the nodes of the grids and solved using the finite element technique, the description of which can be found in reference 22.

To accurately determine the resistivity of the porous medium across the fluid front under different saturation conditions, the cylindrical model was used (Section 5.1.1). The model was filled with glass beads in the same manner as it was done for the sector model to obtain the same porous media. The cylinder was saturated with 200,000 ppm brine and the resistivity at this stage that was obtained by 4-pole measurement was used in the simulator to represent a 100% water saturated zone. With the change of fluid content in

the zone between each pair of electrodes in the cylindrical model, the resistances changed and the ratios of the new resistances to the old ones were used to get the resistivity.

There were seven electrodes on the top plate of the sector model. Each pair of electrodes measured the resistances of the saturated porous medium between the two electrodes. The resistances measured with the 7 pairs of electrodes (at the top plate) were used to simulate the sector model with different positions of oil-water interfaces. It was found that the potentials obtained from the sector model were 15.5 times higher than the simulated ones.

This factor is exactly the ratio of 360/23.3 of the sector model to the radial model (Figure 5.7). The difference in measurements is due to the fact that the numerical simulator assumes that the injected current flows in all directions whereas in the scaled model the injected current is only allowed to flow in the restricted path (unidirectional flow because the other ends were closed using non-conductive Plexiglas plates). Therefore, the calculated resistances were 15.5 times (i.e., 360/23.3) smaller than those of the experimental values. For this reason, resistances obtained experimentally were divided by a factor of 15.5 before comparing them with simulated values.

The sensitivity of the numerical model to the movement of fluid and to the change in resistivity of the fluid was calculated using different resistivity values for different fluid phases and also using different fluid front positions as the input for the numerical model. The sensitivity to the movement of the fluid front and to the change in resistivity across the fluid front was investigated and the average sensitivity with a 1 ohm-m change in the

resistivity of the oil phase was 0.34 V/ohm-m. The sensitivity due to a 1 cm movement of the fluid front varied from 3.5 V/cm to 1.35V/cm for a distance of 23 cm to 63 cm, respectively, while the resistivity for the oil phase was 80 ohm-m and the resistivity of the conductive medium was 0.18 ohm-m.

The sensitivities of the experimental and numerical data were also computed and comparisons of both the sensitivities are shown in Figure 5.8, which clearly indicates that with level of accuracy of our experiment and the hardware used, it is possible to detect the movement of a fluid front up to a distance which equals twice the thickness of the pay zone (the array span). The sudden drop in sensitivity after a distance of 60 cm from the well was due to the segregation of fluid due to gravity, since part of this experiment, in this case, was conducted in two stages separated by a waiting period of about 8 to 12 hours.
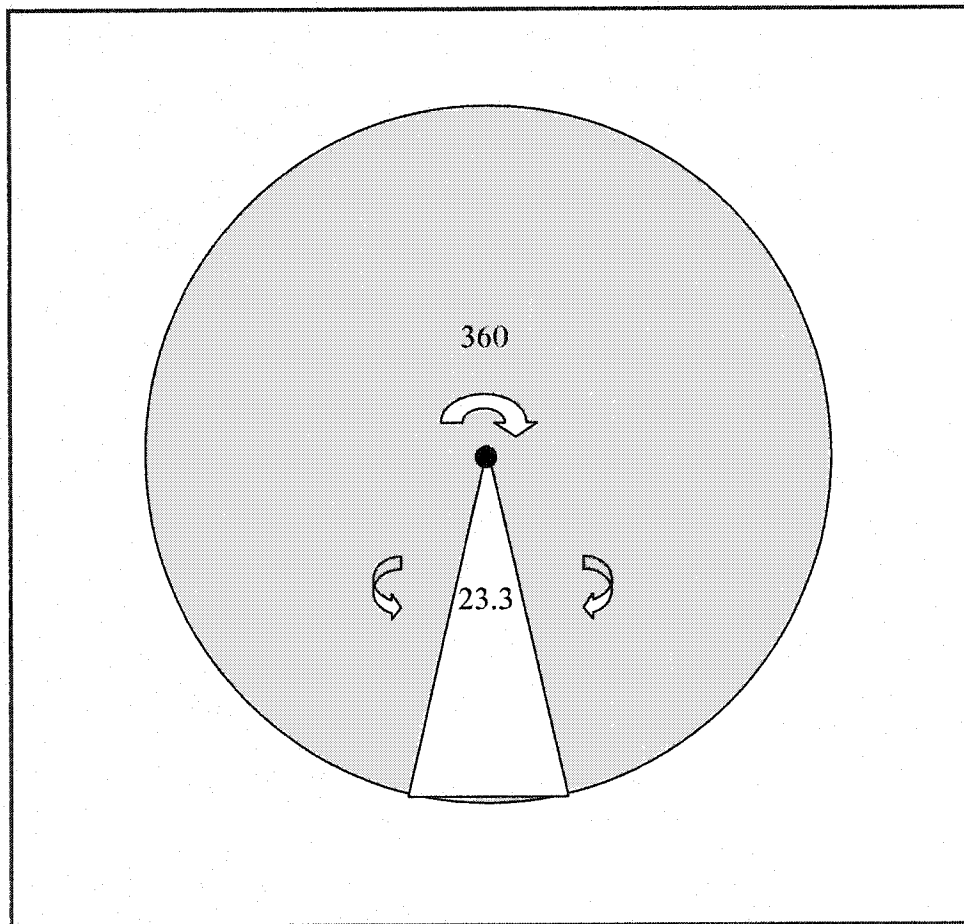
Figure 5.7: Sector Model With an Angle of 23.3 Degree.
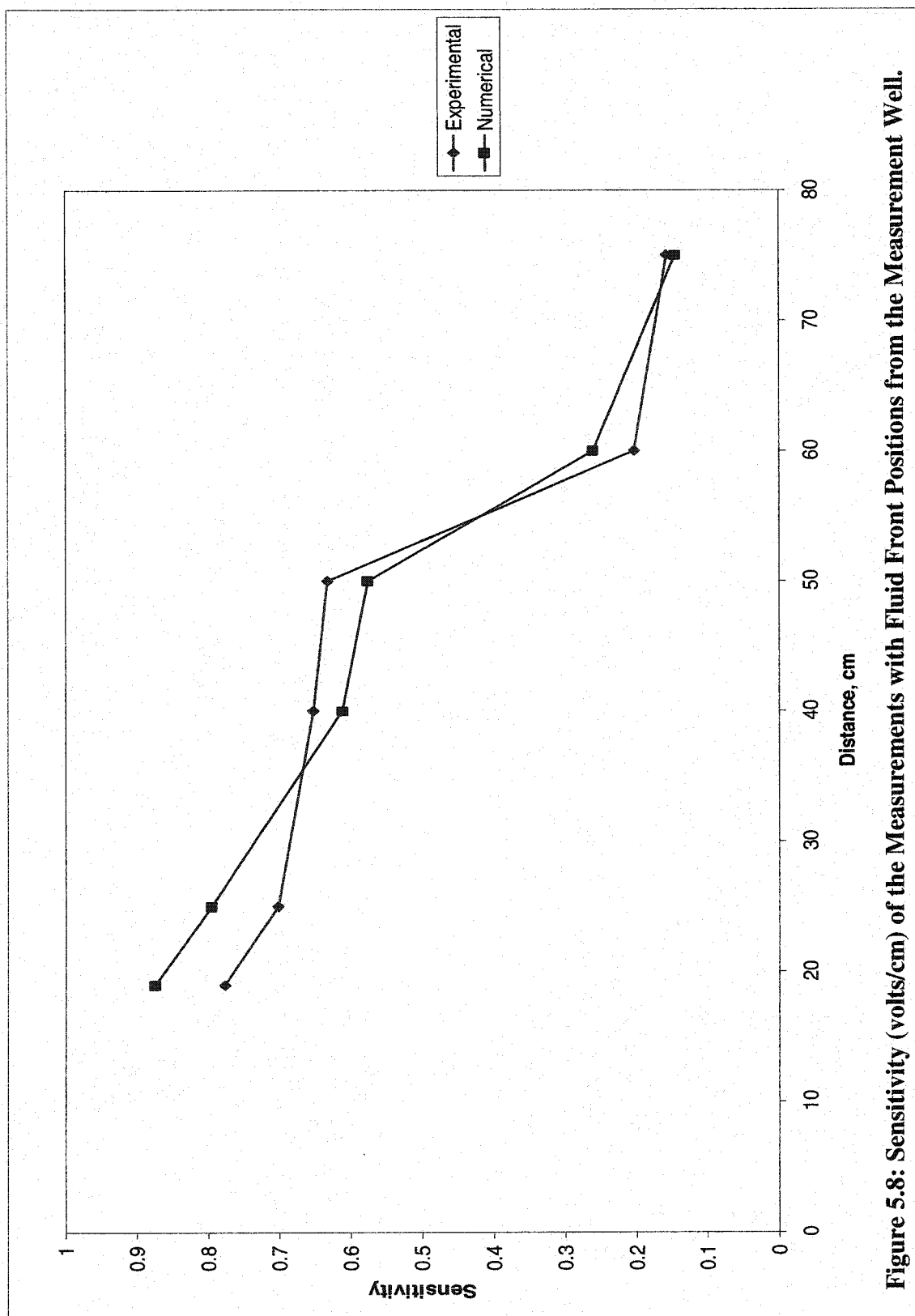
Figure 5.8: Sensitivity (volts/cm) of the Measurements with Fluid Front Positions from the Measurement Well.

5.3 COMPARISON OF RESULTS

Comparison of the results obtained from the experimental and numerical methods are presented in this section. Cases 1 to 5 are considered for this comparison.

5.3.1 CASE 1

Injection of Oil in the

Brine-Saturated Model:
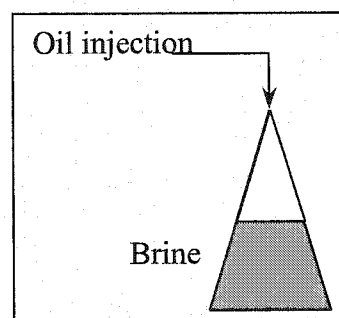
CASE 1

The description of this experiment was presented earlier in Section 5.1.1.1. However, the following is presented to highlight the reasons for differences encountered during numerical simulation.

The model was initially 100% saturated with 200,000 ppm brine. Oil was then injected to reach connate water saturation. During the oil injection, and due to low water saturation, the measured resistances suddenly increased to very high values and it was difficult to inject current using the first set of electrodes. With increasing oil saturation in the model, the resistances continued to increase considerably. As the oil-water interface

reached a distance of 70 cm from the measurement well, it was impossible to inject more than 0.1 mA, which is the limit to obtain reliable measurements from the acquisition system.

However, the above problem did not affect the simulated data. Moreover, comparisons of experimental and numerical results were difficult for the potential electrodes very close to the injection electrode as there was always some residual resistivity or local resistivity in the vicinity of the injection electrode. When the comparisons were made, results for those electrodes were excluded from the rest of the data points.

This kind of problem was significantly reduced using the second set of electrodes and the comparison was better. Comparisons of the experimental and numerical values for the first set of electrodes are shown in Figure 5.2.1 (Case 1-a) for all fluid fronts and also in Figure 5.2.2 for selected front positions. Figure 5.2.3 (Case 1-b) and figure 5.2.4 show the same results as obtained from the second set of electrodes.
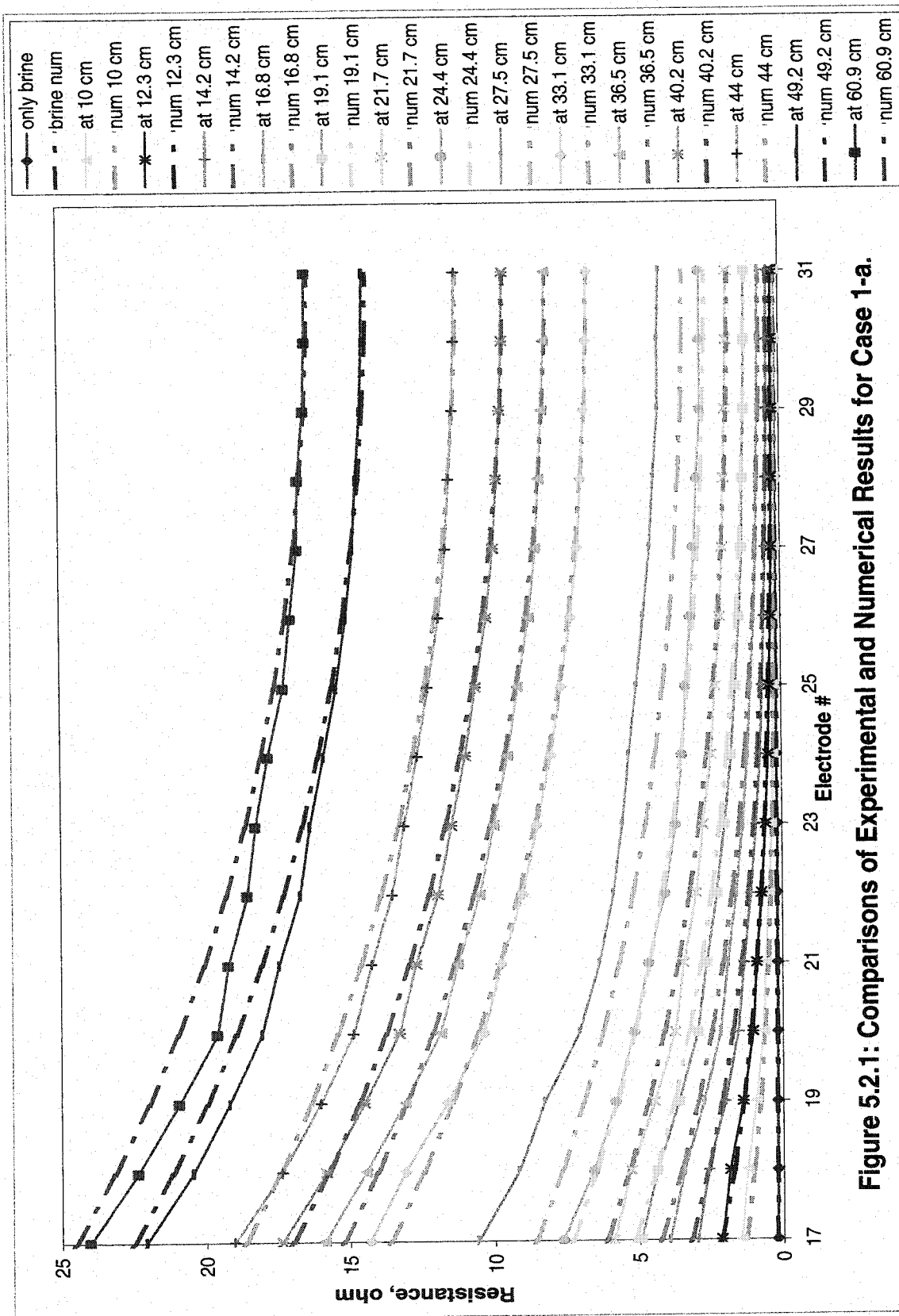
Figure 5.2.1: Comparisons of Experimental and Numerical Results for Case 1-a.

Legend:
- only brine
- brine num
- at 10 cm
- num 10 cm
- at 12.3 cm
- num 12.3 cm
- at 14.2 cm
- num 14.2 cm
- at 16.8 cm
- num 16.8 cm
- at 19.1 cm
- num 19.1 cm
- at 21.7 cm
- num 21.7 cm
- at 24.4 cm
- num 24.4 cm
- at 27.5 cm
- num 27.5 cm
- at 33.1 cm
- num 33.1 cm
- at 36.5 cm
- num 36.5 cm
- at 40.2 cm
- num 40.2 cm
- at 44 cm
- num 44 cm
- at 49.2 cm
- num 49.2 cm
- at 60.9 cm
- num 60.9 cm

Resistance, ohm

Electrode #
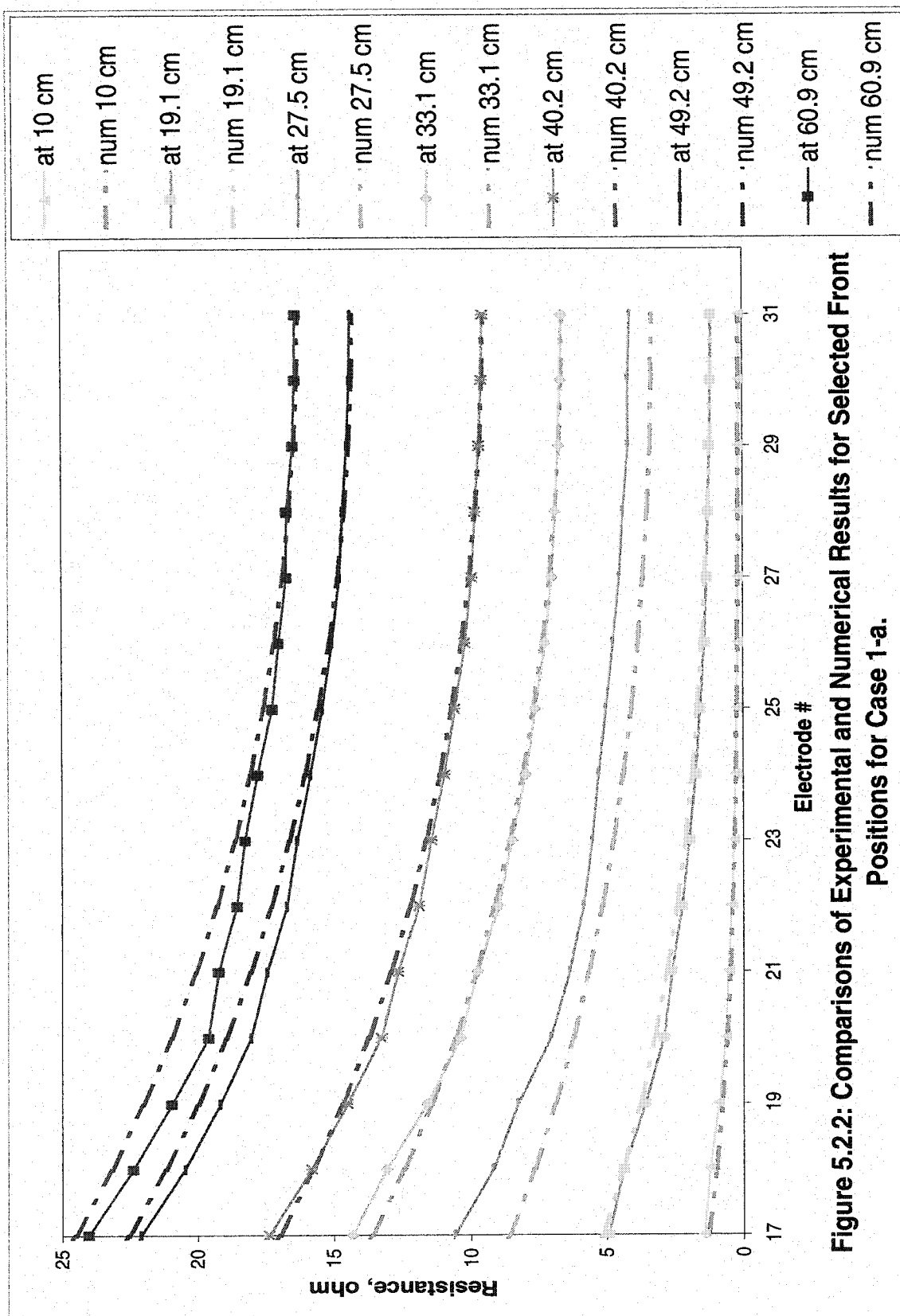
Figure 5.2.2: Comparisons of Experimental and Numerical Results for Selected Front Positions for Case 1-a.
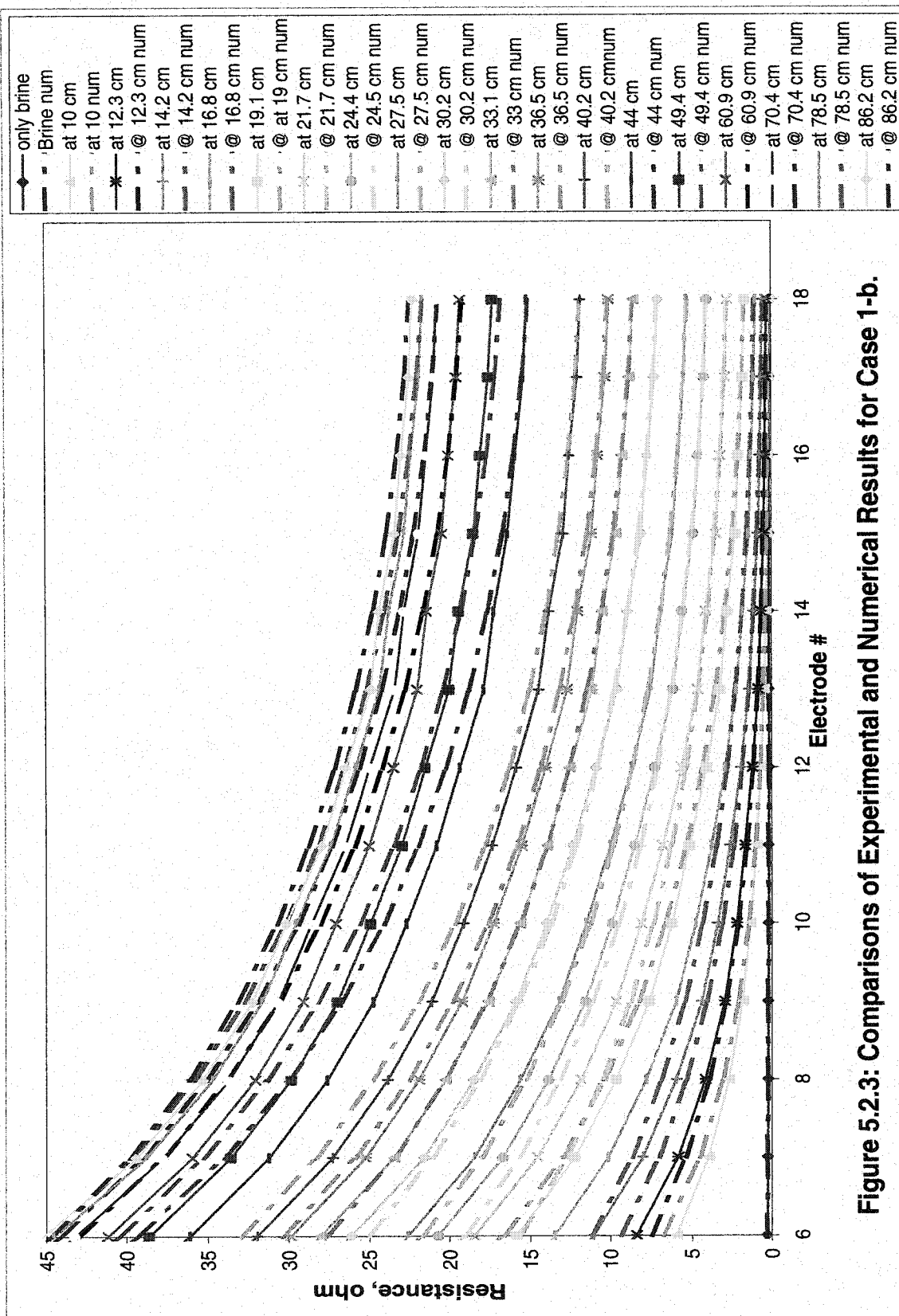
Figure 5.2.3: Comparisons of Experimental and Numerical Results for Case 1-b.

98
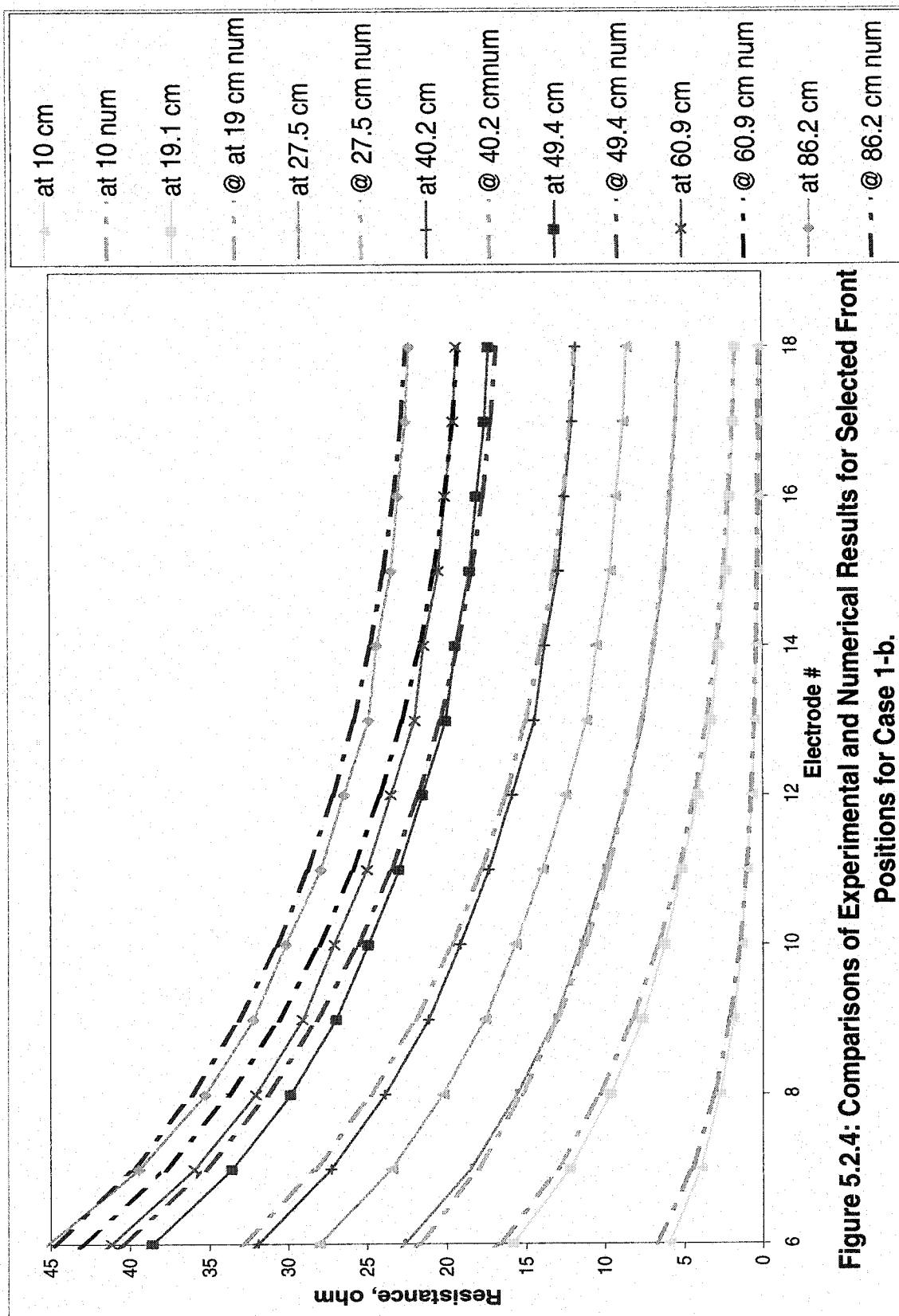
Figure 5.2.4: Comparisons of Experimental and Numerical Results for Selected Front Positions for Case 1-b.

Legend:
- at 10 cm
- at 10 num
- at 19.1 cm
- @ at 19 cm num
- at 27.5 cm
- @ 27.5 cm num
- at 40.2 cm
- @ 40.2 cmnum
- at 49.4 cm
- @ 49.4 cm num
- at 60.9 cm
- @ 60.9 cm num
- at 86.2 cm
- @ 86.2 cm num

X-axis: Electrode #
Y-axis: Resistance, ohm

5.3.2 CASE 2

Injection of Brine in the

Oil Saturated Model:

Oil

Brine injection
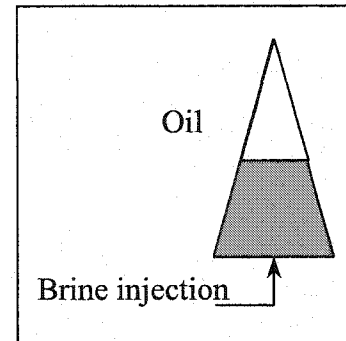
CASE 2

Before presenting the numerical results for this case, it is important to understand the experimental conditions because they have significant impact on the comparison of the two results.

Almost two days were required to conduct the experiment described in Case 1. During this time, there was segregation of oil and connate water due to the force of gravity and high permeability. Based only on visual inspection, the uppermost zone seemed almost water-free. This situation adversely affected current injection as the zone in the vicinity of the injection electrode was almost non-conductive and some of the electrodes were not in good contact with the media and were completely immerged in oil. Accordingly, there were some errors in the measurements based on the first set of electrodes, especially in the vicinity of the injection electrode. For this reason, the closest points (almost 13 cm) to the injection electrode were excluded from comparison with the simulated data. Also, for distances more than 75 cm from the production well, the resistances were too high to measure using the first set of electrodes.

This kind of problem was also found for the second set of electrodes, but it was not as severe. It was possible to detect further than 75 cm using the second set of electrodes as the measurements had less noise interference and were more sensitive. Comparisons for the first set of electrodes are shown in Figure 5.2.5 (Case 2-a) and also in Figure 5.2.6 for selected front positions. Figure 5.2.7 (Case 2-b) and in Figure 5.2.8 present the same results using the second set of electrodes.
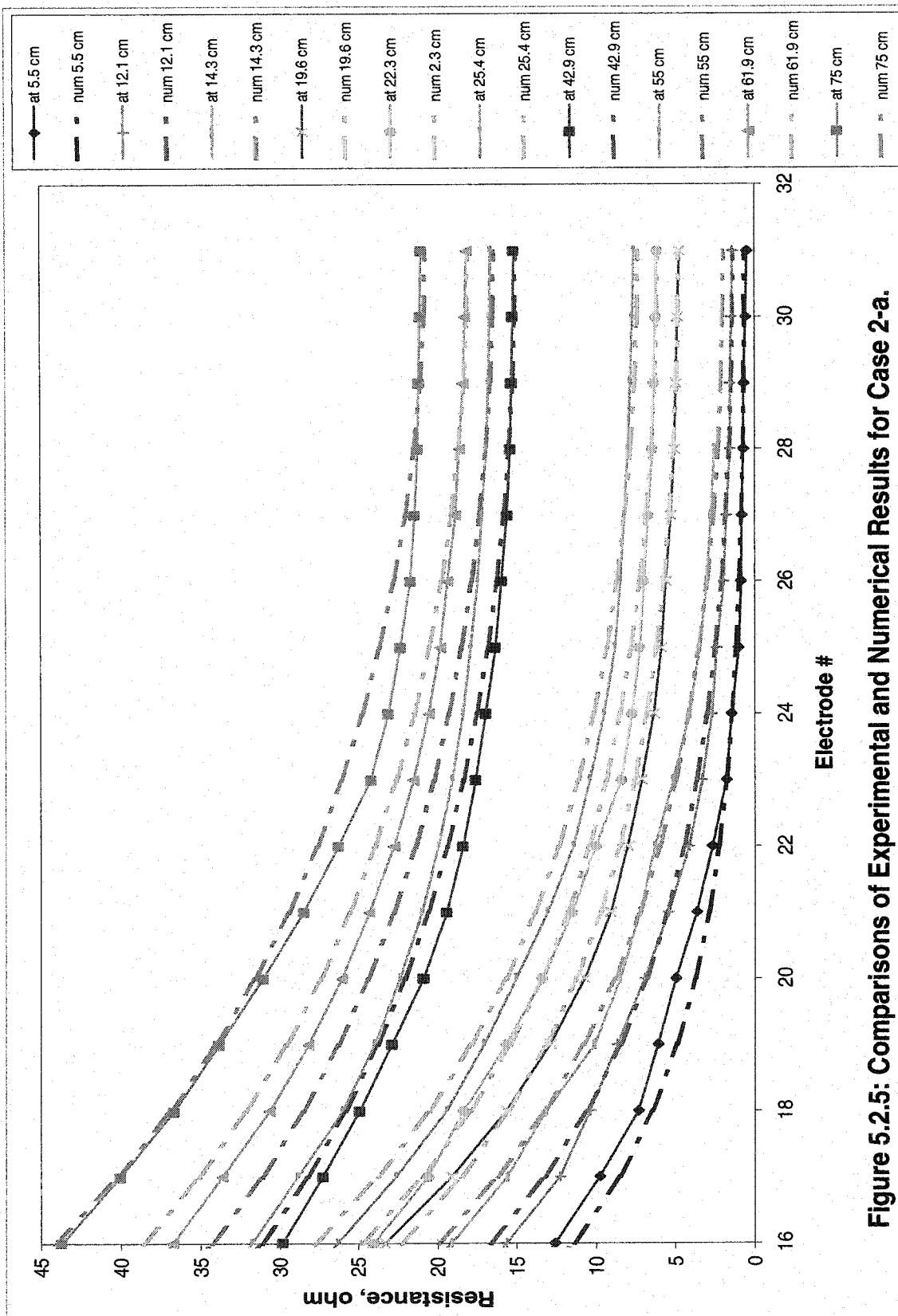
Figure 5.2.5: Comparisons of Experimental and Numerical Results for Case 2-a.
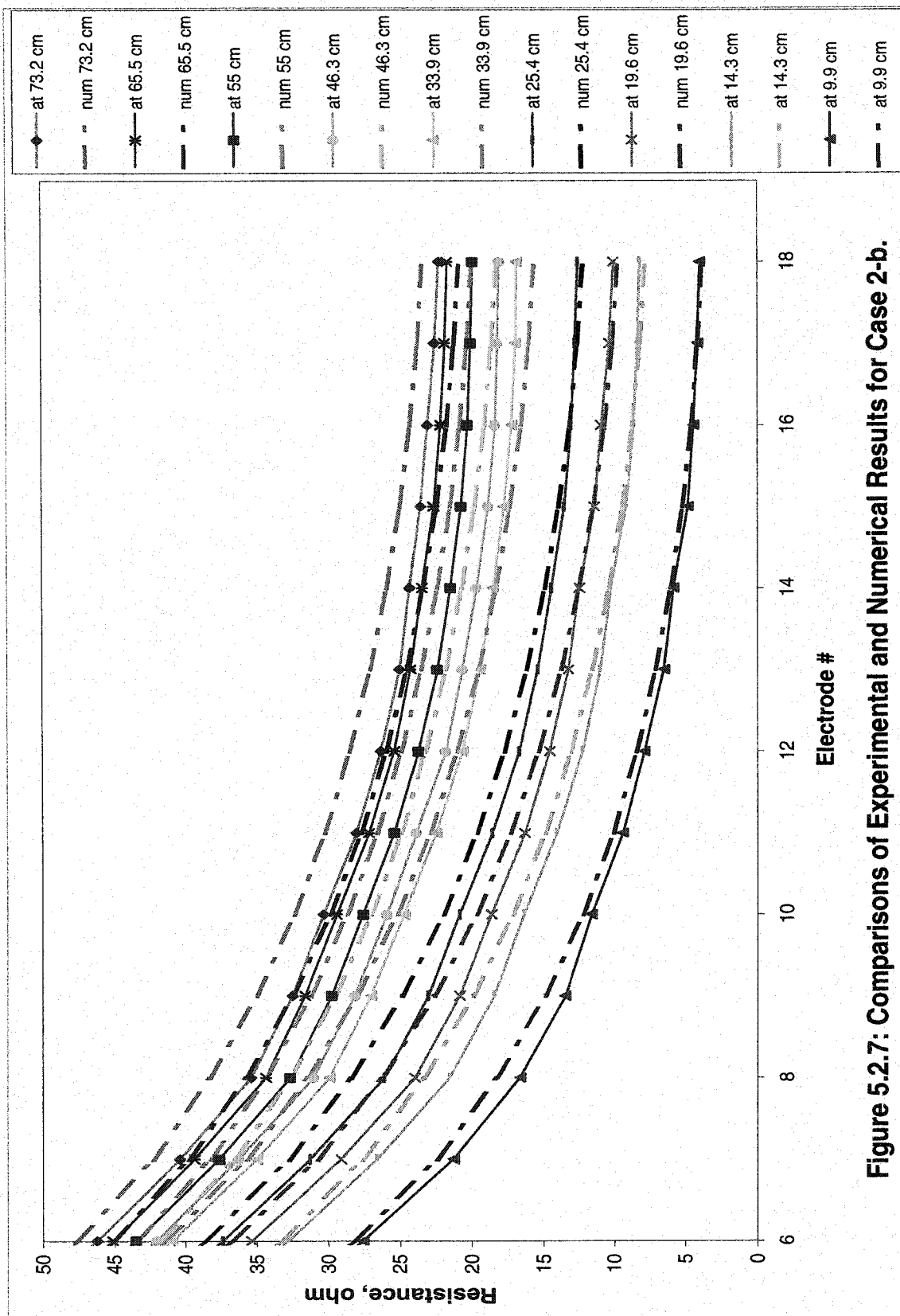
Figure 5.2.7: Comparisons of Experimental and Numerical Results for Case 2-b.
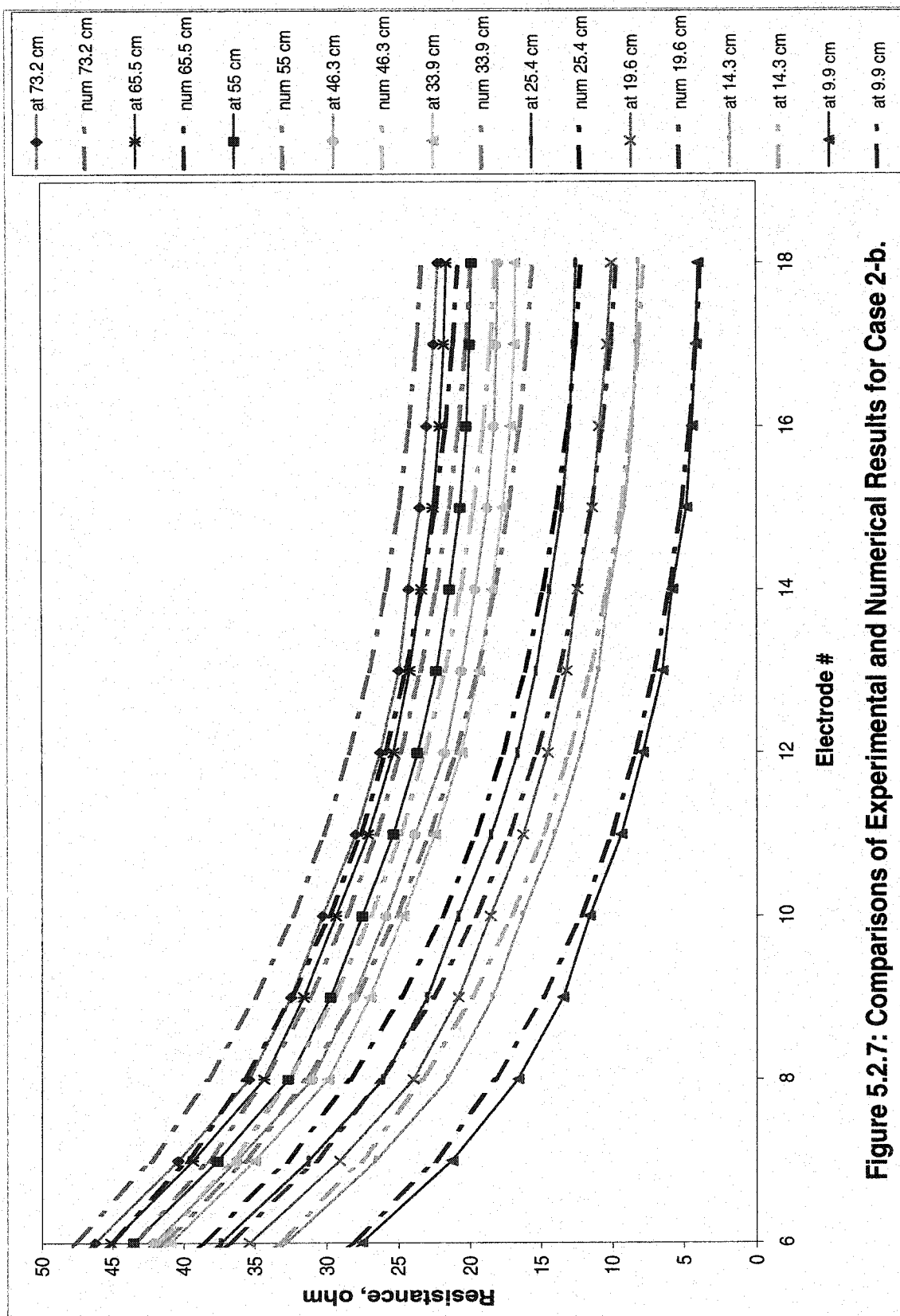
Figure 5.2.7: Comparisons of Experimental and Numerical Results for Case 2-b.
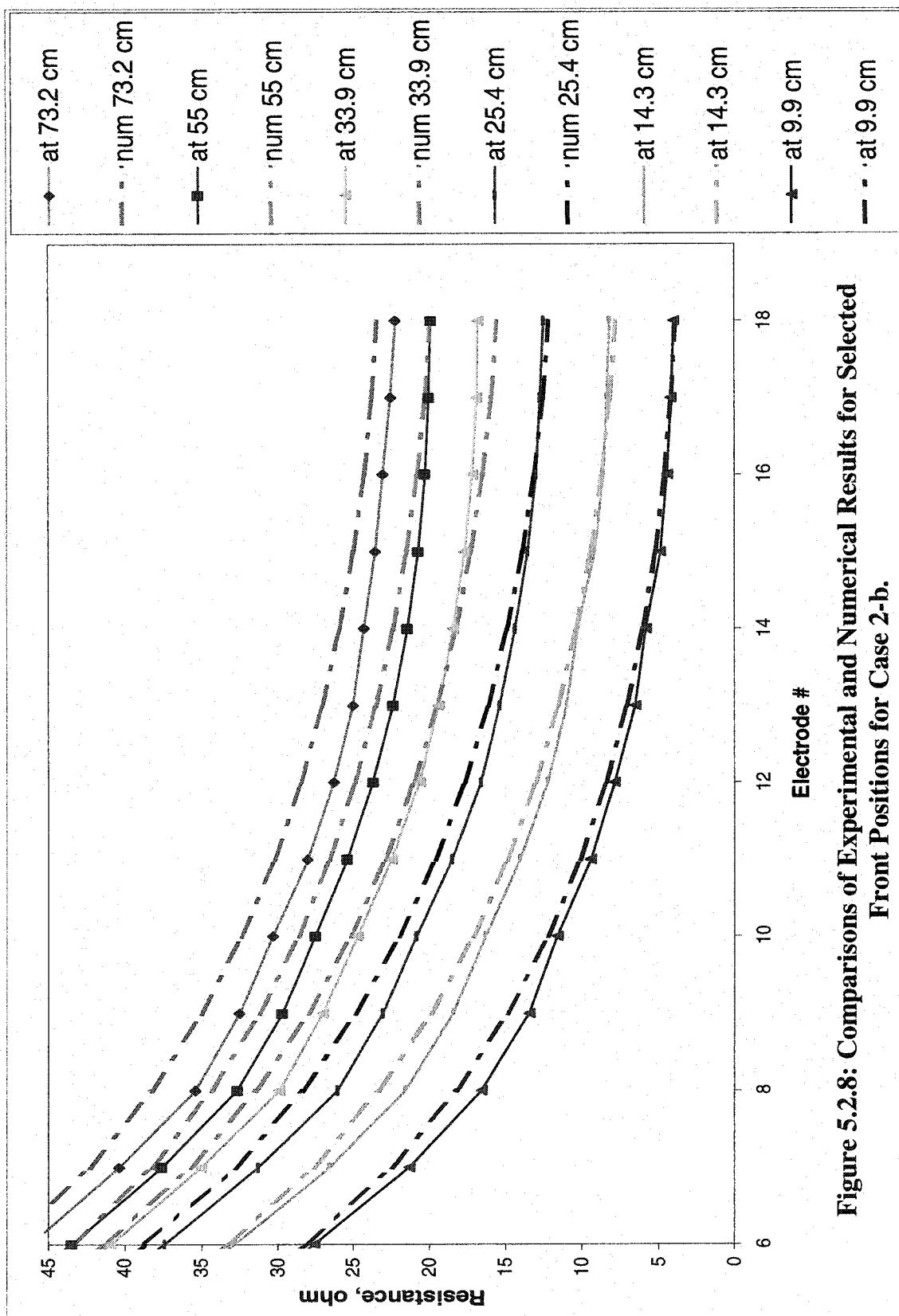
Figure 5.2.8: Comparisons of Experimental and Numerical Results for Selected Front Positions for Case 2-b.

Legend:
- at 73.2 cm
- num 73.2 cm
- at 55 cm
- num 55 cm
- at 33.9 cm
- num 33.9 cm
- at 25.4 cm
- num 25.4 cm
- at 14.3 cm
- at 14.3 cm
- at 9.9 cm
- at 9.9 cm

Axes:
- Y-axis: Resistance, ohm
- X-axis: Electrode #

5.3.3 CASE 3

Injection of Oil in the

100% Brine Saturated Model:
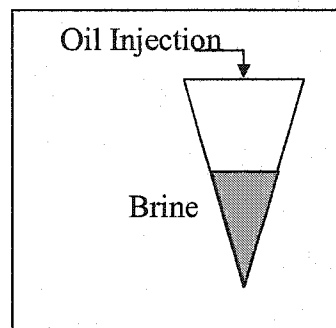
CASE 3

Because of the problem in measurements due to the lack of good contact between electrodes and the porous media and due to fluid segregation, the reservoir model was inverted vertically with the well and electrodes at the bottom to assure more compacted porous media in the vicinity of the well. This approach improved the quality of measurements considerably.

The measurements made in this case, with the injection of oil from the top into the brine-saturated model, and displacement of brine at different oil-water positions were also simulated using the numerical model. Very good matches of the experimental and numerical results were obtained for almost all the electrodes except the first potential electrode using both sets. The first electrode of each set was the injection electrode and therefore, there was always some deflection in measurement due to the presence of high local resistivity in the vicinity of the injection electrode.

Comparisons for the first set of electrodes are shown in Figure 5.2.9 (Case 3-a) and for the second set of electrodes in Figure 5.2.10 (Case 3-b).
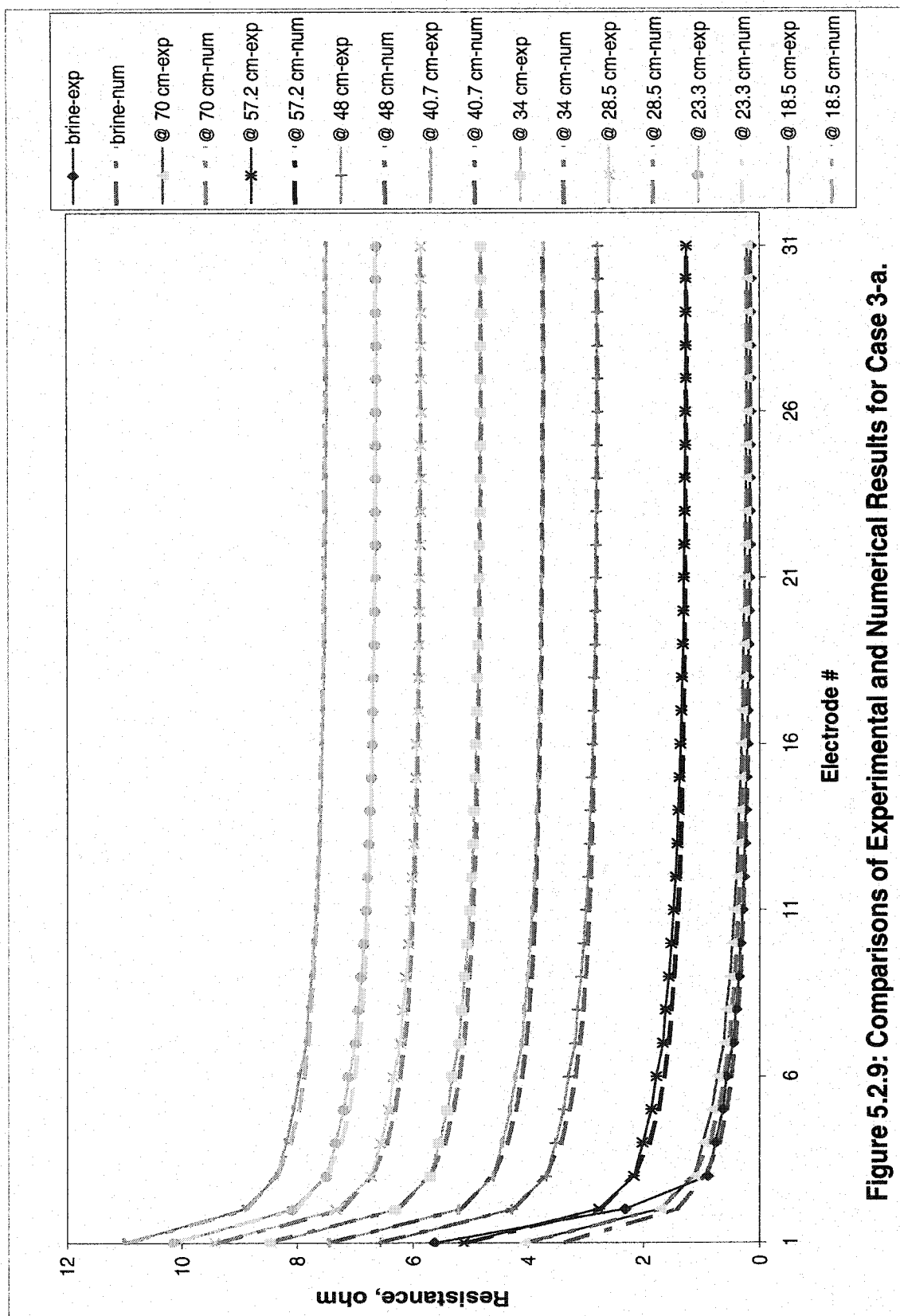
Figure 5.2.9: Comparisons of Experimental and Numerical Results for Case 3-a.
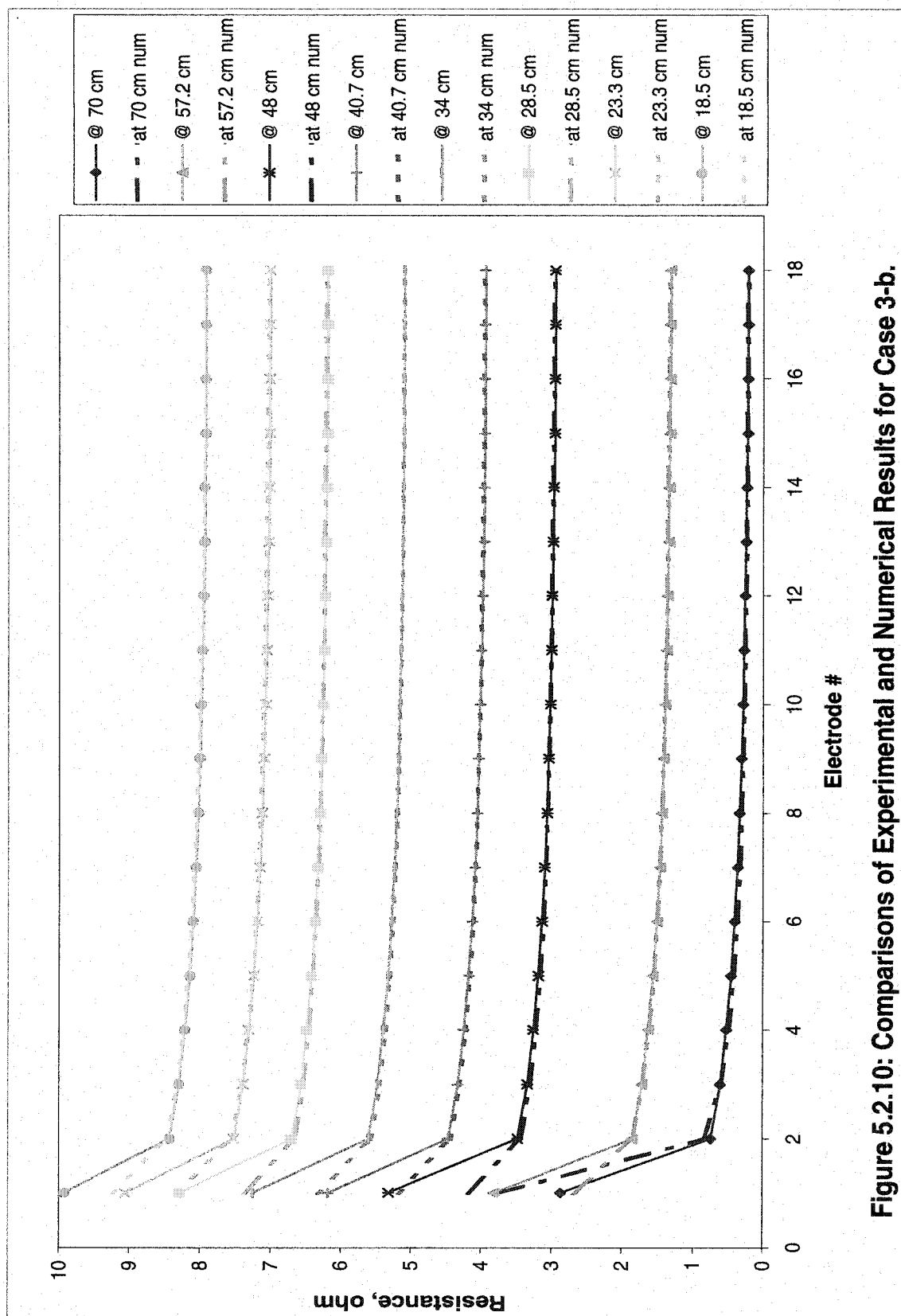
Figure 5.2.10: Comparisons of Experimental and Numerical Results for Case 3-b.

Legend:
- @ 70 cm
- at 70 cm num
- @ 57.2 cm
- at 57.2 cm num
- @ 48 cm
- at 48 cm num
- @ 40.7 cm
- at 40.7 cm num
- @ 34 cm
- at 34 cm num
- @ 28.5 cm
- at 28.5 cm num
- @ 23.3 cm
- at 23.3 cm num
- @ 18.5 cm
- at 18.5 cm num

Y-axis: Resistance, ohm

X-axis: Electrode #

5.3.4   CASE 4

Injection of Brine in the

Oil-Saturated Model:
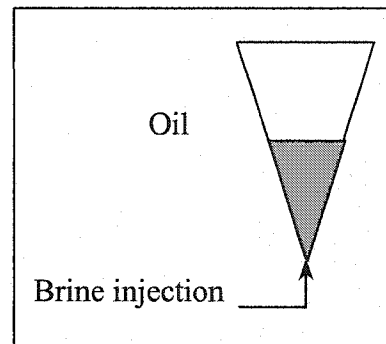
CASE 4

Initially the model was saturated with oil at connate water saturation. Brine was injected from the bottom. A very good match was obtained between the numerical and experimental data.

Comparisons for the first set of electrodes are shown in Figure 5.2.11 (Case 4-a) and for the second set of electrodes in Figure 5.2.12 (Case 4-b). Change in resistance was the highest in the first electrode because it was used as the current injection electrode. Measurements at other electrodes were not that as sensitive to the position of the electrode as the arrays were in highly conductive media.
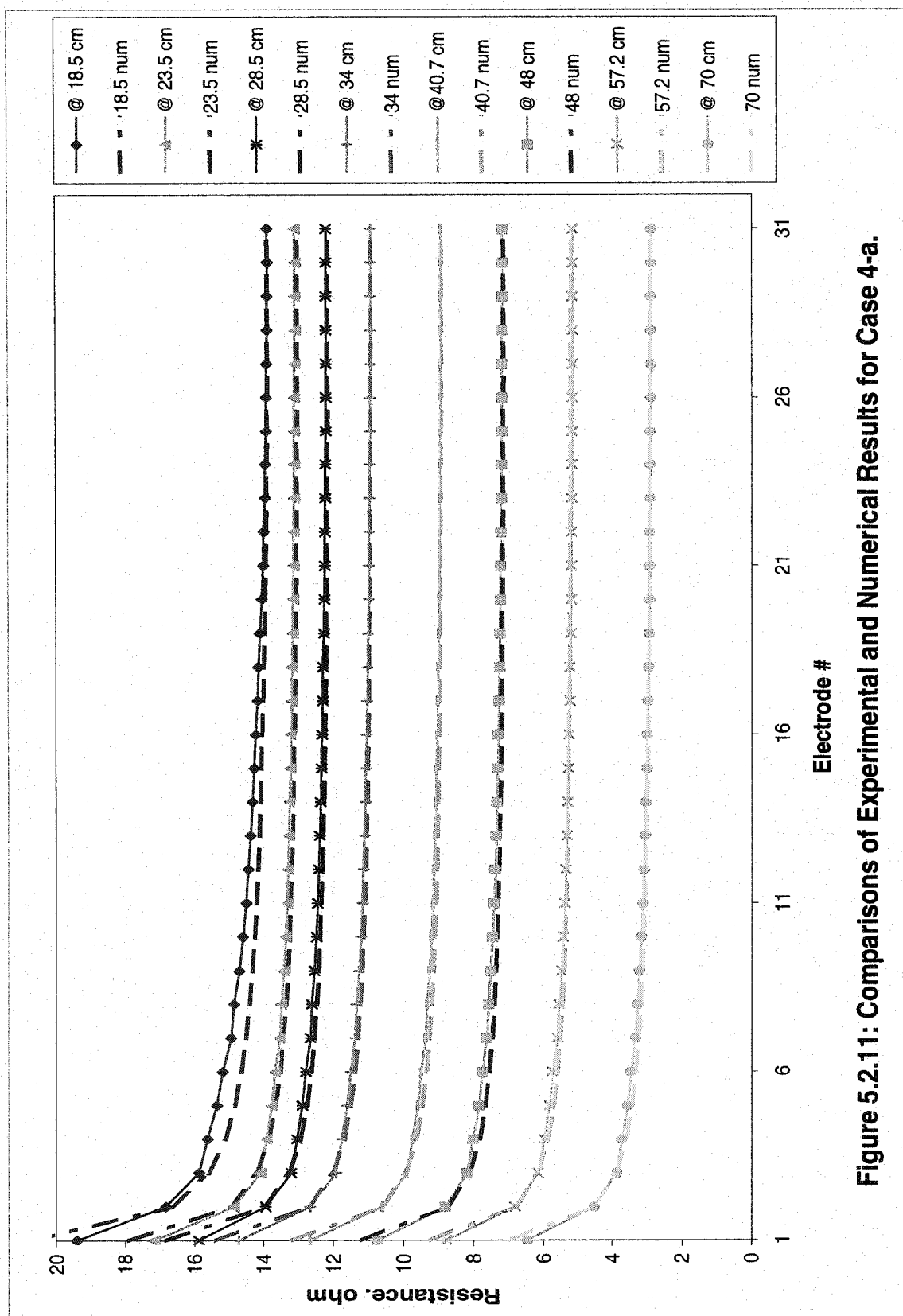
Figure 5.2.11: Comparisons of Experimental and Numerical Results for Case 4-a.
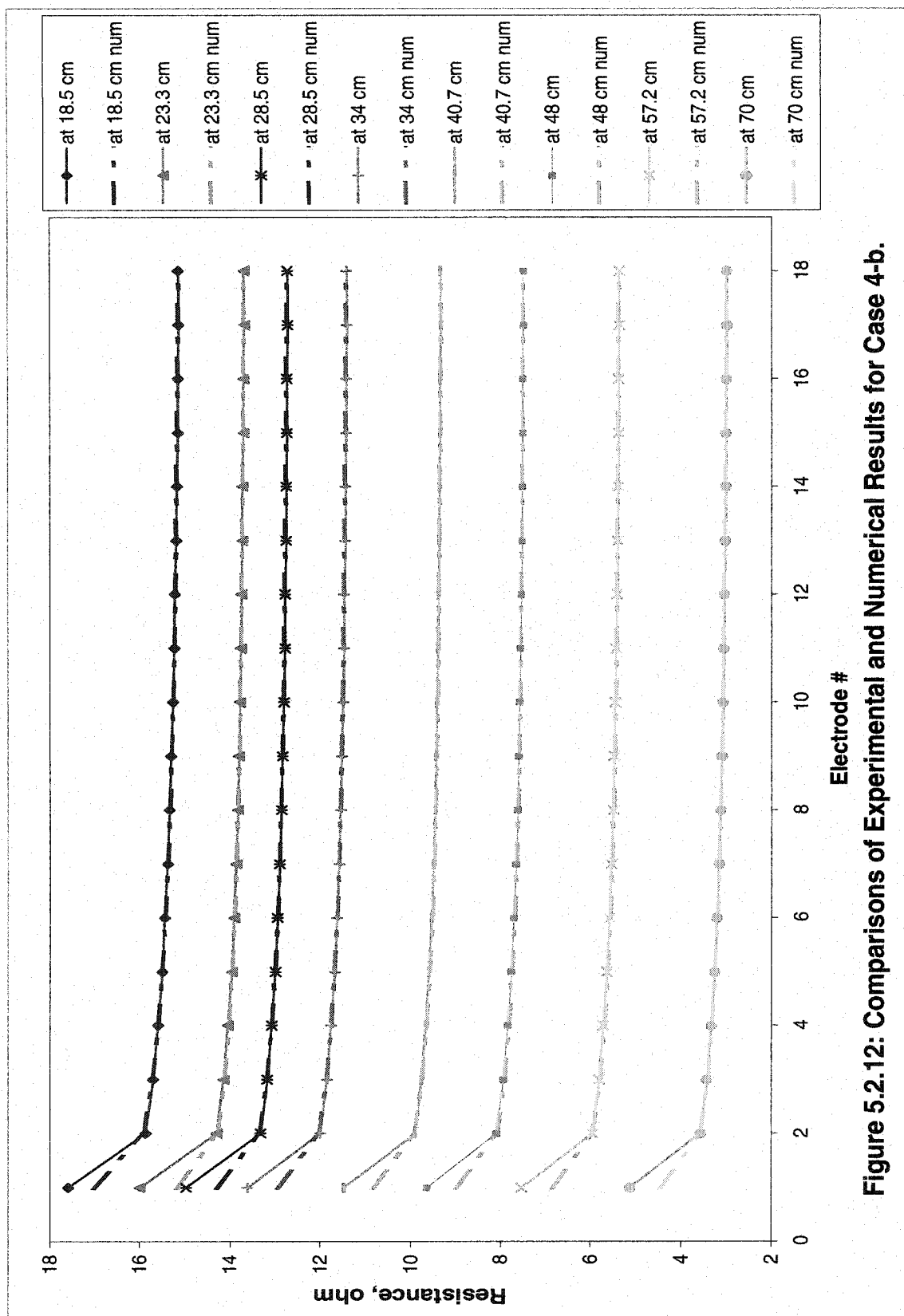
Figure 5.2.12: Comparisons of Experimental and Numerical Results for Case 4-b.

5.3.5 CASE 5

Re-Injection of Oil in the

Model at Residual Oil Saturation:

Oil Injection

Brine
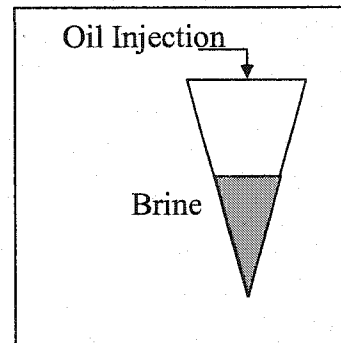
CASE 5

In this case, oil was re-injected into the inverted model from the top. A very good match was obtained between the numerical and experimental data as shown in Figure 5.2.13 and Figure 5.2.14 for the first set and the second set of electrodes, respectively.
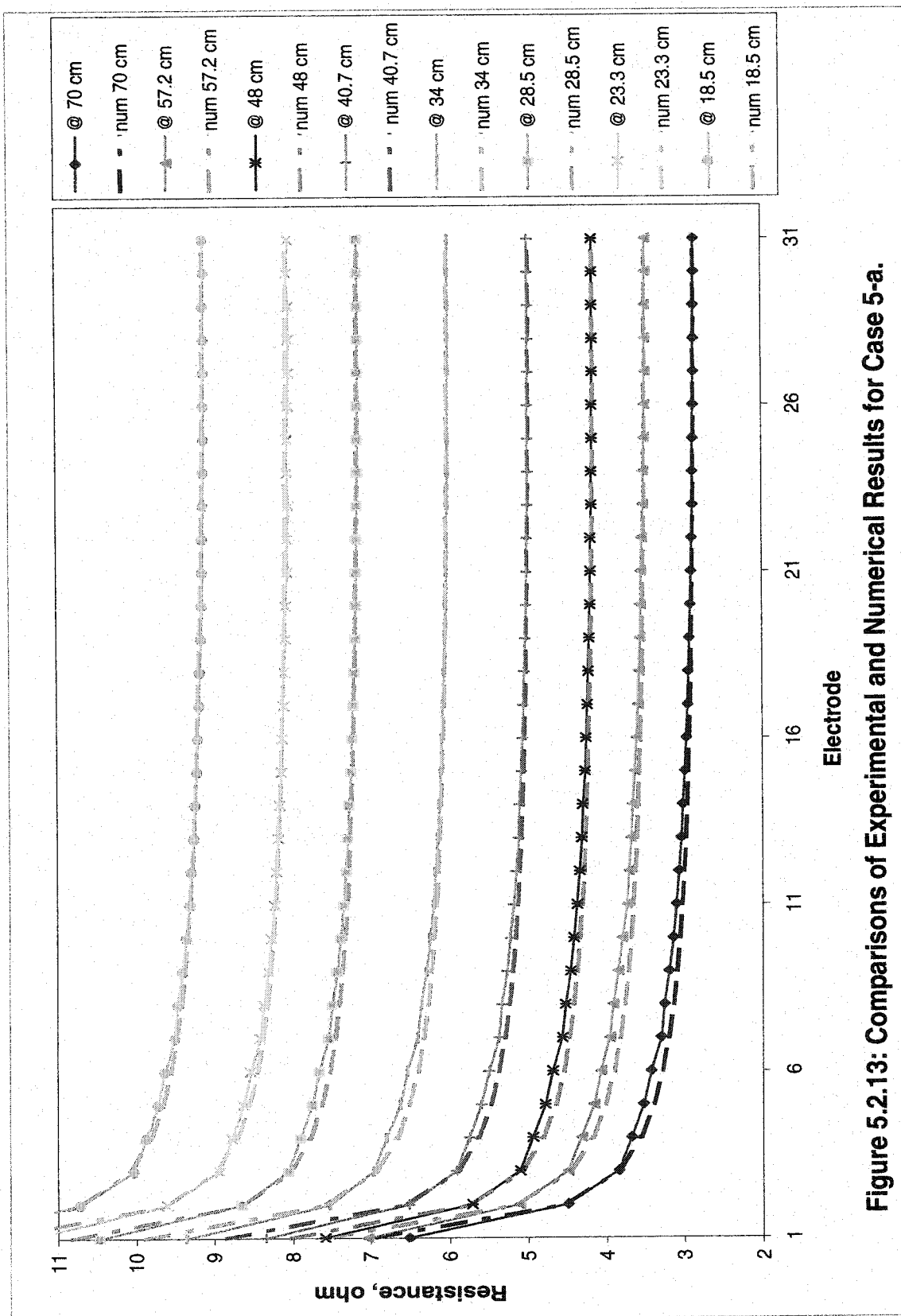
Figure 5.2.13: Comparisons of Experimental and Numerical Results for Case 5-a.
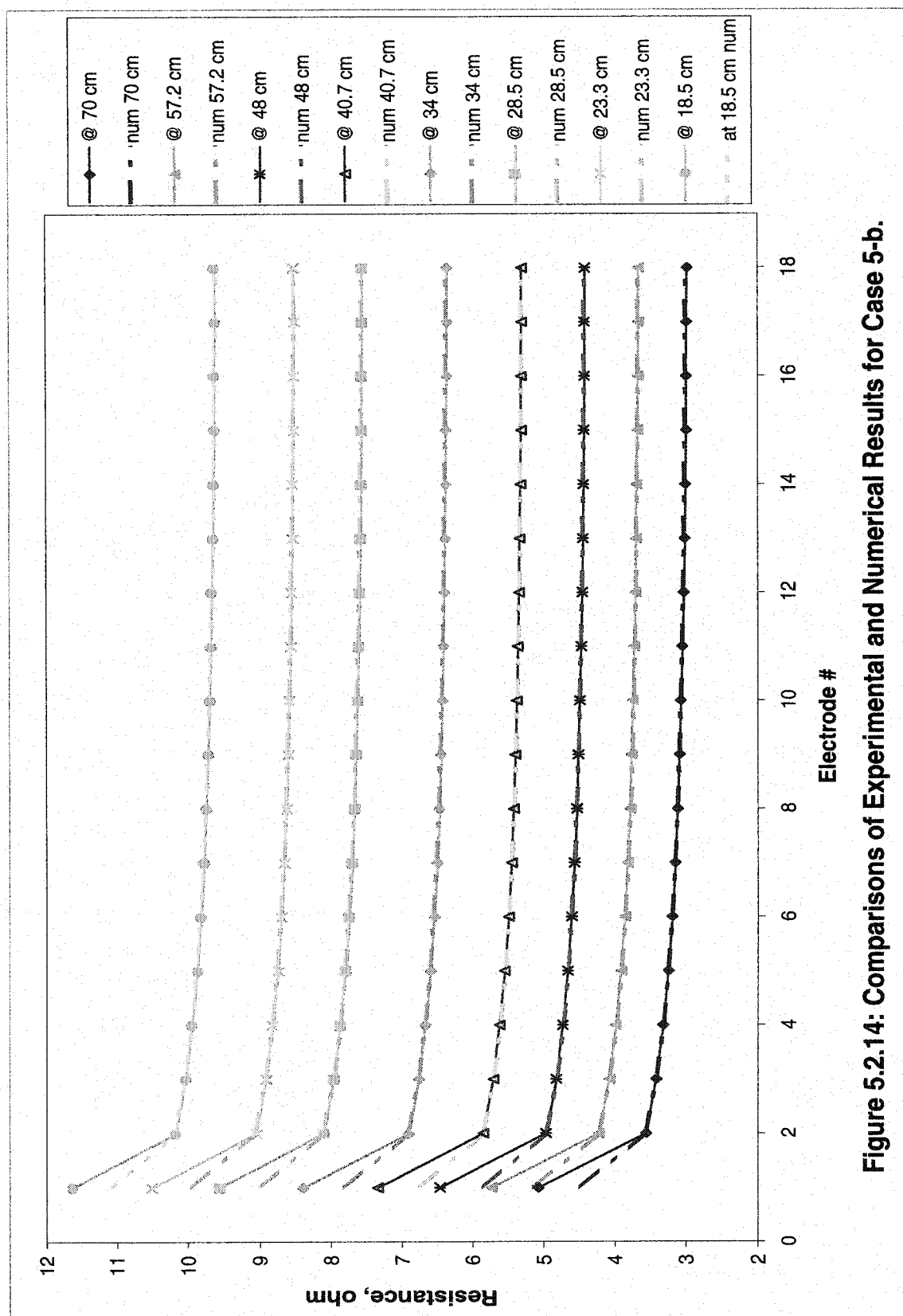
Figure 5.2.14: Comparisons of Experimental and Numerical Results for Case 5-b.

5.4   SUMMARY OF DISCUSSION

The results presented in this work, clearly show that the change of electrical potential due to the displacement of fluid front in a reservoir can be measured. Using the procedures described in this experiment, the fluid front position was detectable up to a distance of twice the length (span) of the electrodes array. Improvement of the measurement accuracy directly translates into an increase of this distance. This can only be done once the actual nature and level of the noise has been characterized. In this study, the noise was exclusively coming from the acquisition system and more especially from its limitation to perform correct measurements in very high impedance environments (created from improper contact of the electrodes with the porous media). This problem is less pronounced in the actual reservoirs. In a field experiment, the noise will have two origins:

- Industrial noise (essentially power supply)

- Natural noise from solar activity

Concerning the first one, the only thing that can be done is to operate at frequencies far from the power supply frequencies (50 and 60 Hz). As for the second source, the best which can be achieved is to operate at frequencies located around the known minimum energy of the natural electrical activity (1-10 Hz) and to use long integration times for the cross-correlation between the source signal and the measured one (lock-in amplifier).

It was also shown that the fluid front position can be detected using measurements from a single well, whether it is an injection or a production well, despite the fact that the measurement conditions (electrodes in brine or in oil) are totally different.

This work was aimed at showing that fluids fronts can be detected and it was not attempted so as to investigate the full inverse problem consisting of deducing from the measurements the exact position of the front. In the very simple case that was treated, there was no need to deal with all the controlling parameters (resistivity and geometry). In an actual case, where the number of unknown parameters is certainly much larger (vertical layering, mixed salinity, noise, etc), the inverse problem is more complex and more measurements are needed to limit the number of possible solutions. One way to increase the number of independent measurements is to use quadru-pole measurements having different vertical extensions. These types of measurements, extensively used in surface exploration, allow one to access resistivity of formation at different lateral distances from the well. This could form the subject of further work.

Chapter 6

CONCLUSIONS AND

SUGGESTIONS

CHAPTER 6

CONCLUSIONS AND SUGGESTIONS

6.1 CONCLUSIONS

Considering the questions asked at the end of chapter one, it could be concluded that:

1. Using a simple electrical method in a scaled model reservoir, it was shown that the displacement (location) of an oil/water front could be detected.

2. Interpretations of the measurements were very easy due to the presence of a minimum number of measurement factors.

3. As the front is detectable,

   a. The maximum distance at which the detection can be reliable depends on the resistivity contrast and on the accuracy of the measurements. In this case, one can safely say that it is possible to detect a front located at a distance of 2 times the thickness (span of the electrodes) of the reservoir.

   b. The technique is very sensitive to the position of the fluid front (potential changes by several tens of mV for a displacement of 1 mm).

117

c. The measurements of resistance or potential drop between electrodes are very simple and can be interpreted easily.

d. By increasing the accuracy of the measurement down to a few microvolts, the maximum distance at which fluid movement is detected can certainly be increased by a factor of 2 or 3.

4. A mathematical model was validated and used successfully to reproduce the experimental data and also to study the various parameters (resistivity of fluid phase, position of front) influencing the measurements.

5. The mathematical model can calculate the change in the potential distribution with the movement of the fluid front position using any electrode in the array with respect to a reference electrode. The model uses only the position of the front and electrodes and the resistivities of different fluid phases as inputs.

6. The numerical model can be used for simulation of any form of fluid movement in a reservoir after a little modification in the input file.

7. With the collected data (using one injection electrode and measurement of potential along an array), it is not possible to delineate the shape of the fluid front approaching the well. This was nevertheless verified that when the model was inclined. However, the measurements clearly reflect change due to the inclination of the front. By taking more measurements (increasing the number of source positions), a simple front orientation can be reconstructed.

6.2 SUGGESTIONS FOR FURTHER WORK

In this study, a number of assumptions and simplifications are made, which may not always be consistent with real field cases. Below is a non-exhaustive list of points that must be considered and whose influence can be tested using the same kind experimental of setup:

a. In most flooding operations, the salinity of the injected water is, in general, different from the reservoir water. In practice, the front will most probably be characterized by a gradual change of resistivity rather than by a sharp contrast. The characteristics of the "buffer zone" are unknown and can probably be simulated by the scaled model.

b. Due to time constraints, measurements were limited to a single source in a "single well" type of measurement condition. Clearly, results can be improved by using, firstly, several current sources, and secondly, cross-well experiments.

c. Fronts are not likely to be perfectly horizontal / vertical; more work is required in order to assess the possibility of describing the shape and orientation of the front.

d. In this study, the reservoir was very simple (uniform permeability and porosity) and was easy to interpret the experimental data. In practice, the interpretation of the measurements will certainly be less straightforward. Introduction of heterogeneities (variations in permeability or porosity) can also be studied.

e. The assessment of doing similar measurements in deviated wells is also worth considering.

f. The same experiment can be transposed to the fields.

g. The numerical model can be validated for planar front movement or inclined advancement of water to the well.

The following recommendations are related to the experimental setup.

1. Glass beads of smaller size should be used to obtain more realistic permeability and irreducible water saturation.

2. Similar laboratory experiments can be used for gas reservoirs undergoing water drives.

3. The fluid front movement can be monitored using similar setup for deviated wells.

NOMENCLATURE

ϕ	Porosity, fraction
k	Permeability, mili-Darcy
cm	Centimeter
ppm	parts per million
cp	Viscosity in Centipoise
Ω	Ohm,
Ω-m	Ohm-meter
J	Current Injected, ampere
V	Potential Distribution, volts
E	Change in Potential, volts
σ	Resistance in ohm
∇	Delta / Gradient
δ	Current Distribution.

REFERENCES

1. Dunlop, K.N., King, G.A., and Breltenbach, E.A.: "Monitoring Oil/Water Fronts by Direct Measurement," *JPT*, May 1991, pp 596-602.

2. Khalaf, A.W.: "Detection of Gas and Water Fronts by Pressure Buildup surveys" *paper SPE* 21336 presented at *SPE* Middle East Oil Show held in Bahrain, 18-19 Noveember, 1991.

3. Mills, A. Andrew: "Reservoir Monitoring in Low-Salinity Environments With Pulsed-Neutron-Capture and Gamma Ray Logs", *SPE* Formation Evaluation, September 1993, pp 177-183.

4. Erga, R., and Knuston, C.A.: "Fluid Distribution in the Beryl Reservoir", *paper SPE* 23080 presented at the Offshore Europe Conference held in Aberdeen, 3-6 September, 1991.

5. Narayan, S., and Dusseault: "Electrical Resistance Tomography for Monitoring Shallow Enhanced Recovery Processes", paper *SPE* 30259 presented at the International Heavy Oil Symposium held in Calgary, Alberta, 19-21 June, 1995.

6. Brady, J.L., Wolcott, D.S., and Ferguson et al: "Water Movement Surveillance with High Resolution Surface Gravity and GPS; A Model Study with Field Test Results", *paper SPE* 30739 presented at the SPE Annual Technical Conference & Exhibition held in Dallas, U.S.A., 22-25 October, 1995.

7. Unneland, T., and Haugland, T.: "Permanent Down hole Gauges Used in Reservoir Management of Complex North Sea Oil Fields," *paper SPE* 26781 presented at the Offshore European Conference held in Aberdeen, 7-10 September, 1993.

8. Philip, A.S., Roy, M.K., and Walter, H.F.: "The Accuracy of Pulsed Neutron Capture Logs for Residual Oil Saturation", *paper SPE* 11148 presented at the 57th Annual Fall Technical Conference and Exhibition of the Society of Petroleum Engineers of AIME, held in New Orleans, LA, 26-29 September, 1982.

9. Donaldson, E.C., Madjidi, A., and White, L.: "Conductivity Mapping to Determine Interwell Fluid Saturation", *Journal of Petroleum Science and Engineering*, vol. 5, pp: 247-259, 1991.

10. Augustin, A.M., Kennedy, W.D., Morison, H.F., and Lee, K.H: "A Theoretical Study of Surface to Borehole Electromagnetic Logging in Cased Holes", Geophysics, vol. 54, no. 1, pp: 90-99, January 1981.

11. Xu, B., and Noel, M.: "On the completeness of Data Sets With Multi-electrode Systems for Electrical Resistivity Survey", *Geophysical prospecting* 41,pp: 791-801, 1993.

12. Poirmeur, C., and Vasseur, G.: "Three Dimensional Modeling of a Hole-to-Hole Electrical Method: Application to the Interpretation of a Field Survey", Geophysics, Vol. 53, no 3, pp: 402-414, March 1988.

13. Gordon, R.M., Lovell, J., Schlumberger-Doll Research; Miriari, M., and Tezaku, K., Japex Research. : "Modeling an Ultra Long Electrical Device; Application in a Fractured Geothermal Reservoir", paper *SPE* presented at the 60th Annual Meeting of Society of Exploration Geoscientists, April 1990.

14. Imamura, S.: "Imaging Technique of Near-Borehole Resistivity Structure from normal Resistivity Logs", SPWLA 33rd Annual Logging Symposium, June 1992.

15. Mansure, A.J., Meldau, R.F., and Weyland, H.V.: "Field Examples of Electrical Resistivity Changes during Steamflooding", SPE Formation Evaluation, pp: 57-64, March 1993.

16. Kleef, R.V., Babour, K.: "Water Flood Monitoring in an Oman Carbonate Reservoir Using a Downhole Permanent Electrode Array", paper *SPE* 68078 presented at the 2001 SPE Middle East Oil Show held in Bahrain, 17-20 March, 2001.

17. Lilley, I.J., Douglas, A.A., Muir, K.R., and Robinson, E.: "Reservoir Monitoring and Wire-line Logging in Sub-sea Wells," paper *SPE* 18357 presented at the SPE European Petroleum Conference, London, UK, 16-19 October, 1998.

18. Shepherd, C.E., Neve, P., and Wilson, D.C.: "Use and Application of Permanent Downhole Pressure Gauges in the Balmoral Field and Satellite Structures," SPE Production Engineering, Volume 6, August 1991, pp 271-276.

19. Narayan, S., and Dusseault: "Electrical Resistance Tomography for Monitoring Shallow Enhanced Recovery Processes", paper *SPE* 30259 presented at the International Heavy Oil Symposium held in Calgary, Alberta, 19-21 June, 1995.

20. Bryant, I. D. et al.: "Utility and Reliability of Cemented Resistivity Arrays in Monitoring Waterflood of the Mansfield Sandstone, Indiana, USA," paper *SPE* 71710 presented at the 2001 *SPE* Annual technical Conference and Exhibition in New Orleans, 30 September – 3 October, 2001.

21. Charara, M., Manin, Y., Bacquet, C., and Delhomme, J.P.: "Use of Permanent Resistivity and Transient-Pressure Measurement for Time-Lapse Saturation Mapping", paper *SPE* 80433 first presented at the 2001 Asia Pacific Improved Oil Recovery Conference in Kuala Lampur, 8-9 October, 2001.

22. Mufti, I. R.: "Finite-Difference Resistivity Modeling for Arbitrarily Shaped Two-Dimensional Structures", paper presented at the 44th Annual International SEG Meeting in Dallas, Texas, November 12, 1974.

23. Johnson, C.: "Numerical Solution of Partial Differential Equations by the Finite Element Method, Studentlitteratur, Lund, Sweden, 1987.

24. Randolph E. B.: "A Software Package for Solving Elliptic Partial Differential Equations", User's Guide 6.0, Society Industrial and Applied Mathematics, Philadelphia, PA, 1990.

25. Carter, P.J., and Morel, E.H.: "Reservoir Monitoring in the Development of Marginal Fields: Ivanhoe, Rob Roy and Hamish," paper *SPE* 20978 presented at Europec 90, The Hague, Netherlands, 22-24 October, 1990.

Appendix A

EXPERIMENTAL DATA

APPENDIX A

EXPERIMENTAL DATA

Apparent resistances measured for different fluid front positions for the 7 cases previously described are presented in the following tables. Resistivity measurements were also performed using the classical 4-point technique. The results obtained by this method were affected by a large noise due to bad contact between some electrodes and the media. Consequently, these results were excluded from the results of this experiment. Two of them are nevertheless presented here as an example in Figure A.4.1 and Figure A.4.2.

Table A.1: Experimental Resistances for case 1-a.

Electrode	100% brine Saturated	Oil front at 10 cm	Oil front at 12.3 cm	Oil front at 14.2 cm	Oil front at 16.8 cm	Oil front at 19.1 cm	Oil front at 21.7 cm	Oil front at 24.4 cm	Oil front at 27.5 cm	Oil front at 3.12 cm
1	88.157	3841.499	3929.159	4056.554	4152.012	4232.615	4558.504	4640.673	4829.121	7066.718
2	36.302	3593.434	3682.358	3803.855	3890.170	3974.564	4292.315	4383.804	4582.170	6757.467
3	13.866	1648.504	1729.978	1805.679	1873.592	1927.961	2149.180	2161.274	2191.482	3436.018
4	11.643	1137.554	1201.366	1245.091	1293.787	1342.047	1457.495	1462.703	1487.063	2328.787
5	9.723	809.405	850.260	874.657	904.864	922.310	964.785	968.388	983.051	1559.496
6	8.867	582.747	621.401	650.280	681.201	704.740	721.676	729.586	748.019	1203.551
7	6.948	345.849	382.297	411.081	437.617	461.050	461.101	540.764	644.152	810.443
8	6.363	267.647	298.529	328.729	356.267	379.798	388.321	434.235	514.301	693.038
9	5.583	186.321	214.319	244.502	271.647	295.431	299.155	358.157	430.875	559.043
10	5.082	130.929	157.935	186.360	212.698	236.340	243.029	298.058	366.504	468.690
11	4.566	93.921	118.363	145.135	170.148	193.528	204.186	251.302	320.250	406.503
12	4.194	70.092	91.668	116.762	140.208	162.589	175.271	218.541	277.302	362.336
13	3.901	55.022	73.884	96.052	117.811	138.876	151.956	184.201	243.365	324.044
14	3.726	45.379	61.950	81.269	100.266	119.648	132.945	166.782	214.589	291.280
15	3.539	32.519	45.910	61.827	78.931	96.299	110.530	149.623	195.658	253.286
16	3.230	27.403	39.453	54.337	70.651	87.383	102.049	136.320	182.306	239.791
17	3.090	22.840	33.401	46.926	61.855	77.525	92.197	120.307	166.304	224.657
18	3.004	19.400	28.717	40.633	53.997	68.777	82.972	103.541	144.705	205.218
19	2.861	14.329	21.471	31.462	43.051	56.521	69.922	91.521	130.219	182.264
20	2.752	10.395	16.022	24.129	33.806	46.098	58.696	81.396	111.437	162.591
21	2.664	8.889	13.849	20.982	29.721	41.353	53.774	73.608	100.025	153.122
22	2.549	7.015	10.983	17.042	25.013	35.511	47.023	64.502	92.625	141.178
23	2.489	5.535	8.732	13.989	21.345	31.177	42.634	58.220	87.592	133.378
24	2.506	4.507	7.150	11.632	18.276	27.198	38.389	54.524	83.234	125.624
25	2.452	3.938	6.204	10.266	16.422	24.760	35.596	52.621	79.109	119.980
26	2.416	3.361	5.275	8.856	14.404	22.344	32.776	49.520	75.728	114.222
27	2.378	3.032	4.685	7.928	13.172	20.841	31.165	47.632	71.592	110.420
28	2.358	2.857	4.360	7.415	12.468	19.972	30.138	45.214	69.221	108.327
29	2.309	2.653	4.033	6.932	11.822	19.184	29.232	43.032	66.527	106.491
30	2.281	2.641	3.924	6.675	11.425	18.638	28.523	43.201	66.219	105.141
31	2.271	2.478	3.714	6.406	11.085	18.249	28.089	43.512	65.059	104.451

Table A.1 (continued): **Experimental Resistances for case 1-a.**

Electrode	Oil front at 36.5 cm	Oil front at 40.2 cm	Oil front at 44 cm	Oil front at 49.2 cm	Oil front at 60.9 cm	Oil front at 70.4 cm	Oil front at 78.5 cm	Oil front at 86.2 cm
1	7304.565	7817.771	8951.313	10104.195	13840.082	28766.306	39511.502	46098.335
2	7183.919	7494.392	8571.111	9762.737	13648.458	34059.957	44598.940	48905.196
3	3653.271	3779.346	4204.251	4779.086	6511.876	14295.340	4783.548	7227.414
4	2462.622	2574.415	2821.382	3279.136	4428.185	13270.714	18895.859	22122.155
5	1616.700	1665.363	1800.858	1969.576	2418.649	8183.761	10160.103	14445.605
6	1275.541	1320.170	1433.296	1550.925	1874.400	6390.207	10881.434	14642.951
7	874.548	913.670	991.492	1068.179	1263.458	3815.436	6627.996	9734.785
8	749.516	783.657	857.326	911.633	1106.207	2588.164	5282.718	7885.640
9	611.607	639.359	701.100	748.034	964.460	1523.634	2670.210	3840.659
10	521.537	548.987	609.886	645.983	768.484	1431.502	2905.121	3883.676
11	460.276	487.762	545.275	579.260	646.145	878.312	1603.821	2356.499
12	418.349	446.459	499.523	532.227	586.911	732.112	1832.951	2795.339
13	378.013	405.028	457.376	489.166	532.531	625.272	1442.889	2088.740
14	342.792	369.532	421.964	451.854	493.521	612.344	1377.620	2007.435
15	301.653	329.062	384.397	414.170	451.189	501.799	877.828	1323.509
16	287.992	315.368	365.956	397.141	433.166	470.524	645.057	843.906
17	272.449	298.702	346.260	376.989	411.840	439.150	603.247	831.673
18	248.301	272.464	320.925	350.818	385.167	402.915	505.289	645.378
19	227.512	251.211	300.883	328.423	347.160	349.032	443.056	616.067
20	208.445	233.248	283.080	307.422	323.762	355.294	455.235	573.319
21	198.898	223.332	273.430	301.620	330.884	340.007	388.380	452.267
22	186.813	212.083	261.980	290.997	321.259	343.711	375.559	406.018
23	179.542	205.210	256.316	286.326	318.648	342.238	362.052	377.607
24	172.084	197.970	248.768	279.159	311.793	335.422	353.783	367.776
25	166.146	191.820	241.821	270.459	301.594	326.131	344.486	358.653
26	160.190	185.974	236.303	266.726	298.088	321.659	338.445	351.424
27	156.311	182.005	232.031	262.309	294.211	317.962	334.573	347.198
28	154.251	179.965	230.094	261.995	292.871	316.438	332.715	345.161
29	152.132	177.763	227.779	258.578	290.469	314.143	330.355	342.512
30	150.770	176.466	226.436	257.342	289.340	313.235	329.296	341.511
31	150.127	175.849	225.984	257.096	289.156	312.609	328.831	340.763

Table A.2: Numerical Resistances for case 1-a.

Electrode	100% brine saturated	Oil front at 10 cm	Oil front at 12.3 cm	Oil front at 14.2 cm	Oil front at 16.8 cm	Oil front at 19.1 cm	Oil front at 21.7 cm	Oil front at 24.4 cm	Oil front at 27 cm	Oil front at 36.5 cm	Oil front at 40.2 cm	Oil front at 44 cm	Oil front at 49.2 cm	Oil front at 60.9 cm
2	1.406	199.874	195.829	202.000	205.349	169.665	167.797	169.590	168.386	204.150	215.221	216.960	240.313	241.566
3	0.904	109.224	109.613	115.596	118.891	100.123	99.786	101.568	101.887	125.262	133.237	134.974	150.283	151.846
4	0.680	69.438	71.566	77.248	80.454	69.125	69.453	71.217	72.187	90.008	96.594	98.330	110.043	111.744
5	0.553	47.510	50.394	55.701	58.791	51.571	52.258	53.997	55.307	69.951	75.742	77.477	87.142	88.921
6	0.467	33.475	36.651	41.528	44.476	39.890	40.796	42.505	44.012	56.508	61.761	63.493	71.785	73.616
7	0.406	23.968	27.165	31.578	34.363	31.558	32.601	34.274	35.893	46.822	51.682	53.411	60.712	62.582
8	0.360	17.475	20.534	24.487	27.098	25.498	26.625	28.256	29.930	39.685	44.251	45.977	52.547	54.443
9	0.324	12.809	15.638	19.139	21.563	20.816	21.988	23.574	25.264	34.080	38.410	40.132	46.126	48.044
10	0.296	9.451	12.002	15.076	17.310	17.157	18.348	19.885	21.564	29.613	33.751	35.469	41.003	42.938
11	0.273	7.009	9.266	11.945	13.989	14.246	15.436	16.923	18.570	25.980	29.957	31.670	36.828	38.777
12	0.253	5.222	7.189	9.508	11.367	11.900	13.075	14.509	16.112	22.977	26.816	28.524	33.371	35.331
13	0.237	3.905	5.596	7.593	9.272	9.984	11.134	12.514	14.062	20.457	24.175	25.878	30.463	32.432
14	0.224	2.936	4.377	6.088	7.597	8.418	9.533	10.860	12.347	18.332	21.946	23.643	28.005	29.983
15	0.212	2.218	3.433	4.894	6.244	7.121	8.198	9.472	10.893	16.517	20.037	21.730	25.901	27.885
16	0.202	1.685	2.703	3.944	5.147	6.044	7.078	8.299	9.655	14.957	18.394	20.081	24.087	26.076
17	0.193	1.289	2.136	3.188	4.255	5.146	6.136	7.306	8.596	13.611	16.974	18.655	22.518	24.512
18	0.185	0.995	1.695	2.586	3.530	4.397	5.343	6.464	7.689	12.448	15.743	17.420	21.158	23.156
19	0.179	0.776	1.353	2.105	2.939	3.772	4.672	5.747	6.911	11.441	14.676	16.347	19.977	21.979
20	0.173	0.612	1.086	1.719	2.454	3.246	4.103	5.134	6.240	10.565	13.745	15.411	18.946	20.950
21	0.168	0.490	0.878	1.412	2.059	2.807	3.624	4.613	5.665	9.808	12.938	14.600	18.052	20.059
22	0.164	0.400	0.716	1.166	1.737	2.441	3.219	4.170	5.173	9.154	12.240	13.897	17.278	19.287
23	0.160	0.332	0.591	0.971	1.476	2.136	2.878	3.796	4.754	8.592	11.640	13.293	16.612	18.623
24	0.157	0.281	0.493	0.816	1.264	1.884	2.594	3.481	4.399	8.114	11.128	12.777	16.043	18.055
25	0.154	0.244	0.419	0.695	1.095	1.680	2.362	3.222	4.106	7.716	10.700	12.346	15.568	17.581
26	0.152	0.216	0.362	0.599	0.960	1.513	2.170	3.007	3.862	7.382	10.341	11.984	15.168	17.183
27	0.150	0.196	0.319	0.527	0.856	1.383	2.020	2.838	3.669	7.116	10.055	11.696	14.851	16.866
28	0.149	0.182	0.288	0.474	0.779	1.285	1.907	2.711	3.522	6.914	9.838	11.476	14.608	16.624
29	0.148	0.173	0.267	0.437	0.725	1.215	1.826	2.618	3.416	6.767	9.679	11.316	14.431	16.447
30	0.147	0.167	0.255	0.416	0.693	1.175	1.778	2.564	3.353	6.680	9.585	11.221	14.327	16.343
31	0.147	0.165	0.250	0.408	0.682	1.160	1.761	2.544	3.331	6.649	9.551	11.187	14.289	16.306

Table A.3: Experimental Resistances for case 1-b.

Electrode	Brine	10 cm	12.3 cm	14.2 cm	16.8 cm	19.1 cm	21.7 cm	24.4 cm	27.5 cm
1	37.047	1847.33	1961.90	2070.86	2172.66	2258.54	2613.39	2715.76	2815.81
2	8.555	601.393	680.340	751.937	810.279	860.893	951.561	990.459	1028.270
3	6.757	342.486	409.987	471.843	522.996	567.937	634.761	671.071	704.398
4	5.901	221.429	278.389	332.868	379.025	419.843	469.685	505.919	537.207
5	5.068	135.474	180.508	227.106	268.143	305.682	349.006	384.312	414.028
6	4.525	89.235	125.689	165.727	202.680	237.423	276.753	310.812	339.128
7	4.048	59.346	87.435	120.285	152.132	183.480	218.161	250.255	277.027
8	3.707	40.703	62.389	89.248	116.714	144.740	177.032	207.695	233.812
9	3.419	27.715	44.237	65.880	89.241	114.137	144.207	173.068	197.970
10	3.208	20.189	33.074	50.914	71.080	93.407	121.246	148.485	172.406
11	3.052	14.989	25.100	39.724	57.007	76.953	101.484	127.141	149.929
12	2.884	10.331	17.812	29.361	43.834	61.443	84.361	108.689	130.506
13	2.620	7.264	12.633	21.564	33.467	48.824	69.507	92.169	112.892
14	2.645	5.626	9.851	17.286	27.711	41.759	61.730	83.611	103.923
15	2.528	4.217	7.236	13.031	21.766	34.102	52.329	72.949	92.498
16	2.495	3.706	6.232	11.339	19.339	30.964	48.460	68.518	87.690
17	2.441	3.272	5.242	9.496	16.551	27.219	43.740	62.973	81.616
18	2.414	2.914	4.604	8.442	15.072	25.319	41.472	60.381	78.848

Table A.3 (continued): Experimental Resistances for case 1-b.

Electrode	30.2 cm	33.1 cm	36.5 cm	40.2 cm	44 cm	49.4 cm	60.9 cm	70.4 cm	78.5 cm
1	2943.38	3074.84	3216.96	3352.62	3869.95	4222.99	5091.01	5976.28	6751.63
2	1128.29	1174.46	1216.35	1261.81	1390.96	1462.91	1582.62	1675.22	1734.69
3	785.95	822.79	856.05	894.27	988.99	1042.24	1113.55	1170.61	1202.08
4	606.09	638.37	669.58	704.70	782.89	828.67	882.65	924.47	947.59
5	473.58	503.27	532.51	564.77	633.01	672.75	715.94	749.51	767.50
6	391.76	420.32	448.09	479.13	541.68	579.00	617.91	648.74	668.47
7	323.94	351.52	378.41	409.03	468.49	503.84	539.46	566.58	581.84
8	277.11	303.24	328.89	357.94	413.91	447.90	481.04	505.67	520.39
9	237.96	263.56	288.24	316.74	370.94	404.23	436.41	459.94	474.38
10	209.69	234.69	258.70	286.75	340.62	373.67	405.75	428.51	443.26
11	184.72	209.26	232.66	259.97	312.20	344.66	375.32	396.93	410.33
12	163.25	187.41	210.62	237.76	289.80	322.21	352.70	374.06	387.62
13	143.54	167.22	190.09	216.84	267.97	300.01	329.90	351.05	365.08
14	133.79	157.39	180.45	207.26	258.59	290.64	321.06	342.38	356.17
15	121.00	144.27	167.24	193.83	245.08	276.99	306.83	328.18	342.03
16	115.55	138.57	161.36	187.80	238.68	270.44	300.22	321.68	335.73
17	108.68	131.50	154.14	180.47	231.00	262.78	292.47	313.97	327.99
18	105.53	128.24	150.81	177.00	227.15	258.83	289.10	310.66	324.76

Table A.4: Numerical Resistances for case 1-b

Electrode	Brine	10 cm	12.3 cm	14.2 cm	16.8 cm	19.1 cm	21.7 cm	24.4 cm	27.5 cm
1	1.266	120.426	93.079	96.033	95.949	138.697	109.000	125.916	136.636
2	0.584	36.120	30.947	33.774	35.491	51.770	42.804	50.251	55.287
3	0.469	22.933	20.850	23.494	25.398	37.233	31.660	37.496	41.563
4	0.395	15.099	14.610	17.030	18.972	27.960	24.496	29.285	32.719
5	0.342	10.067	10.402	12.574	14.471	21.447	19.412	23.444	26.421
6	0.303	6.756	7.472	9.387	11.185	16.678	15.639	19.098	21.726
7	0.271	4.498	5.343	6.996	8.659	12.996	12.678	15.674	18.020
8	0.248	3.074	3.905	5.323	6.841	10.333	10.493	13.139	15.268
9	0.229	2.103	2.853	4.052	5.418	8.237	8.736	11.090	13.038
10	0.214	1.454	2.097	3.101	4.316	6.607	7.336	9.449	11.245
11	0.201	1.019	1.551	2.387	3.460	5.332	6.213	8.126	9.795
12	0.191	0.727	1.158	1.850	2.794	4.334	5.310	7.055	8.618
13	0.183	0.532	0.875	1.446	2.276	3.552	4.585	6.191	7.665
14	0.176	0.401	0.671	1.145	1.876	2.945	4.006	5.498	6.898
15	0.171	0.313	0.526	0.922	1.570	2.479	3.552	4.951	6.290
16	0.166	0.255	0.425	0.760	1.342	2.129	3.204	4.530	5.821
17	0.163	0.218	0.355	0.647	1.178	1.878	2.949	4.221	5.476
18	0.161	0.195	0.312	0.574	1.071	1.713	2.779	4.014	5.245

Table A.4 (continued): Numerical Resistances for case 1-b

Electrode	30.2 cm	33 cm	36.5 cm	40.2 cm	44 cm	49.4 cm	60.9 cm	70.4 cm	78.5 cm
1	149.440	158.731	169.529	177.443	205.272	202.390	206.281	204.721	202.649
2	61.463	66.021	71.142	75.271	87.962	87.918	90.863	91.195	91.015
3	46.611	50.366	54.526	58.014	68.147	68.581	71.367	72.019	72.158
4	37.034	40.268	43.807	46.880	55.362	56.104	58.787	59.646	59.991
5	30.207	33.066	36.160	38.937	46.241	47.201	49.812	50.817	51.310
6	25.111	27.688	30.449	33.002	39.425	40.548	43.104	44.220	44.822
7	21.081	23.433	25.927	28.303	34.027	35.279	37.792	38.995	39.684
8	18.083	20.264	22.559	24.801	30.005	31.351	33.833	35.100	35.855
9	15.648	17.688	19.820	21.953	26.732	28.155	30.612	31.932	32.739
10	13.687	15.611	17.610	19.654	24.090	25.574	28.010	29.373	30.223
11	12.096	13.923	15.814	17.784	21.942	23.475	25.895	27.292	28.176
12	10.801	12.549	14.350	16.260	20.189	21.762	24.169	25.594	26.507
13	9.748	11.431	13.159	15.019	18.762	20.367	22.763	24.212	25.148
14	8.900	10.528	12.196	14.016	17.609	19.239	21.627	23.094	24.048
15	8.226	9.810	11.431	13.218	16.691	18.341	20.722	22.204	23.173
16	7.705	9.255	10.838	12.600	15.979	17.645	20.022	21.515	22.495
17	7.320	8.845	10.400	12.143	15.454	17.132	19.504	21.006	21.995
18	7.062	8.569	10.106	11.837	15.101	16.786	19.156	20.663	21.658

Table A.5: Experimental Resistances for case 2-a.

Electrode	5.5 cm	12.1 cm	14.3 cm	19.6 cm	22.3 cm	25.4 cm	42.9 cm	55 cm	61.9 cm	75 cm	86.3 cm	96.5 cm
1	64767.625	61491.188	46267.124	45945.970	49179.279	52115.327	32924.421	34523.286	56055.752	75791.94	40310.379	39857.571
2	75753.410	70032.711	51581.698	50289.350	56940.281	59213.042	35574.186	36603.340	61741.025	76085.91	42560.494	39847.129
3	25611.680	22617.673	18104.389	18454.435	19238.368	19797.085	16246.834	17322.416	21338.403	26229.70	6636.418	4351.530
4	16519.773	15033.965	12934.861	12139.609	13187.732	13480.790	11672.677	12091.334	15743.081	27984.17	18918.529	14802.492
5	11327.239	9478.664	8558.315	8085.905	8416.293	8452.105	7822.550	7971.743	10290.541	19714.88	12043.461	7850.368
6	8769.050	7390.254	6613.785	6299.425	6545.091	6870.580	6400.469	6807.733	8361.335	12157.55	14426.049	11145.308
7	3955.401	3302.388	3061.015	3969.154	4089.291	4119.725	3066.852	3133.727	4187.350	8022.894	10275.800	7552.372
8	3426.080	2786.634	2563.827	2538.729	2613.048	2703.065	2130.474	2187.037	2936.953	6219.984	10347.935	5409.604
9	1294.415	1153.351	1289.621	1306.961	1363.713	1409.261	1240.135	1312.991	1567.451	4397.804	2058.212	4265.064
10	952.670	938.635	988.188	1048.269	1093.919	1138.505	1059.155	1108.566	1325.543	2928.509	5180.756	3989.948
11	669.921	759.537	829.422	891.522	936.210	956.182	921.843	965.191	1057.167	1705.918	4340.041	3405.831
12	512.245	618.128	675.321	727.783	768.351	801.072	795.499	814.461	911.172	1250.928	3822.429	3286.131
13	412.649	486.483	540.591	595.215	647.922	688.245	672.064	695.705	793.021	1073.477	3013.428	2992.387
14	305.103	381.602	447.205	506.767	531.055	575.042	578.831	621.063	708.096	913.471	2353.798	2862.201
15	250.670	302.090	375.850	435.862	459.352	483.405	518.370	552.224	634.910	774.259	1534.214	2254.514
16	208.791	245.428	299.674	365.505	376.728	412.755	467.761	498.474	576.784	685.603	1298.362	1746.156
17	153.568	192.943	244.705	299.933	322.587	354.939	427.585	453.255	527.670	628.478	1175.521	1375.398
18	115.451	163.406	206.391	245.487	287.798	305.132	390.657	407.390	480.697	575.229	1086.132	1177.186
19	95.847	136.473	158.911	202.353	245.848	267.771	358.816	375.778	442.118	530.475	983.857	1118.903
20	78.253	109.025	133.534	168.667	210.048	235.948	327.621	350.956	408.633	487.226	771.654	1050.367
21	57.269	85.465	113.759	142.827	180.333	205.094	304.372	328.819	381.286	446.907	643.770	854.899
22	42.261	65.294	98.515	125.856	157.464	179.482	288.224	312.906	356.575	411.967	571.789	580.184
23	28.173	52.192	80.796	112.003	132.179	163.353	276.051	298.704	337.078	379.297	427.693	436.086
24	23.049	42.731	64.449	99.611	121.605	149.395	265.663	288.148	322.485	362.238	396.162	400.873
25	18.393	37.716	54.435	92.347	114.207	138.828	256.230	280.536	310.764	350.342	379.387	382.747
26	13.282	30.639	46.698	87.418	109.450	132.977	249.959	273.551	302.943	340.194	362.916	365.328
27	12.538	28.129	43.485	83.093	105.235	128.668	244.072	268.936	295.390	335.773	356.307	358.634
28	9.279	24.633	39.785	78.984	100.931	125.290	241.433	265.435	291.690	332.844	352.457	354.623
29	10.430	24.544	38.954	77.752	99.757	123.226	239.720	262.678	287.916	331.204	349.202	351.441
30	8.772	23.011	38.2631	75.995	97.941	121.407	238.498	261.534	285.740	330.164	348.204	350.624
31	7.047	21.533	37.428	74.268	96.188	119.461	237.650	260.600	284.540	329.027	347.410	349.661

Table A.6: Numerical Resistances for case 2-a.

Electrode	5.5 cm	12.1 cm	14.3 cm	19.6 cm	22.3 cm	25.4 cm	42.9 cm	55 cm	61.9 cm	75 cm	86.3 cm	96.5 cm
1	6283.279	2802.086	2627.833	3176.069	2636.209	2279.463	1353.054	1358.983	1422.804	1524.885	1568.225	1571.670
2	2230.745	1063.695	1005.293	1205.926	1013.613	888.558	541.636	547.548	576.578	620.689	640.839	644.281
3	1163.900	601.247	573.526	681.933	581.663	517.947	325.251	331.106	350.808	379.424	393.365	396.796
4	704.975	396.517	382.189	450.090	390.036	353.089	228.759	234.518	249.994	271.652	282.793	286.204
5	459.899	281.995	274.951	320.532	282.447	260.084	174.080	179.712	192.722	210.387	219.906	223.291
6	309.178	207.149	204.642	235.982	211.749	198.537	137.652	143.125	154.421	169.374	177.778	181.130
7	211.619	155.060	155.475	177.248	162.183	154.975	111.630	116.915	126.915	139.877	147.447	150.760
8	148.082	118.329	120.571	135.922	126.908	123.607	92.670	97.749	106.734	118.194	125.122	128.390
9	104.505	90.961	94.335	105.203	100.335	99.649	77.984	82.836	90.968	101.215	107.611	110.828
10	74.503	70.452	74.458	82.242	80.169	81.182	66.475	71.088	78.487	87.735	93.679	96.842
11	53.570	54.883	59.168	64.851	64.638	66.716	57.291	61.655	68.411	76.814	82.366	85.470
12	38.813	42.957	47.276	51.557	52.552	55.252	49.863	53.975	60.155	67.833	73.036	76.078
13	28.290	33.733	37.918	41.291	43.040	46.058	43.775	47.634	53.290	60.333	65.221	68.200
14	20.778	26.603	30.549	33.362	35.549	38.679	38.774	42.385	47.565	54.049	58.651	61.564
15	15.350	21.041	24.683	27.175	29.585	32.690	34.618	37.986	42.729	48.714	53.054	55.900
16	11.407	16.687	19.993	22.326	24.815	27.809	31.147	34.282	38.623	44.160	48.258	51.037
17	8.532	13.273	16.237	18.514	20.989	23.822	28.241	31.154	35.125	40.261	44.134	46.847
18	6.428	10.594	13.222	15.509	17.911	20.559	25.805	28.508	32.141	36.915	40.581	43.230
19	4.881	8.486	10.799	13.132	15.428	17.882	23.757	26.265	29.591	34.038	37.515	40.100
20	3.732	6.818	8.838	11.235	13.410	15.673	22.028	24.355	27.399	31.552	34.854	37.379
21	2.882	5.505	7.262	9.728	11.777	13.860	20.577	22.739	25.530	29.421	32.562	35.031
22	2.249	4.468	5.992	8.525	10.451	12.370	19.358	21.372	23.936	27.592	30.589	33.005
23	1.776	3.650	4.971	7.565	9.376	11.148	18.339	20.220	22.582	26.033	28.900	31.266
24	1.422	3.007	4.154	6.801	8.507	10.151	17.492	19.257	21.442	24.713	27.465	29.787
25	1.161	2.509	3.512	6.201	7.817	9.352	16.803	18.467	20.503	23.620	26.273	28.557
26	0.963	2.118	2.999	5.723	7.260	8.704	16.235	17.814	19.721	22.706	25.274	27.524
27	0.820	1.825	2.610	5.360	6.834	8.204	15.792	17.302	19.105	21.985	24.483	26.705
28	0.719	1.611	2.324	5.093	6.518	7.833	15.459	16.916	18.638	21.436	23.881	26.081
29	0.650	1.462	2.122	4.904	6.293	7.567	15.220	16.637	18.300	21.039	23.444	25.627
30	0.611	1.376	2.006	4.794	6.162	7.413	15.080	16.474	18.102	20.805	23.187	25.360
31	0.597	1.345	1.964	4.755	6.115	7.357	15.029	16.415	18.030	20.720	23.093	25.263

Table A.7: Experimental Resistances for case 2-b.

Electr.	73.2 cm	65.5 cm	55 cm	46.3 cm	33.9 cm	25.4 cm	19.6 cm	14.3 cm	9.9 cm	5.5 cm
1	106558	120760	105154	73358	77229	76455.1	69244.5	87426.2	96136.0	103434
2	2140.10	2092.77	2060.16	2070.17	2038.57	2004.66	1972.13	1932.78	1872.77	1849.50
3	1336.42	1313.14	1292.13	1282.02	1258.88	1202.54	1163.80	1123.34	1070.83	1041.60
4	1035.06	1012.29	983.42	974.69	955.26	892.54	857.58	810.54	752.56	719.45
5	842.82	822.14	795.92	776.54	757.96	700.62	667.03	624.58	568.95	537.59
6	724.77	707.66	682.11	659.46	642.11	587.03	555.20	515.16	461.94	432.73
7	633.80	617.19	590.00	569.51	549.32	491.06	456.26	417.22	363.12	334.02
8	555.51	539.46	512.75	486.40	468.96	408.97	375.69	338.29	287.86	260.48
9	510.24	496.38	466.28	441.31	423.68	361.25	326.71	289.48	238.45	211.07
10	475.60	460.69	431.82	405.91	387.24	326.98	291.78	256.39	207.01	181.85
11	439.56	425.85	398.17	374.21	352.41	290.78	255.19	220.53	171.56	147.57
12	412.44	398.06	371.25	341.61	323.69	260.99	228.30	192.03	146.03	123.62
13	392.31	379.88	350.75	323.62	304.03	241.20	207.47	172.26	125.49	102.03
14	380.84	367.02	336.21	308.18	289.70	225.92	195.07	160.88	113.67	91.24
15	368.87	354.36	325.01	295.27	277.85	212.50	179.04	144.00	98.20	76.08
16	361.39	347.24	317.87	287.59	269.82	204.52	171.37	135.13	90.56	69.32
17	353.70	342.42	314.06	284.76	265.08	200.14	162.40	131.31	86.81	65.37
18	348.59	339.86	312.28	282.81	263.55	196.45	157.61	128.61	83.49	62.37

Table A.8: Numerical Resistances for case 2-b.

Electrode	73.2 cm	65.5 cm	55 cm	46.3 cm	33.9 cm	25.4 cm	19.6 cm	14.3 cm	12.1 cm	9.9 cm
1	213.570	211.019	203.997	202.299	218.024	220.588	223.980	212.405	216.941	214.483
2	96.259	93.709	90.471	88.773	93.146	91.929	91.543	85.657	84.562	82.142
3	76.444	73.894	71.295	69.597	72.053	70.202	69.187	64.278	62.291	59.929
4	63.658	61.108	58.922	57.224	58.443	56.188	54.773	50.506	47.989	45.701
5	54.535	51.985	50.093	48.395	48.733	46.192	44.499	40.702	37.850	35.649
6	47.718	45.168	43.495	41.798	41.478	38.727	36.832	33.397	30.336	28.233
7	42.319	39.769	38.271	36.573	35.732	32.818	30.771	27.634	24.449	22.454
8	38.295	35.745	34.376	32.679	31.450	28.419	26.263	23.357	20.116	18.227
9	35.020	32.470	31.208	29.511	27.966	24.842	22.603	19.895	16.640	14.860
10	32.376	29.826	28.649	26.952	25.154	21.957	19.656	17.114	13.877	12.203
11	30.226	27.676	26.568	24.872	22.867	19.613	17.267	14.866	11.667	10.096
12	28.472	25.922	24.870	23.174	21.001	17.703	15.323	13.043	9.895	8.419
13	27.043	24.493	23.488	21.792	19.482	16.150	13.745	11.568	8.476	7.088
14	25.888	23.338	22.370	20.674	18.254	14.895	12.473	10.382	7.348	6.038
15	24.968	22.418	21.480	19.784	17.277	13.897	11.463	9.443	6.464	5.220
16	24.256	21.706	20.791	19.095	16.520	13.125	10.682	8.718	5.788	4.599
17	23.730	21.180	20.282	18.586	15.961	12.555	10.107	8.186	5.295	4.148
18	23.376	20.826	19.940	18.244	15.585	12.172	9.721	7.829	4.966	3.849

Table A.9: Experimental Resistances for case 3-a.

Electr.	Only brine	70 cm	57.2 cm	48 cm	40.7 cm	34 cm	28.5 cm	23.3 cm	18.5 cm
1	88.157	63.617	80.342	103.000	116.881	132.711	147.848	159.104	172.512
2	36.302	26.648	43.433	67.371	81.905	98.952	114.869	126.826	139.970
3	13.866	17.436	33.955	57.868	72.433	89.588	105.556	117.627	131.083
4	11.643	15.010	31.495	55.399	69.966	87.132	103.107	115.177	128.637
5	9.723	12.752	29.244	53.146	67.723	84.892	100.874	112.943	126.417
6	8.867	11.366	27.867	51.785	66.374	83.546	99.533	111.612	125.087
7	6.948	9.467	26.019	49.929	64.505	81.684	97.666	109.751	123.220
8	6.363	8.880	25.384	49.301	63.892	81.076	97.063	109.151	122.621
9	5.583	7.953	24.429	48.333	62.935	80.140	96.127	108.211	121.682
10	5.082	7.301	23.769	47.674	62.286	79.490	95.481	107.565	121.036
11	4.566	6.642	23.103	47.010	61.624	78.826	94.819	106.904	120.375
12	4.194	6.187	22.656	46.573	61.196	78.398	94.396	106.487	119.959
13	3.901	5.747	22.223	46.149	60.782	77.980	93.989	106.086	119.556
14	3.726	5.487	21.949	45.876	60.514	77.712	93.724	105.822	119.296
15	3.539	5.098	21.564	45.493	60.137	77.337	93.353	105.457	118.930
16	3.230	4.867	21.335	45.273	59.920	77.123	93.145	105.252	118.725
17	3.090	4.581	21.049	44.990	59.646	76.847	92.871	104.981	118.454
18	3.004	4.429	20.894	44.845	59.504	76.710	92.740	104.853	118.325
19	2.861	4.199	20.664	44.619	59.282	76.489	92.519	104.638	118.109
20	2.752	4.031	20.495	44.455	59.123	76.328	92.366	104.486	117.962
21	2.664	3.901	20.376	44.343	59.016	76.220	92.263	104.387	117.865
22	2.549	3.788	20.266	44.244	58.925	76.128	92.178	104.306	117.787
23	2.489	3.672	20.134	44.115	58.802	76.007	92.060	104.192	117.671
24	2.506	3.589	20.070	44.062	58.755	75.961	92.019	104.156	117.640
25	2.452	3.513	20.004	44.004	58.702	75.907	91.972	104.114	117.601
26	2.416	3.455	19.948	43.958	58.662	75.866	91.937	104.084	117.574
27	2.378	3.398	19.888	43.906	58.614	75.821	91.897	104.047	117.536
28	2.358	3.362	19.851	43.876	58.590	75.796	91.878	104.033	117.523
29	2.309	3.322	19.811	43.845	58.565	75.771	91.859	104.018	117.515
30	2.281	3.299	19.790	43.831	58.555	75.759	91.854	104.015	117.514
31	2.271	3.285	19.782	43.835	58.565	75.769	91.870	104.036	117.538

138

Table A.10: Numerical Resistances for case 3-a.

Electrode	Only brine	70 cm	57.2 cm	48 cm	40.7 cm	34 cm	28.5 cm	23.3 cm	18.5 cm
1	3.342	3.984	5.025	6.563	7.416	8.505	9.353	10.134	10.933
2	1.429	1.723	2.765	4.302	5.213	6.302	7.267	8.047	8.904
3	0.919	1.120	2.161	3.699	4.625	5.714	6.710	7.490	8.363
4	0.691	0.850	1.892	3.429	4.363	5.451	6.461	7.241	8.120
5	0.561	0.697	1.738	3.276	4.213	5.302	6.319	7.099	7.981
6	0.474	0.594	1.635	3.173	4.113	5.202	6.224	7.004	7.888
7	0.411	0.520	1.561	3.099	4.041	5.129	6.155	6.935	7.820
8	0.365	0.465	1.507	3.044	3.987	5.076	6.105	6.884	7.770
9	0.328	0.422	1.464	3.001	3.945	5.034	6.065	6.844	7.730
10	0.299	0.388	1.429	2.967	3.912	5.000	6.033	6.812	7.697
11	0.276	0.360	1.401	2.939	3.885	4.973	6.007	6.785	7.670
12	0.256	0.337	1.378	2.916	3.862	4.950	5.985	6.763	7.648
13	0.240	0.317	1.359	2.896	3.843	4.931	5.967	6.744	7.628
14	0.226	0.301	1.342	2.880	3.827	4.915	5.952	6.729	7.611
15	0.214	0.287	1.328	2.866	3.813	4.901	5.939	6.715	7.597
16	0.203	0.274	1.316	2.853	3.801	4.890	5.927	6.703	7.584
17	0.194	0.264	1.305	2.843	3.791	4.879	5.917	6.693	7.572
18	0.187	0.255	1.296	2.834	3.782	4.870	5.909	6.684	7.562
19	0.180	0.247	1.288	2.826	3.774	4.863	5.901	6.676	7.553
20	0.174	0.240	1.281	2.819	3.768	4.856	5.894	6.669	7.545
21	0.169	0.234	1.275	2.813	3.762	4.850	5.889	6.662	7.538
22	0.165	0.229	1.270	2.808	3.757	4.845	5.884	6.657	7.531
23	0.161	0.224	1.266	2.803	3.752	4.840	5.879	6.652	7.526
24	0.158	0.220	1.262	2.800	3.749	4.837	5.876	6.648	7.521
25	0.155	0.217	1.259	2.796	3.746	4.833	5.873	6.645	7.517
26	0.153	0.215	1.256	2.794	3.743	4.831	5.870	6.642	7.513
27	0.151	0.212	1.254	2.792	3.741	4.829	5.868	6.640	7.511
28	0.150	0.211	1.252	2.790	3.739	4.827	5.866	6.638	7.508
29	0.149	0.210	1.251	2.789	3.738	4.826	5.865	6.637	7.507
30	0.148	0.209	1.250	2.788	3.737	4.825	5.865	6.636	7.506
31	0.148	0.209	1.250	2.788	3.737	4.825	5.864	6.636	7.506

Table A.11: Experimental Resistances for case 3-b.

Electrode	70 cm	57.2 cm	48 cm	40.7 cm	34 cm	28.5 cm	23.3 cm	18.5 cm
1	42.956	57.213	79.724	92.646	108.796	124.330	135.722	148.916
2	11.107	27.727	52.118	66.977	84.158	100.493	112.779	126.408
3	9.104	25.738	50.107	64.976	82.167	98.500	110.784	124.419
4	7.878	24.508	48.871	63.748	80.944	97.277	109.564	123.197
5	6.830	23.459	47.821	62.704	79.904	96.243	108.522	122.157
6	6.092	22.717	47.080	61.970	79.172	95.513	107.794	121.428
7	5.483	22.106	46.470	61.365	78.570	94.911	107.197	120.827
8	5.038	21.656	46.022	60.922	78.125	94.472	106.758	120.385
9	4.682	21.300	45.671	60.577	77.783	94.133	106.419	120.047
10	4.373	20.990	45.364	60.276	77.483	93.834	106.121	119.747
11	4.121	20.737	45.113	60.029	77.236	93.589	105.878	119.505
12	3.894	20.516	44.901	59.824	77.031	93.392	105.681	119.310
13	3.695	20.316	44.703	59.629	76.837	93.197	105.488	119.115
14	3.569	20.195	44.590	59.524	76.733	93.099	105.393	119.021
15	3.441	20.068	44.470	59.408	76.616	92.987	105.284	118.916
16	3.373	20.003	44.411	59.356	76.563	92.940	105.238	118.871
17	3.292	19.919	44.333	59.277	76.488	92.870	105.167	118.799
18	3.253	19.885	44.307	59.259	76.468	92.855	105.158	118.791

Table A.12: Numerical Resistances for case 3-b.

Electrode	70 cm	57.2 cm	48 cm	40.7 cm	34 cm	28.5 cm	23.3 cm	18.5 cm
1	3.718	2.684	4.191	5.185	6.327	7.373	8.327	9.247
2	0.841	1.851	3.434	4.428	5.570	6.654	7.532	8.451
3	0.601	1.711	3.306	4.300	5.442	6.532	7.397	8.315
4	0.485	1.620	3.224	4.218	5.359	6.454	7.310	8.226
5	0.414	1.555	3.165	4.159	5.300	6.398	7.247	8.162
6	0.366	1.507	3.121	4.115	5.256	6.355	7.200	8.112
7	0.331	1.469	3.086	4.080	5.221	6.322	7.162	8.072
8	0.304	1.440	3.060	4.054	5.195	6.297	7.134	8.041
9	0.284	1.417	3.039	4.033	5.174	6.277	7.110	8.015
10	0.268	1.398	3.022	4.016	5.157	6.260	7.091	7.994
11	0.255	1.383	3.008	4.002	5.143	6.246	7.076	7.975
12	0.245	1.370	2.997	3.991	5.132	6.235	7.062	7.960
13	0.236	1.360	2.987	3.981	5.122	6.226	7.052	7.947
14	0.229	1.352	2.980	3.974	5.115	6.219	7.043	7.936
15	0.224	1.345	2.974	3.968	5.109	6.213	7.036	7.927
16	0.220	1.340	2.969	3.963	5.104	6.208	7.030	7.920
17	0.217	1.337	2.966	3.960	5.101	6.205	7.026	7.915
18	0.215	1.334	2.964	3.958	5.098	6.203	7.023	7.912

Table A.13: Experimental Resistances for case 4-a.

Electrode	18.5 cm	23.5 cm	28.5 cm	34 cm	40.7 cm	48 cm	57.2 cm	70 cm
1	304.444	269.087	248.993	230.939	198.717	168.504	137.533	101.361
2	263.869	233.468	218.731	198.632	166.296	138.058	106.722	70.687
3	249.130	221.370	207.243	187.170	155.501	128.300	96.438	60.658
4	245.037	218.588	204.540	184.519	152.900	125.679	93.750	58.144
5	241.056	216.202	202.180	182.187	150.547	123.136	91.253	55.649
6	238.470	214.671	200.663	180.684	149.052	121.624	89.706	54.080
7	234.550	212.543	198.539	178.600	146.996	119.530	87.597	51.980
8	233.086	211.857	197.874	177.951	146.361	118.831	86.898	51.274
9	230.835	210.755	196.789	176.915	145.354	117.795	85.841	50.242
10	229.316	209.908	195.906	176.045	144.511	117.020	85.065	49.483
11	227.739	209.232	195.219	175.341	143.792	116.270	84.299	48.761
12	226.783	208.809	194.791	174.914	143.349	115.791	83.826	48.279
13	225.660	208.374	194.322	174.476	142.894	115.289	83.320	47.772
14	224.909	207.989	193.914	174.108	142.545	115.010	83.033	47.469
15	223.954	207.682	193.565	173.775	142.188	114.573	82.583	47.017
16	223.354	207.420	193.286	173.512	141.937	114.332	82.344	46.773
17	222.496	207.053	192.926	173.164	141.599	113.990	82.006	46.441
18	222.067	206.916	192.775	173.008	141.442	113.817	81.827	46.270
19	221.280	206.602	192.458	172.720	141.164	113.556	81.554	46.002
20	220.575	206.315	192.173	172.437	140.899	113.346	81.350	45.803
21	219.932	206.149	192.004	172.273	140.744	113.203	81.213	45.670
22	219.627	206.188	192.021	172.281	140.726	113.085	81.095	45.545
23	219.066	205.971	191.807	172.078	140.536	112.915	80.935	45.388
24	218.884	205.956	191.781	172.055	140.503	112.835	80.856	45.310
25	218.585	205.809	191.630	171.919	140.379	112.746	80.765	45.226
26	218.462	205.815	191.622	171.908	140.361	112.685	80.702	45.158
27	218.224	205.670	191.478	171.780	140.247	112.613	80.633	45.092
28	218.080	205.568	191.374	171.688	140.152	112.570	80.593	45.051
29	218.140	205.656	191.446	171.758	140.203	112.522	80.552	45.009
30	217.916	205.437	191.232	171.569	140.050	112.485	80.519	44.980
31	218.102	205.580	191.354	171.682	140.138	112.476	80.512	44.967

Table A.14: Numerical Resistances for case 4-a.

Electrode	18.5 cm	23.5 cm	28.5 cm	34 cm	40.7 cm	48 cm	57.2 cm	70 cm
1	20.738	17.881	16.802	15.389	13.176	11.193	9.239	6.955
2	16.681	14.983	14.020	12.722	10.625	8.758	6.804	4.521
3	15.597	14.209	13.278	12.011	9.945	8.109	6.154	3.871
4	15.112	13.863	12.946	11.693	9.640	7.818	5.864	3.581
5	14.835	13.666	12.757	11.512	9.467	7.653	5.699	3.416
6	14.648	13.534	12.630	11.390	9.351	7.542	5.588	3.305
7	14.513	13.438	12.538	11.303	9.267	7.462	5.508	3.225
8	14.412	13.367	12.471	11.238	9.206	7.403	5.449	3.166
9	14.331	13.312	12.418	11.187	9.157	7.357	5.403	3.120
10	14.266	13.267	12.375	11.147	9.118	7.320	5.366	3.083
11	14.212	13.230	12.340	11.114	9.087	7.290	5.336	3.052
12	14.167	13.199	12.312	11.086	9.061	7.265	5.311	3.027
13	14.128	13.173	12.287	11.063	9.039	7.244	5.290	3.006
14	14.094	13.151	12.267	11.044	9.020	7.226	5.272	2.989
15	14.065	13.132	12.249	11.027	9.004	7.211	5.257	2.974
16	14.039	13.116	12.234	11.013	8.990	7.198	5.244	2.960
17	14.016	13.101	12.220	11.000	8.978	7.186	5.232	2.949
18	13.995	13.088	12.209	10.989	8.968	7.177	5.223	2.939
19	13.977	13.077	12.199	10.980	8.959	7.168	5.214	2.931
20	13.961	13.068	12.190	10.972	8.951	7.161	5.207	2.923
21	13.947	13.059	12.182	10.964	8.945	7.154	5.200	2.917
22	13.934	13.052	12.176	10.958	8.939	7.149	5.195	2.911
23	13.923	13.045	12.170	10.953	8.934	7.144	5.190	2.906
24	13.913	13.039	12.165	10.948	8.929	7.140	5.186	2.902
25	13.905	13.035	12.161	10.944	8.926	7.136	5.182	2.899
26	13.898	13.031	12.157	10.941	8.923	7.133	5.179	2.896
27	13.893	13.028	12.155	10.939	8.920	7.131	5.177	2.894
28	13.888	13.025	12.153	10.937	8.918	7.129	5.175	2.892
29	13.885	13.023	12.151	10.935	8.917	7.128	5.174	2.891
30	13.883	13.022	12.150	10.934	8.916	7.127	5.173	2.890
31	13.883	13.022	12.150	10.934	8.916	7.127	5.173	2.890

Table A.15: Experimental Resistances for case 4-b.

Electrode	18 cm	23.3 cm	28.5 cm	34 cm	40.7 cm	48 cm	57.2 cm	70 cm
1	263.847	239.809	224.544	204.251	172.118	144.373	112.971	76.788
2	237.931	214.489	199.848	180.037	148.510	121.236	89.363	53.610
3	235.532	212.270	197.640	177.860	146.344	118.973	87.098	51.394
4	233.945	210.837	196.230	176.470	144.972	117.579	85.695	50.033
5	232.482	209.568	194.974	175.242	143.761	116.375	84.494	48.873
6	231.609	208.821	194.231	174.501	143.016	115.533	83.653	48.029
7	230.716	208.103	193.522	173.816	142.338	114.853	82.966	47.363
8	229.946	207.496	192.922	173.233	141.779	114.352	82.460	46.867
9	229.483	207.169	192.590	172.910	141.444	113.956	82.055	46.461
10	228.924	206.760	192.191	172.527	141.071	113.611	81.711	46.127
11	228.478	206.449	191.882	172.227	140.783	113.323	81.419	45.841
12	228.290	206.356	191.780	172.117	140.645	113.077	81.167	45.588
13	227.752	205.951	191.396	171.759	140.314	112.852	80.945	45.372
14	227.683	205.947	191.380	171.732	140.268	112.709	80.798	45.225
15	227.352	205.709	191.153	171.517	140.066	112.560	80.649	45.079
16	227.360	205.745	191.180	171.538	140.074	112.487	80.572	45.003
17	226.941	205.416	190.865	171.213	139.825	112.382	80.471	44.905
18	227.099	205.575	191.012	171.378	139.920	112.347	80.435	44.869

Table A.16: Numerical Resistances for case 4-b.

Electrode	18.5 cm	23.3 cm	28.5 cm	34 cm	40.7 cm	48 cm	57.2 cm	70 cm
1	17.044	15.194	14.316	12.971	10.854	8.996	6.870	4.474
2	15.907	14.286	13.351	12.024	9.908	8.069	5.943	3.566
3	15.713	14.131	13.188	11.865	9.748	7.912	5.786	3.413
4	15.586	14.032	13.083	11.761	9.645	7.811	5.685	3.314
5	15.494	13.960	13.007	11.688	9.571	7.739	5.613	3.243
6	15.423	13.906	12.951	11.633	9.516	7.685	5.559	3.190
7	15.366	13.863	12.906	11.589	9.473	7.643	5.517	3.149
8	15.321	13.830	12.872	11.556	9.440	7.611	5.485	3.117
9	15.284	13.803	12.845	11.530	9.414	7.585	5.459	3.092
10	15.253	13.782	12.823	11.508	9.392	7.564	5.438	3.072
11	15.227	13.763	12.804	11.491	9.375	7.547	5.421	3.055
12	15.205	13.748	12.789	11.477	9.361	7.533	5.407	3.041
13	15.186	13.736	12.777	11.465	9.349	7.522	5.396	3.030
14	15.171	13.726	12.767	11.455	9.340	7.513	5.387	3.021
15	15.158	13.718	12.759	11.448	9.332	7.505	5.379	3.014
16	15.148	13.711	12.753	11.442	9.327	7.500	5.374	3.009
17	15.140	13.707	12.749	11.438	9.322	7.496	5.370	3.005
18	15.135	13.703	12.745	11.435	9.320	7.493	5.367	3.002

Table A.17 Experimental Resistances for case 5-a.

Electrode	70 cm	57.2 cm	48 cm	40.7 cm	34 cm	28.5 cm	23.3 cm	18.5 cm
1	102.144	110.303	118.87	130.888	146.669	164.305	179.130	198.616
2	70.500	80.225	89.579	102.236	117.978	135.682	150.576	168.142
3	60.260	70.472	80.009	92.727	109.121	126.406	140.178	157.429
4	57.659	67.883	77.481	90.218	106.613	123.936	137.631	154.806
5	55.196	65.271	74.998	87.731	103.911	121.470	135.293	152.446
6	53.689	63.854	73.550	86.268	102.479	120.027	133.873	151.001
7	51.665	62.073	71.617	84.304	100.480	118.098	131.919	149.038
8	50.983	61.347	70.929	83.648	99.664	117.428	131.272	148.374
9	49.970	60.296	69.918	82.653	98.639	116.424	130.263	147.356
10	49.225	59.486	69.190	81.951	97.928	115.730	129.656	146.591
11	48.528	58.538	68.495	81.254	97.216	115.028	128.984	145.912
12	48.052	58.125	68.067	80.831	96.781	114.605	128.593	145.513
13	47.555	57.609	67.585	80.354	96.319	114.133	128.170	145.083
14	47.257	57.301	67.326	80.094	96.062	113.887	127.850	144.743
15	46.813	56.855	66.915	79.693	95.650	113.480	127.518	144.405
16	46.573	56.498	66.685	79.484	95.442	113.273	127.296	144.172
17	46.242	56.196	66.400	79.206	95.154	112.994	127.011	143.871
18	46.072	56.019	66.249	79.068	95.016	112.853	126.880	143.735
19	45.812	55.742	66.006	78.836	94.777	112.611	126.619	143.450
20	45.617	55.606	65.824	78.677	94.617	112.452	126.600	143.227
21	45.485	55.475	65.718	78.569	94.512	112.349	126.120	143.096
22	45.363	55.353	65.629	78.486	94.423	112.267	126.129	143.106
23	45.207	55.121	65.464	78.358	94.288	112.138	125.985	142.943
24	45.131	55.009	65.422	78.321	94.248	112.102	126.263	142.946
25	45.049	54.814	65.366	78.273	94.200	112.057	126.225	142.853
26	44.985	54.762	65.334	78.242	94.168	112.029	125.912	142.858
27	44.919	54.664	65.292	78.208	94.134	111.994	125.844	142.779
28	44.881	54.638	65.273	78.195	94.126	111.985	125.820	142.736
29	44.842	54.606	65.264	78.187	94.116	111.981	125.884	142.805
30	44.816	54.575	65.258	78.188	94.116	111.976	126.161	142.678
31	44.804	54.569	65.268	78.210	94.138	112.005	125.892	142.808

Table A.18: Numerical Resistances for case 5-a.

Electrode	70 cm	57.2 cm	48 cm	40.7 cm	34 cm	28.5 cm	23.3 cm	18.5 cm
1	6.922	7.549	8.024	8.845	9.878	10.823	11.840	13.031
2	4.488	5.114	5.705	6.527	7.560	8.620	9.579	10.712
3	3.838	4.465	5.086	5.908	6.941	8.032	8.976	10.093
4	3.548	4.174	4.810	5.631	6.664	7.770	8.706	9.816
5	3.382	4.009	4.652	5.474	6.507	7.620	8.552	9.657
6	3.272	3.898	4.547	5.368	6.401	7.520	8.449	9.551
7	3.192	3.818	4.471	5.292	6.325	7.447	8.374	9.473
8	3.133	3.759	4.415	5.236	6.269	7.394	8.319	9.415
9	3.086	3.713	4.370	5.192	6.225	7.352	8.275	9.369
10	3.049	3.676	4.335	5.157	6.190	7.318	8.241	9.332
11	3.019	3.646	4.307	5.128	6.161	7.290	8.212	9.302
12	2.994	3.621	4.283	5.104	6.137	7.268	8.188	9.276
13	2.973	3.600	4.263	5.084	6.117	7.248	8.168	9.253
14	2.956	3.582	4.246	5.067	6.100	7.232	8.151	9.234
15	2.940	3.567	4.231	5.053	6.085	7.218	8.136	9.217
16	2.927	3.554	4.219	5.040	6.073	7.206	8.123	9.202
17	2.916	3.543	4.208	5.029	6.062	7.196	8.111	9.189
18	2.906	3.533	4.199	5.020	6.052	7.186	8.102	9.177
19	2.898	3.524	4.191	5.012	6.044	7.178	8.093	9.167
20	2.890	3.517	4.184	5.005	6.037	7.171	8.085	9.158
21	2.884	3.510	4.177	4.999	6.031	7.165	8.079	9.150
22	2.878	3.505	4.172	4.993	6.026	7.160	8.073	9.142
23	2.873	3.500	4.168	4.989	6.021	7.156	8.068	9.136
24	2.869	3.496	4.164	4.985	6.017	7.152	8.063	9.130
25	2.866	3.492	4.160	4.982	6.014	7.148	8.060	9.126
26	2.863	3.490	4.158	4.979	6.011	7.146	8.057	9.122
27	2.861	3.487	4.155	4.977	6.009	7.143	8.054	9.119
28	2.859	3.485	4.154	4.975	6.007	7.142	8.052	9.116
29	2.858	3.484	4.153	4.974	6.006	7.141	8.051	9.114
30	2.857	3.483	4.152	4.973	6.005	7.140	8.050	9.113
31	2.857	3.483	4.152	4.973	6.005	7.140	8.050	9.113

Table A.19: Experimental Resistances for case 5-b.

Electrode	70 cm	57.2 cm	48 cm	40.7 cm	34 cm	28.5 cm	23.3 cm	18.5 cm
1	76.153	86.017	96.942	110.025	125.842	143.411	157.681	174.451
2	53.417	63.347	74.485	87.793	103.670	121.460	135.689	152.593
3	51.214	61.190	72.339	85.641	101.512	119.314	133.597	150.492
4	49.858	59.850	71.020	84.324	100.189	117.999	132.282	149.164
5	48.704	58.728	69.907	83.209	99.065	116.884	131.128	147.985
6	47.870	57.920	69.099	82.407	98.258	116.081	130.410	147.257
7	47.210	57.276	68.477	81.784	97.630	115.450	129.776	146.604
8	46.718	56.798	68.013	81.324	97.168	114.987	129.254	146.055
9	46.320	56.420	67.647	80.961	96.801	114.628	128.934	145.716
10	45.986	56.105	67.341	80.656	96.496	114.325	128.603	145.363
11	45.704	55.834	67.083	80.398	96.239	114.067	128.331	145.072
12	45.457	55.603	66.863	80.182	96.025	113.858	128.211	144.951
13	45.242	55.401	66.673	79.994	95.836	113.667	127.923	144.623
14	45.098	55.275	66.547	79.880	95.723	113.557	127.898	144.599
15	44.954	55.138	66.427	79.766	95.610	113.441	127.728	144.406
16	44.880	55.049	66.380	79.719	95.566	113.398	127.763	144.443
17	44.785	54.965	66.307	79.652	95.497	113.326	127.559	144.201
18	44.748	54.946	66.295	79.641	95.490	113.326	127.672	144.331

Table A.20: Numerical Resistances for case 5-b.

Electrode	70 cm	57.2 cm	48 cm	40.7 cm	34 cm	28.5 cm	23.3 cm	18.5 cm
1	4.474	5.135	5.838	6.746	7.790	8.974	9.936	11.063
2	3.566	4.227	4.967	5.857	6.919	8.104	9.065	10.192
3	3.413	4.073	4.820	5.706	6.772	7.957	8.917	10.043
4	3.314	3.974	4.725	5.609	6.677	7.861	8.822	9.945
5	3.243	3.904	4.658	5.540	6.609	7.793	8.753	9.874
6	3.190	3.851	4.607	5.488	6.559	7.742	8.701	9.820
7	3.149	3.809	4.567	5.447	6.519	7.702	8.660	9.776
8	3.117	3.778	4.537	5.417	6.489	7.672	8.629	9.742
9	3.092	3.753	4.513	5.392	6.464	7.647	8.603	9.714
10	3.072	3.732	4.493	5.372	6.444	7.627	8.582	9.690
11	3.055	3.716	4.477	5.356	6.428	7.610	8.565	9.670
12	3.041	3.702	4.464	5.342	6.415	7.597	8.551	9.653
13	3.030	3.691	4.454	5.332	6.404	7.586	8.539	9.639
14	3.021	3.682	4.445	5.323	6.396	7.577	8.529	9.627
15	3.014	3.675	4.438	5.316	6.389	7.570	8.521	9.617
16	3.009	3.669	4.433	5.310	6.384	7.564	8.515	9.610
17	3.005	3.665	4.429	5.306	6.380	7.560	8.511	9.604
18	3.002	3.663	4.427	5.304	6.377	7.557	8.507	9.600

Table A.21: Experimental Resistances for case 6.

Electrode	70 cm	57.2 cm	48 cm	40.7 cm	34 cm	28.5 cm	23.3 cm	18.5 cm
1	94.174	103.171	115.174	129.173	147.081	199.147	215.403	232.613
2	66.248	76.919	88.616	102.859	120.883	171.163	187.125	204.423
3	57.082	68.297	79.894	94.225	112.339	161.879	177.163	194.195
4	54.456	65.867	77.560	91.938	109.987	158.975	174.584	191.538
5	51.811	63.417	75.212	89.624	107.661	156.811	172.422	189.277
6	50.296	62.004	73.798	88.231	106.316	155.427	171.034	187.870
7	48.369	60.107	71.933	86.370	104.487	153.446	169.102	185.923
8	47.797	59.514	71.273	85.745	103.895	152.864	168.492	185.326
9	46.888	58.590	70.326	84.835	103.002	151.918	167.515	184.342
10	46.173	57.859	69.629	84.184	102.373	151.228	166.844	183.663
11	45.554	57.194	68.980	83.563	101.781	150.602	166.237	183.040
12	45.067	56.749	68.579	83.152	101.372	150.200	165.851	182.646
13	44.529	56.258	68.104	82.690	100.906	149.787	165.473	182.267
14	44.273	55.993	67.867	82.478	100.688	149.476	165.150	181.934
15	43.854	55.585	67.460	82.089	100.300	149.178	164.861	181.641
16	43.620	55.346	67.250	81.886	100.101	148.948	164.627	181.412
17	43.264	55.034	66.966	81.600	99.813	148.706	164.394	181.174
18	43.110	54.886	66.832	81.479	99.689	148.549	164.235	181.000
19	42.867	54.645	66.611	81.261	99.468	148.290	163.980	180.738
20	42.697	54.458	66.460	81.110	99.316	148.091	163.774	180.515
21	42.554	54.329	66.359	81.013	99.216	147.987	163.670	180.402
22	42.432	54.207	66.262	80.931	99.132	148.015	163.707	180.445
23	42.262	54.051	66.122	80.795	98.989	147.841	163.533	180.255
24	42.203	53.990	66.086	80.775	98.965	147.905	163.602	180.318
25	42.135	53.914	66.022	80.732	98.928	147.814	163.515	180.218
26	42.085	53.853	65.974	80.706	98.900	147.868	163.569	180.274
27	42.023	53.793	65.942	80.674	98.865	147.791	163.494	180.188
28	41.970	53.758	65.930	80.667	98.854	147.738	163.439	180.127
29	41.920	53.717	65.898	80.670	98.846	147.830	163.547	180.234
30	41.886	53.690	65.883	80.665	98.837	147.653	163.350	180.020
31	41.879	53.684	65.899	80.693	98.863	147.856	163.585	180.261

Table A.22 Experimental Resistances for case 7-a.

Electrode	At 18.5 cm	At 23.3 cm	At 28.5 cm	At 34 cm	At 40.7 cm
1	244.180	231.620	194.928	130.263	96.302
2	216.626	203.067	165.183	100.563	68.236
3	206.196	193.049	154.953	90.873	58.974
4	203.400	190.373	152.385	88.309	56.556
5	201.036	188.129	150.119	85.966	54.229
6	199.568	186.596	148.583	84.473	52.756
7	197.581	184.530	146.480	82.440	50.755
8	196.977	183.874	145.774	81.784	50.120
9	195.961	182.838	144.697	80.732	49.127
10	195.254	182.045	143.971	79.972	48.418
11	194.613	181.329	143.226	79.246	47.743
12	194.217	180.859	142.731	78.761	47.281
13	193.827	180.413	142.256	78.278	46.801
14	193.479	180.013	141.856	77.938	46.499
15	193.169	179.645	141.469	77.549	46.102
16	192.922	179.358	141.157	77.285	45.846
17	192.648	179.056	140.821	76.969	45.523
18	192.446	178.824	140.585	76.771	45.350
19	192.141	178.503	140.237	76.486	45.081
20	191.884	178.201	139.949	76.255	44.868
21	191.747	178.023	139.728	76.115	44.747
22	191.759	178.003	139.677	76.033	44.652
23	191.544	177.764	139.428	75.819	44.462
24	191.587	177.774	139.424	75.802	44.432
25	191.456	177.611	139.279	75.689	44.339
26	191.493	177.592	139.252	75.640	44.295
27	191.383	177.454	139.126	75.552	44.221
28	191.292	177.349	139.037	75.486	44.175
29	191.384	177.401	139.062	75.490	44.162
30	191.139	177.130	138.852	75.354	44.088
31	191.367	177.300	138.980	75.432	44.130

Table A.23: Experimental Resistances for case 7-b.

Electrode	40.7 cm	34 cm	28.5 cm	23.3 cm	18.5 cm
1	96.302	103.751	119.046	139.560	164.086
2	68.236	75.766	92.481	113.447	137.046
3	58.974	66.865	83.962	104.763	126.466
4	56.556	64.315	81.474	102.505	123.889
5	54.229	62.012	79.283	100.415	121.589
6	52.756	60.551	77.871	99.071	120.168
7	50.755	58.614	75.978	97.213	118.295
8	50.120	57.932	75.402	96.624	117.729
9	49.127	56.899	74.450	95.677	116.793
10	48.418	56.150	73.765	95.035	116.169
11	47.743	55.459	73.132	94.431	115.578
12	47.281	55.006	72.724	94.054	115.201
13	46.801	54.564	72.299	93.661	114.833
14	46.499	54.320	72.034	93.399	114.562
15	46.102	53.973	71.690	93.085	114.259
16	45.846	53.777	71.472	92.881	114.056
17	45.523	53.504	71.211	92.649	113.826
18	45.350	53.379	71.067	92.518	113.687
19	45.081	53.179	70.840	92.303	113.457
20	44.868	53.007	70.663	92.115	113.259
21	44.747	52.967	70.557	92.038	113.175
22	44.652	52.971	70.512	92.023	113.168
23	44.462	52.729	70.341	91.849	112.969
24	44.432	52.692	70.363	91.904	113.046
25	44.339	52.604	70.301	91.851	112.987
26	44.295	52.572	70.302	91.871	113.027
27	44.221	52.508	70.246	91.822	112.985
28	44.175	52.462	70.222	91.803	113.097
29	44.162	52.463	70.255	91.868	113.170
30	44.088	52.383	70.179	91.775	113.048
31	44.130	52.446	70.258	91.909	113.221

Figure # A 4.1: Measurements at different fluid front using the last electrode of the array as the reference electrode for Case 1(a).
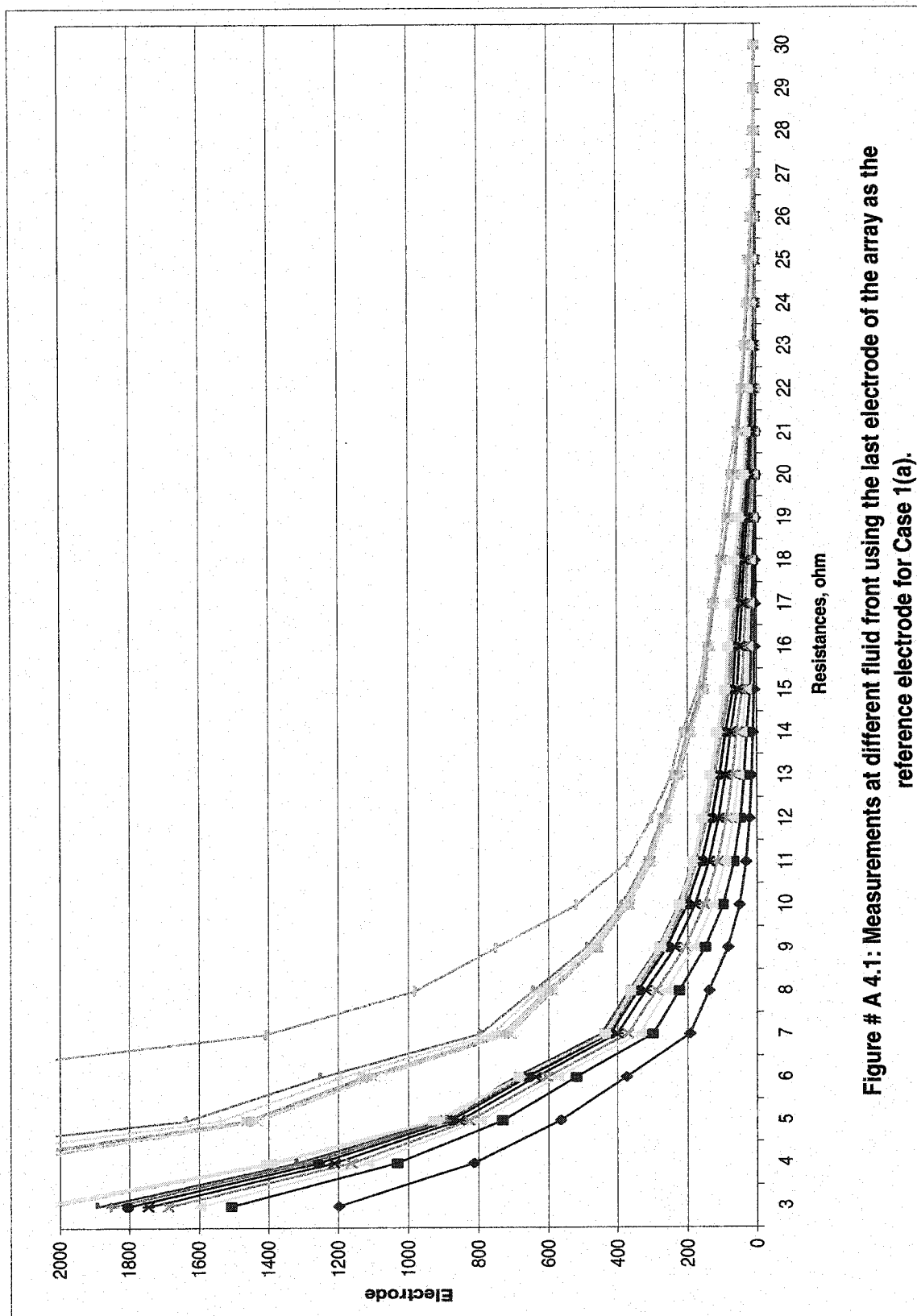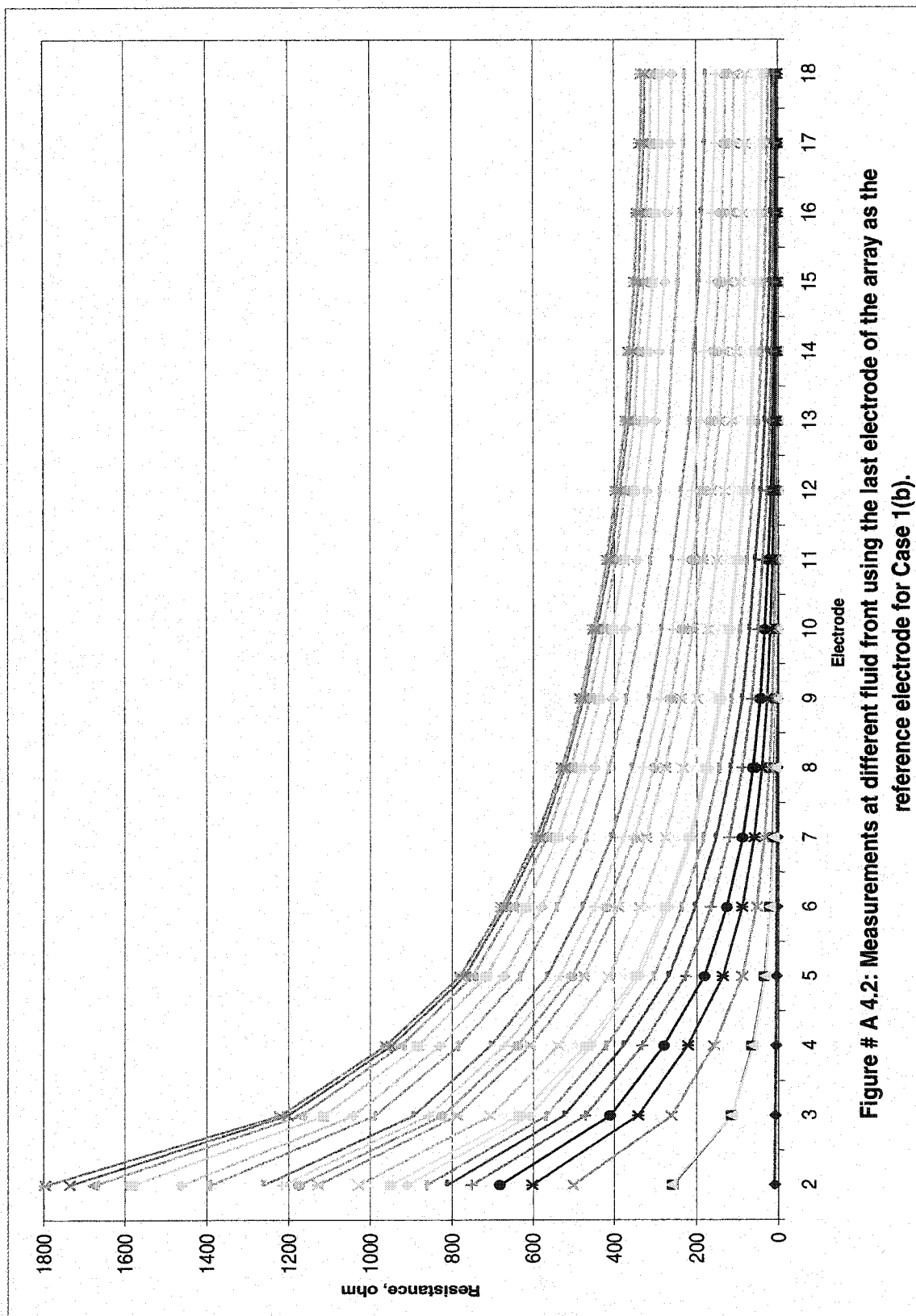
150

Figure # A 4.2: Measurements at different fluid front using the last electrode of the array as the reference electrode for Case 1(b).

Appendix B

CALCULATIONS OF PROPERTIES

APPENDIX B

CALCULATIONS OF PROPERTIES

B.1 PERMEABILITY MEASUREMENT

Permeability was calculated on the basis of Darcy's law. A cylindrical Plexiglas model was used to measure the permeability of the porous media. According to Darcy's law:

$$q = -\frac{kA}{\mu} \cdot \frac{\Delta P}{\Delta x} \quad\text{..} Equation - B.1$$

$$k = -\frac{\mu q}{A} \cdot \frac{\Delta x}{\Delta P} \quad\text{..} Equation - B.2$$

where, q is the flow rate in cc/sec, k is the permeability in Darcy, μ is the viscosity in cp, x is the distance traveled by the fluid (x=L in our case), and ΔP is the pressure drop along the path. Expressing the permeability in md, equation - B.2 can be written as:

$$k = \frac{\mu q L}{A \Delta P} \cdot 10^3 \quad\text{..,..................} Equation - B.3$$

For the set-up used, the following numerical values were there: viscosity: 0.9 cp, Length of the Cylinder: 53 cm, Diameter of the Cylinder: 3.98 cm, besides, 30 cc of brine was collected during 96 second. The manometer read 0.7 cm -, which is equivalent to a pressure of 0.1354-psi From equation – A.3 we obtained a permeability of 128.86 Darcy.

POROSITY CALCULATION

Equations used for the Helium Porosimeter:

$$V_{REF} = \frac{V_{BR}}{\left(\dfrac{P_{REFFULL} - P_{ZERO}}{P_{CUPFULL} - P_{ZERO}}\right) - \left(\dfrac{P_{REFREM} - P_{ZERO}}{P_{CUPREM} - P_{ZERO}}\right)} \dotfill Equation - A.4$$

$$V_{DEAD} = \left[\left(\frac{P_{REF} - P_{ZERO}}{P_{DV} - P_{ZERO}}\right) - 1\right].V_{REF} \dotfill Equation - A.5$$

$$V_{TOTAL} = \left[\left(\frac{P_{REF} - P_{ZERO}}{P_{TOTAL} - P_{ZERO}}\right) - 1\right].V_{REF} \dotfill Equation - A.6$$

$$V_{PORE} = V_{TOTAL} - V_{DEAD} \dotfill Equation - A.7$$

Where,

V_{PORE} is the pore volume in cc

V_{REF} is the reference volume in cc

V_{BR} is the volume of the removed Billets in cc

$P_{REFFULL}$ is the reference pressure for full cup measurement, psi

P_{ZERO} is the zero pressure with the Helium Source valve closed, psi

$P_{CUPFULL}$ is the cup pressure with no billets removed, psi

P_{REFREM} is the reference pressure with a billet removed, psi

P_{CUPREM} is the cup pressure with a billet removed, psi

P_{DV} is the pressure when the reference system is opened to the new dead volume,

psi.

Appendix C

GENERAL OBSERVATIONS

APPENDIX C

GENERAL OBSERVATIONS

This appendix contains some basic remarks concerning the construction of the model and suggestions to improve the construction of such experimental set-up:

1.   A new set of electrode was inserted at a distance of 1.5 cm from the well later on by making holes in the body of the model reservoir and copper rods were used as electrodes. These electrodes were exactly in the desired position and were in good contact with the media throughout the experiment, regardless of the position of the model.

2.   The top plate was kept separate from the rest of the body of the model to facilitate any kind of change inside the model. The other sides were fixed to each other using screws and glue. The top plate was attached with rods and nuts to the bottom part. The top plate was broken while fixing it on the model. This was due to imbalanced forces applied through the 40 rods used. It was needed to fabricate another top plate before starting the experiment.

3. The model was heavy (150 kg) and could not be easily moved once filled. During injection of fluids and measurements, care was taken to avoid any kind of imbalance and tilting. Besides, the base of the model, also made of Plexiglas, was too weak to support the total weight. Any displacement of the model was done very carefully. A more robust construction is required in order to easily manipulate such a heavy construction.

4. An alternate and certainly better solution would have been to put the opening in the bottom plate and to incorporate hooks to allow transportation. While putting the model upside-down, the model fell and several cracks appeared on the body of the sector model. The last part of the experiment was conducted by keeping the model in a fixed position.

5. The holes drilled in the Teflon type plastic pipe, used as the well in the model reservoir, were small enough (0.4 mm) to prevent the glass beads (0.5-0.6 mm) from flowing out. So, there was no need to put any screen to the well.

6. At the sharp end of the model, the velocity of fluid was high due to the small size of the flow area. This caused some glass beads to be displaced from the compacted location and created bad contact of electrodes with the porous media.

7. Keeping the sector model in the reverse direction (the well at the bottom) was a better idea to increase pressure in the vicinity of the well and to have a compacted media close to the well. This arrangement allowed less permeability and higher connate water saturation and provided better measurement.

A correct positioning of the electrodes is a key factor for the interpretation of the measurements. The second set of electrodes, which was inserted once the model was closed, gave good measurements.

1. The acquisition system was originally designed for the monitoring of water saturation changes in an actual reservoir and was not optimum for measurements performed in an oil-bearing medium where the impedance of the medium can reach several $M\Omega.m$.

2. The acquisition system was powered by 220 volts supply line. The injected current was limited to 20 mA and the maximum voltage to 300 V; all measurements have been done at 10 Hz. At this frequency, the DC approximation is valid and polarization effects of electrodes are avoided. The shapes of the measured potential and injected current are displayed together with the corresponding values during measurement sequences. This feature allows one to detect any error during measurement.

3. Current was injected through the first electrode of the array (source electrode) with respect to a reference electrode and the potential distribution was measure using the other electrodes of the array with respect to another reference electrode.

Appendix D

NUMERICAL MODEL INPUTS

APPENDIX D

INPUT FILES FOR NUMERICAL MODEL

Different input files were needed for to use the simulation model.. Some of the input files are included below. <u>Contents in lines of Input Files:</u>

Line 1: Name of the file

Line 2: skip

Line 3: Angles, Radiuses, and Elevation points for grids.

Line 4: Number of co-ordinates

Line-5: Values for radiuses (continues to other lines also).

Line 6: Z values (Continues to other lines also).

Line 7: Skip

Line 8: Position of reference electrode.

Line 9: Number of total electrode, number of current electrode

Line 10: Position of the electrodes (after C).

Line 11: Resistivities of the porous zones.

Line 12: Definition of zones with various resistivities.

Line 13: Name of the output file.

Input file for a reservoir model in a large area of interest

```
REAZ TEST (2D case: symmetry of revolution-for large reservoir)
0 0 0
2 53 381
0 0 3
23.3  0
12 14 18 22 26 32 38 46 56 68 82 100 120 148 180 216 260 312
380 460 560 680 820 1000 1220 1480 1800 2180 2640 3200 3880
4700 5700 6900 8300 10200 12300 14900 18100 22000 26600
32300 39100 47500 57500 69800 84600 102600 124300 151000
183000 222000 270000
-250000 -180000 -120000 -70000 -40000 -20000 -10000 -5000 -3000
-2000 -1500 -1200 -1000 -850 -760 -700 -660 -640 -625 -615 -608
-604 -602 -601 -600 -599 -598 -597 -596 -594 -590 -582 -574 -568
-564 -562 -561 -560 -559 -558 -556 -552 -544 -536 -528 -524 -522
-521 -520 -519 -518 -516 -512 -504 -496 -488 -484 -482 -481 -480
-479 -478 -476 -472 -464 -456 -448 -444 -442 -441 -440 -439 -438
-436 -432 -424 -416 -408 -404 -402 -401 -400 -399 -398 -396 -392
-384 -376 -368 -364 -362 -361 -360 -359 -358 -356 -352 -344 -336
-328 -324 -322 -321 -320 -319 -318 -316 -312 -304 -296 -288 -284
-282 -281 -280 -279 -278 -276 -272 -264 -256 -248 -244 -242 -241
-240 -239 -238 -236 -232 -224 -216 -208 -204 -202 -201 -200 -199
-198 -196 -192 -184 -176 -168 -164 -162 -161 -160 -159 -158 -156
-152 -144 -136 -128 -124 -122 -121 -120 -119 -118 -116 -112 -104
-96 -88 -84 -82 -81 -80 -79 -78 -76 -72 -64 -56 -48 -44 -42 -41
-40 -39 -38 -36 -32 -24 -16 -8 -4 -2 -1
0 1 2 4 8 16 24 32 36 38 39 40 41 42 44 48 56 64 72 76 78 79 80
81 82 84 88 96 104 112 116 118 119 120 121 122 124 128 136 144
152 156 158 159 160 161 162 164 168 176 184 192 196 198 199 200
201 202 204 208 216 224 232 236 238 239 240 241 242 244 248 256
264 272 276 278 279 280 281 282 284 288 296 304 312 316 318 319
320 321 322 324 328 336 344 352 356 358 359 360 361 362 364 368
376 384 392 396 398 399 400 401 402 404 408 416 424 432 436 438
439 440 441 442 444 448 456 464 472 476 478 479 480 481 482 484
488 496 504 512 516 518 519 520 521 522 524 528 536 544 552 556
558 559 560 561 562 564 568 576 584 592 596 598 599 600 601 602
604 608 615 625 640 660 700 760 850 1000 1200 1500 2000 3000
5000 10000 20000 40000 70000 120000 180000 250000
0 0 0 0
0 270000 0
31 31
C
0 12 -598
0 12 -560
0 12 -520
0 12 -480
```

```
0 12 -440
0 12 -400
0 12 -360
0 12 -320
0 12 -280
0 12 -240
0 12 -200
0 12 -160
0 12 -120
0 12 -80
0 12 -40
0 12 0
0 12 40
0 12 80
0 12 120
0 12 160
0 12 200
0 12 240
0 12 280
0 12 320
0 12 360
0 12 400
0 12 440
0 12 480
0 12 520
0 12 560
0 12 600
1    1.  /End
2    5.  /Water zone
3  100.  /Oil zone
99/
1    23.3   3880        -250000    0    270000    250000
2    23.3   100         -250000    0    3880      250000
3    23.3   12          -250000    0    100       250000
10   23.3   270000      -250000    0    270000    250000
10   23.3   12   -599   0    12   -597
10   23.3   12   -561   0    12   -559
10   23.3   12   -521   0    12   -519
10   23.3   12   -481   0    12   -479
10   23.3   12   -441   0    12   -439
10   23.3   12   -401   0    12   -399
10   23.3   12   -361   0    12   -359
10   23.3   12   -321   0    12   -319
10   23.3   12   -281   0    12   -279
10   23.3   12   -241   0    12   -239
10   23.3   12   -201   0    12   -199
10   23.3   12   -161   0    12   -159
10   23.3   12   -121   0    12   -119
```

```
10    23.3     12    -81     0      12     -79
10    23.3     12    -41     0      12     -39
10    23.3     12    -1      0      12     1
10    23.3     12    39      0      12     41
10    23.3     12    79      0      12     81
10    23.3     12    119     0      12     121
10    23.3     12    159     0      12     161
10    23.3     12    199     0      12     201
10    23.3     12    239     0      12     241
10    23.3     12    279     0      12     281
10    23.3     12    319     0      12     321
10    23.3     12    359     0      12     361
10    23.3     12    399     0      12     401
10    23.3     12    439     0      12     441
10    23.3     12    479     0      12     481
10    23.3     12    519     0      12     521
10    23.3     12    559     0      12     561
10    23.3     12    599     0      12     601
99/
99/
ar2dmat.dat
```

Input file for a case with the first set of electrode for the fabricated model

```
REAZ TEST (2D case: first set of electrode) Modified by Reaz
November 17-02
0  0  0
3 69 336
0  0  3
11.65 0 -11.65
0.64  0.66  0.69  0.72  0.75  0.79  0.83  0.88  0.93  0.97
1.03  1.11  1.19  1.27  1.36  1.45  1.54  1.64  1.74  1.85
1.96  2.08  2.2   2.33  2.46  2.6   2.74  2.89  3.04  3.2
3.36  3.53  3.7   3.98  4.16  4.35  4.54  4.74  4.95  5.16
5.38  5.5   5.84  6.09  6.34  6.62  6.95  7.25  7.58  7.93
8.31  8.71  9.15  9.75  10.4  11.1  12.2  13.3  14.65 16.0
17.4  18.9  20.6  22.5  24.8  27.55 30.5  34.0  38.69
-5.91 -5.83 -5.787
-5.77 -5.76 -5.75 -5.74 -5.73 -5.71 -5.67 -5.59 -5.55 -5.53
-5.52 -5.51 -5.5  -5.49 -5.47 -5.43 -5.35 -5.28 -5.197
-5.16 -5.14 -5.13 -5.12 -5.11 -5.1  -5.08 -5.04 -4.96 -4.88
```

```
-4.8  -4.76 -4.74 -4.73 -4.72 -4.71 -4.7  -4.69 -4.65 -4.57
-4.49 -4.41 -4.37 -4.35 -4.34 -4.33 -4.32 -4.31 -4.29 -4.25
-4.17 -4.09 -4.02 -3.976 -3.957 -3.947 -3.937
-3.927 -3.917 -3.898 -3.858 -3.78 -3.7
-3.62 -3.583 -3.563 -3.55 -3.54 -3.53 -3.52 -3.504
-3.465 -3.386 -3.307 -3.23 -3.189 -3.17
-3.16 -3.15 -3.14 -3.13 -3.11 -3.07 -2.99 -2.91 -2.835
-2.795 -2.776 -2.766 -2.756 -2.746
-2.736 -2.717 -2.677 -2.598 -2.5197
-2.44 -2.402 -2.382 -2.372 -2.362 -2.3524
-2.343 -2.32 -2.283 -2.205 -2.126 -2.0472
-2.01 -1.988 -1.978 -1.969 -1.959 -1.949
-1.929 -1.89 -1.811 -1.732 -1.654 -1.614
-1.595 -1.585 -1.575 -1.565 -1.555
-1.535 -1.496 -1.417 -1.339 -1.26 -1.22 -1.2
-1.19 -1.181 -1.171 -1.161 -1.142 -1.102
-1.024 -0.945 -0.866 -0.827 -0.807
-0.797 -0.787 -0.778 -0.768 -0.748 -0.7087
-0.63 -0.551 -0.472 -0.433 -0.4134 -0.404 -0.394
-0.384 -0.374 -0.354 -0.315 -0.236 -0.1575
-0.0787 -0.0394 -0.0197 -0.0098 0 0.0098 0.0197
0.0394 0.0787 0.1575 0.236 0.315 0.354 0.374 0.384 0.394
0.404 0.4134 0.433 0.472 0.551 0.63 0.7087 0.748 0.768 0.778
0.787 0.797 0.807 0.827 0.866 0.945 1.024 1.102 1.142 1.161
1.171 1.181 1.19 1.2 1.22 1.26 1.339 1.417 1.496 1.535
1.555 1.565 1.575 1.585 1.595 1.614 1.654 1.732 1.811 1.89
1.929 1.949 1.959 1.969 1.978 1.988 2.01 2.0472    2.126 2.205
2.283 2.32 2.345 2.3524 2.362 2.372 2.382 2.402 2.44 2.5197
2.598 2.677 2.717 2.736 2.746 2.756 2.766 2.776 2.795 2.835
2.91 2.99 3.07 3.11 3.13 3.14 3.15 3.16 3.17 3.189
3.23 3.307 3.386 3.465 3.504 3.52 3.53 3.54 3.55 3.563
3.583 3.62 3.7   3.78 3.858 3.898 3.917 3.927 3.937 3.947
3.957 3.976 4.02 4.09 4.17 4.25 4.29 4.31 4.32 4.33
4.34 4.35 4.37 4.41 4.49 4.57 4.65 4.69 4.7   4.71
4.72 4.73 4.74 4.76 4.8  4.88 4.96 5.04 5.08 5.1
5.11 5.12 5.13 5.14 5.16 5.197 5.28 5.35 5.43 5.47
5.49 5.5  5.51 5.52 5.53 5.55 5.59 5.67 5.75 5.83
5.87 5.89 5.9  5.91 5.92 5.93
0 0 0 0
0 38.69 5.9
32 32
C
0 0.64 -5.75
0 0.64 -5.51
0 0.64 -5.12
0 0.64 -4.72
0 0.64 -4.33
0 0.64 -3.937
```

```
0 0.64 -3.54
0 0.64 -3.15
0 0.64 -2.756
0 0.64 -2.362
0 0.64 -1.969
0 0.64 -1.575
0 0.64 -1.181
0 0.64 -0.787
0 0.64 -.394
0 0.64 0
0 0.64 0.394
0 0.64 0.787
0 0.64 1.181
0 0.64 1.575
0 0.64 1.969
0 0.64 2.362
0 0.64 2.756
0 0.64 3.15
0 0.64 3.54
0 0.64 3.937
0 0.64 4.33
0 0.64 4.72
0 0.64 5.12
0 0.64 5.51
0 0.64 5.91
0 38.69 0.433
1      1.   /End
2      1000000. / Outside
3      80.0    / oil zone
4      25.   / mixed 1
5      20. /mixed 2
6      32. / mixed 3
7      0.22 / water zone
99/
3      11.65      0.64     -5.91    -11.65     9.15      5.93
4      11.65      9.15     -5.91    -11.65     9.75      5.93
5      11.65      9.75     -5.91    -11.65     12.2      5.93
6      11.65      12.2     -5.91    -11.65     20.6      5.93
7      11.65      20.6     -5.91    -11.65     38.69     5.93
10     11.65      0.64     -5.76    -11.65     0.64      -5.74
10     11.65      0.64     -5.52    -11.65     0.64      -5.5
10     11.65      0.64     -5.13    -11.65     0.64      -5.11
10     11.65      0.64     -4.73    -11.65     0.64      -4.71
10     11.65      0.64     -4.34    -11.65     0.64      -4.32
10     11.65      0.64     -3.947   -11.65     0.64      -3.927
10     11.65      0.64     -3.55    -11.65     0.64      -3.53
10     11.65      0.64     -3.16    -11.65     0.64      -3.14
10     11.65      0.64     -2.766   -11.65     0.64      -2.746
```

```
10     11.65     0.64     -2.372    -11.65     0.64     -2.3524
10     11.65     0.64     -1.978    -11.65     0.64     -1.959
10     11.65     0.64     -1.585    -11.65     0.64     -1.565
10     11.65     0.64     -1.19     -11.65     0.64     -1.171
10     11.65     0.64     -0.797    -11.65     0.64     -0.778
10     11.65     0.64     -0.404    -11.65     0.64     -0.384
10     11.65     0.64     -0.0098   -11.65     0.64      0.0098
10     11.65     0.64      0.384    -11.65     0.64      0.404
10     11.65     0.64      0.778    -11.65     0.64      0.797
10     11.65     0.64      1.171    -11.65     0.64      1.19
10     11.65     0.64      1.565    -11.65     0.64      1.585
10     11.65     0.64      1.959    -11.65     0.64      1.978
10     11.65     0.64      2.3524   -11.65     0.64      2.372
10     11.65     0.64      2.746    -11.65     0.64      2.766
10     11.65     0.64      3.14     -11.65     0.64      3.16
10     11.65     0.64      3.53     -11.65     0.64      3.55
10     11.65     0.64      3.927    -11.65     0.64      3.947
10     11.65     0.64      4.32     -11.65     0.64      4.34
10     11.65     0.64      4.71     -11.65     0.64      4.73
10     11.65     0.64      5.11     -11.65     0.64      5.13
10     11.65     0.64      5.5      -11.65     0.64      5.52
10     11.65     0.64      5.9      -11.65     0.64      5.92
99/
99/
smtstmo.dat
```

Input file for a case with the second set of electrode for the fabricated model

```
REAZ TEST (2D case: Second set of electrode) Modified by Reaz
November 11-02
0 0 0
3 69 264
0 0 3
12     0   -12
0.64  0.66  0.69  0.72  0.75  0.79  0.83  0.88  0.93  0.97
1.04  1.11  1.18  1.26  1.35  1.44  1.53  1.63  1.74  1.85
1.96  2.08  2.2   2.33  2.46  2.6   2.74  2.89  3.04  3.2
3.36  3.53  3.7   3.98  4.16  4.35  4.54  4.74  4.95  5.16
5.38  5.5   5.84  6.09  6.34  6.62  6.95  7.25  7.58  7.93
8.31  8.71  9.15  9.75  10.4  11.1  12.2  13.3  14.65 16.0
17.4  18.9  20.6  22.5  24.8  27.55 30.5  34.0  38.69
-5.91 -5.83 -5.79 -5.77 -5.76 -5.75 -5.74 -5.73 -5.71 -5.67
```

```
-5.59 -5.55 -5.53 -5.52 -5.51 -5.5  -5.49 -5.47 -5.43 -5.35
-5.28 -5.2  -5.16 -5.14 -5.13 -5.12 -5.11 -5.10 -5.08 -5.04
-4.96 -4.84 -4.69 -4.61 -4.57 -4.55 -4.54 -4.53 -4.52 -4.51
-4.49 -4.45 -4.37 -4.24 -4.1  -4.02 -3.98 -3.96 -3.95 -3.94
-3.93 -3.92 -3.9  -3.86 -3.78 -3.64 -3.51 -3.43 -3.39 -3.37
-3.36 -3.35 -3.34 -3.33 -3.31 -3.27 -3.19 -3.06 -2.92 -2.84
-2.8  -2.78 -2.77 -2.76 -2.75 -2.74 -2.72 -2.68 -2.6  -2.46
-2.33 -2.25 -2.21 -2.19 -2.18 -2.17 -2.16 -2.15 -2.13 -2.09
-2.01 -1.86 -1.72 -1.64 -1.6  -1.58 -1.57 -1.56 -1.55 -1.54
-1.52 -1.48 -1.4  -1.27 -1.14 -1.06 -1.02 -1.0  -0.99 -0.98
-0.97 -0.96 -0.94 -0.9  -0.82 -0.67 -0.55 -0.47 -0.43 -0.41
-0.4  -0.39 -0.38 -0.37 -0.35 -0.31 -0.24 -0.16 -0.08 0
0.08  0.12  0.16  0.18  0.19  0.2   0.21  0.22  0.24  0.28
0.36  0.5   0.63  0.71  0.75  0.77  0.78  0.79  0.80  0.81
0.83  0.87  0.95  1.08  1.22  1.3   1.34  1.36  1.37  1.38
1.39  1.4   1.42  1.46  1.54  1.68  1.81  1.89  1.93  1.95
1.96  1.97  1.98  1.99  2.01  2.05  2.13  2.26  2.4   2.48
2.52  2.54  2.55  2.56  2.57  2.58  2.6   2.64  2.72  2.86
2.99  3.07  3.11  3.13  3.14  3.15  3.16  3.17  3.19  3.23
3.31  3.45  3.58  3.66  3.7   3.72  3.73  3.74  3.75  3.76
3.78  3.82  3.9   4.03  4.17  4.25  4.29  4.31  4.32  4.33
4.34  4.35  4.37  4.41  4.49  4.62  4.76  4.84  4.88  4.9
4.91  4.92  4.93  4.94  4.96  5.0   5.04  5.1   5.11  5.12
5.13  5.14  5.16  5.197 5.28  5.35  5.43  5.47  5.49  5.5
5.51  5.52  5.53  5.55  5.59  5.67  5.75  5.83  5.87  5.89
5.9   5.91  5.92 5.93
0 0 0 0
0 38.69 5.9
19 19
C
0 1.53 -5.12
0 1.53 -4.53
0 1.53 -3.94
0 1.53 -3.35
0 1.53 -2.76
0 1.53 -2.17
0 1.53 -1.56
0 1.53 -0.98
0 1.53 -0.39
0 1.53 0.2
0 1.53 0.79
0 1.53 1.38
0 1.53 1.97
0 1.53 2.56
0 1.53 3.15
0 1.53 3.74
0 1.53 4.33
0 1.53 4.92
```
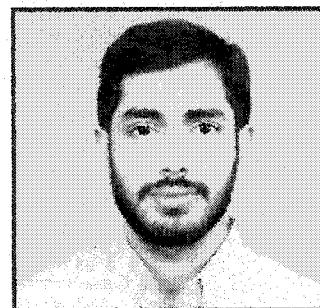
```
0 38.69 0.08
1      1.   /End
2      1000000. / Outside
5      31. /Oil zone
3      21.5   /foam
4      0.22 /Water zone
99/
5    12    0.64    -5.91    -12   24.8    5.93
3    12    24.8    -5.91    -12   30.5    5.93
4    12    30.5    -5.91    -12   38.69   5.93
10   12    1.53    -5.13    0     1.53    -5.11
10   0     1.53    -4.54    -12   1.53    -4.52
10   12    1.53    -3.95    0     1.53    -3.93
10   0     1.53    -3.36    -12   1.53    -3.34
10   12    1.53    -2.77    0     1.53    -2.75
10   0     1.53    -2.18    -12   1.53    -2.16
10   12    1.53    -1.57    0     1.53    -1.55
10   0     1.53    -0.99    -12   1.53    -0.97
10   12    1.53    -0.40    0     1.53    -0.38
10   0     1.53    0.19     -12   1.53    0.21
10   12    1.53    0.78     0     1.53    0.80
10   0     1.53    1.37     -12   1.53    1.39
10   12    1.53    1.96     0     1.53    1.98
10   0     1.53    2.55     -12   1.53    2.57
10   12    1.53    3.14     0     1.53    3.16
10   0     1.53    3.73     -12   1.53    3.75
10   12    1.53    4.32     0     1.53    4.34
10   0     1.53    4.91     -12   1.53    4.93
99/
99/
smtstmn.dat
```

VITA

OF

MUHAMMAD REAZ UDDIN CHOWDHURY

Addresses:

Saudi Arabia:	*Bangladesh*	*U.A.E.*
KFUPM Box # 1182	126 New Paltan Lane	C/o, A. H. Chowdhury
Dhahran 31261	Azimpur	P.O. Box # 8437
Ph: 03-860-5437	Dhaka-1205	Musaffah, Abu Dhabi

Email: g200427@kfupm.edu.sa, mdreaz@hotmail.com

Date & Place of Birth: 22nd November 1975, Dhaka, Bangladesh.

Education:

Sept. 2000 – Dec. 2002: M.S. in Petroleum Engineering, King Fahd University of Petroleum & Minerals, (KFUPM), Dhahran –31261, Saudi Arabia.

Jun. 1994 –Sept. 1999: B.Sc. in Chemical Engineering, Bangladesh University of Engineering & Technology (BUET), Dhaka –1000.

Experiences:

- Served as a Project Engineer in "Tetrahedron Inc. Bangladesh- An Arsenic Mitigation Project" from February 2000 to August 2000. The job involved working with water analysis and fieldwork with the installation and supervision of 'Tetrahedron Arsenic Mitigation Filter' as a team leader.

- Working as a Research Assistant in the Petroleum Engineering Department of King Fahd University of Petroleum & Minerals.

Professional Memberships:

American Institute of Chemical Engineers (AIChE), Saudi Arabia section and Society of Petroleum Engineers (SPE).